

International Atomic Energy Agency

---

**INDC**

---

---

**INTERNATIONAL NUCLEAR DATA COMMITTEE**

---

CONSOLIDATED PROGRESS REPORT FOR 1975

ON NUCLEAR DATA ACTIVITIES

OUTSIDE THE NDS SERVICE AREA

Austria

Belgium

Greece

Spain

Switzerland

Turkey

December 1975

---

**IAEA NUCLEAR DATA SECTION, KÄRNTNER RING 11, A-1010 VIENNA**

CONSOLIDATED PROGRESS REPORT FOR 1975

ON NUCLEAR DATA ACTIVITIES

OUTSIDE THE NDS SERVICE AREA

Austria

Belgium

Greece

Spain

Switzerland

Turkey

December 1975

## FOREWORD

This consolidated progress report for 1975 has been prepared for the countries outside the NDS service area. A second report, INDC(SEC)-50/L, covers countries within the NDS service area.

The report is arranged alphabetically by country, and reproduces the content of each individual report as it was received by the INDC Secretariat. Also included in the Table of Contents is a list of each laboratory, institute and university referred to in the report, preceded by its internationally used EXFOR code.

As in all progress reports the information included here is partly preliminary and is to be considered as private communication. Consequently, the individual reports are not to be quoted without the permission of the authors.



TABLE OF CONTENTS

	<u>pages</u>
<u>Austria</u> .....	1-8
(2AUSATI) Atominstitut der Oesterreichischen Hochschulen, Vienna	
(2AUSIRK) Institut fuer Radiumforschung und Kernphysik	
(2AUSSGA) Oesterreichische Studiengesellschaft fuer Atom- energie, Seibersdorf	
(2AUSGFK) Gesellschaft zur Foerderung der Kernenergie, Graz	
<u>Belgium</u> .....	9-93
(2BLGGHT) University of Ghent, Ghent	
(2BLGLVN) University of Louvain, Louvain	
(2BLGMOL) Nuclear Energy Center, Mol	
<u>Greece</u> .....	95-101
(2GRCATH) N.R.C. "Demokritos", Athens	
<u>Spain</u> .....	103-115
(2SPNJNE) Junta de Energia Nuclear, Madrid	
(2SPNUCM) Universidad Complutense, Madrid	
(2SPNUAM) Universidad Autonoma de Madrid, Madrid	
(2SPNIFC) Instituto de Fisica Corpuscular, Valencia	
(2SPNVU) Universidad de Valladolid	
(2SPNZU) Universidad de Zaragoza	
<u>Switzerland</u> .....	117-136
(2SWTNEU) University of Neuchatel, Neuchatel	
(2SWTFRS) University of Fribourg, Fribourg	

	<u>pages</u>
<u>Switzerland</u> continued	
(2SWTZUR) University of Zuerich, Zuerich	
(2SWTETH) Eidgenoessische Technische Hochschule, Zuerich	
(2SWTWUR) Institute for Reactor Research, Wuerenlingen	
<u>Turkey</u> .....	137-145
(2TUKCNA) Cekmece Nuclear Research Center, Istanbul	

PROGRESS REPORT TO NEANDC AND INDC  
FROM AUSTRIA

August 1975

O.J.Eder, Editor

This report contains abstracts about work performed at

Atominstitut der Österreichischen Hochschulen, Wien

Institut für Radiumforschung und Kernphysik der Österreichischen Akademie der Wissenschaften, Wien

Physikinstitut des Forschungszentrums Seibersdorf der Österreichischen Studiengesellschaft für Atomenergie

Institut für Reaktorphysik der Technischen Hochschule Graz

Österreichische  
Studiengesellschaft für  
Atomenergie Ges.m.b.H.  
A-2444 Seibersdorf  
Austria

This report contains  
partly preliminary data.  
The information given  
is to be considered as  
private communication  
and is not to be quoted.





ATOMINSTITUT DER ÖSTERREICHISCHEN HOCHSCHULEN, WIEN

1. NEUTRON SOURCES AND NEUTRON DETECTION

1.1 Flux depression and the absolute measurement of the thermal neutron flux density  
Atomkernenergie (1975)

F.Bensch

The thermal neutron flux depression in a diffusing medium by an absorbing foil has been treated in numerous papers. The results are re-examined in an attempt to find a uniform and physically meaningful representation of the "activation correction". This quantity can be split up into a combination of probabilities. Thus it is possible to determine the activation correction for any moderator and foil material. Measurements confirm the utility of the concepts introduced.

1.2 Measurement of emission spectra of some low-energy photo-neutron sources by the proton recoil method

E.Zankl

The spectroscopy of photoneutron sources poses serious difficulties due to their intense gamma field. Therefore a comprehensive n- $\gamma$ -discrimination is required. The results obtained by the division method developed by Bennett have been compared with those obtained by the anticoincidence method as used by Moler-Zagotta. It could be shown that the division method is more effective at high count rates and unfavourable neutron-to-gamma ratios. At the Ga-D<sub>2</sub>O source a good agreement with the calculations by Mueck has been achieved. At the Sb-Be source it was possible to show - besides the well-known  $^9\text{Be}(\gamma, n)^8\text{Be}$  reaction - the  $^9\text{Be}(\gamma, n)^2\alpha$  reaction.

2. NUCLEAR PHYSICS

2.1 Neutron inelastic scattering cross sections of some low lying levels in Sb, Ag and I

H.Jasicek, F.Bensch

The inelastic neutron scattering cross sections of Ag, Sb and I have been measured for three neutron energies at 390, 755 and 960 keV, using photoneutron sources and a spherical shell-geometry arrangement. A proton recoil neutron spectrometer has been used to resolve the neutron groups inelastic scattered by low lying levels. The inelastic excitation of states in Ag at 80, 320, 420 and 730 keV; in Sb at 30, 160 and 550 keV; in I at 60, 200, 410 and 600 keV was observed. Hauser-Feshbach calculations were carried out and the results fit well the experimental data.

## 2.2 Fission at high excited heavy nuclei

F.Bensch, G.Eder, H.Jasicek, H.Müller\*, H.Oberhummer, P.Riehs

Continuing our plans on fission investigations it is intended to measure the mass distribution of fission fragments using Si-surface barrier detectors. It is foreseen to distinguish between primary fissions and multiple chance fissions by means of the angular distribution of neutron time-of-flight spectrometry. The equipment will be installed at the Swiss Institute for Nuclear Research in the near future.

## 2.3 Investigation of (p, $\alpha$ ) transfer-reactions

H.Gryer\*, V.Meyer\*, H.Müller\*, W.Reichart\*, R.Wagner\*\*, H.Jasicek, H.Oberhummer, P.Riehs

The (p, $\alpha$ )-reactions are investigated for medium-weight target-nuclei in the energy range  $E_p = 30 - 70$  MeV. The differential cross-section is measured for these transfer-reactions and compared with DWBA-calculations using improved form-factors. Results for the Zr-isotopes have already been obtained.

## 2.4 The shape of $\gamma$ -ray spectra after thermal neutron capture in coincidence to low energy $\gamma$ -transitions

H.P.Korn\*\*\*, P.Weinzierl\*\*\*, P.Riehs

The continuous shape of  $\gamma$ -ray spectra of  $^{149}\text{Sm}(n,\gamma)$ ,  $^{157}\text{Gd}(n,\gamma)$  and  $^{181}\text{Ta}(n,\gamma)$  has been measured in coincidence to various low energy  $\gamma$ -transitions. Some differences of the shapes were found and are explained by calculations of the shapes of  $\gamma$ -ray spectra leading to low energy levels. The changes of the spectrum shape due to energy, spin and parity of the low energy level have been studied.

---

\* Universität Zürich

\*\* Universität Basel

\*\*\* Forschungszentrum Seibersdorf, Institut für Physik

2.5 Low energy  $\gamma$ -rays from resonance neutron capture in  $^{133}\text{Cs}$  and  $^{167}\text{Er}$

P.Riehs, B.W.Thomas\*

The intensities of prominent low energy  $\gamma$ -transitions in  $^{133}\text{Cs}(n,\gamma)$  and  $^{167}\text{Er}(n,\gamma)$  have been measured for a number of neutron resonances using a Ge(Li) detector. Both nuclides indicate a grouping of s-wave capture spins 3 and 4. Spin assignments and  $\gamma$ -cascade calculations for population rates of low energy levels have been made.

INSTITUT FÜR RADIUMFORSCHUNG UND KERNPHYSIK DER  
ÖSTERREICHISCHEN AKADEMIE DER WISSENSCHAFTEN, WIEN

1. Cross Sections for 14 MeV Neutron Capture

O.Schwerer, M.Winkler, H.Warhanek, G.Winkler

Activation cross sections for neutron capture have been measured at an energy of  $(14.6 \pm 0.2)$  MeV relative to  $^{27}\text{Al}(n,\alpha)^{24}\text{Na} = 114.2 \text{ mb} \pm 1.2\%$ . Measurements were carried out by  $\gamma$ -detection using a Ge(Li) detector. Special attention has been paid to taking into account all possible sources of error, especially contributions of lower energy neutrons. Capture cross sections have been measured on the isotopes  $^{37}\text{Cl}$ ,  $^{41}\text{K}$ ,  $^{50}\text{Ti}$ ,  $^{55}\text{Mn}$ ,  $^{71}\text{Ga}$ ,  $^{87}\text{Rb}$ ,  $^{89}\text{Y}$ ,  $^{127}\text{I}$ ,  $^{130}\text{Te}$ ,  $^{138}\text{Ba}$ ,  $^{139}\text{La}$ ,  $^{142}\text{Ce}$ ,  $^{186}\text{W}$ ,  $^{198}\text{Pt}$ ,  $^{197}\text{Au}$ .

The work is to be published in Nucl. Phys.

2. M.Wagner, H.Warhanek

The work mentioned above has been continued and capture cross sections have been measured on the following isotopes:

$^{45}\text{Sc}$ ,  $^{75}\text{As}$ ,  $^{81}\text{Br}$ ,  $^{96}\text{Zr}$ ,  $^{100}\text{Mo}$ ,  $^{104}\text{Ru}$ ,  $^{115}\text{In}$ ,  $^{123}\text{Sb}$ ,  $^{133}\text{Cs}$ ,  $^{141}\text{Pr}$ ,  $^{181}\text{Ta}$ ,  $^{187}\text{Re}$ .

---

\* Nuclear Physics Division, AERE Harwell

3. Measurement of energy spectra and angular distributions of charged particles emitted in nuclear reactions induced by 14 MeV neutrons

P.Hille, M.Uhl, K.Richter, W.Weisz, C.Derndorfer

Work described in the last reports is continued by measuring the  $^{50}\text{Cr}(n,\alpha)$ -reaction. A new improved version of the cylindrical multiwire chamber is under construction.

4. Age-determination of bones by activation with 14MeV neutrons

P.Eisenbarth, P.Hille

Work described in the last report has been completed. Routine analysis of N/F-, N/Ca-, N/P-, F/P- and F/Ca-ratios can now be carried out in order to estimate ages of bones up to some  $10^7$  years back from present. Co-operation with institutions interested in such age-determinations has been initiated.

5. Measurement of  $\gamma$ -multiplicities after  $(n,n')$ -reactions with 14 MeV neutrons

P.Hille, P.Grabmayer

With a  $\gamma$ -detector having almost constant efficiency between 0.1 and 10 MeV the number of  $\gamma$ -quanta emitted after  $(n,n')$ -reactions will be measured in coincidence with the scattered neutrons using TOF-technique. The result is to be compared with statistical calculations using different models for the  $\gamma$ -width.

6. Measurement of  $(n,n'\gamma)$ -reaction on  $^{56}\text{Fe}$

G.Stengl

The work described in the last report has been completed and will be published.

PHYSIKINSTITUT DES FORSCHUNGSZENTRUMS SEIBERSDORF,  
ÖSTERREICHISCHE STUDIENGESELLSCHAFT FÜR ATOMENERGIE

Electron-neutrino angular correlation coefficient  $a$   
measured from free-neutron decay - Phys.Rev. D 11 (1975)

R.Dobrozemsky, E.Kerschbaum, G.Moraw, H.Paul\*,  
C.Stratowa, P.Weinzierl

Measurements of the electron-neutrino angular correlation coefficient  $a$  in the free-neutron decay are reported. The method is based on the measurement of the energy spectrum of recoil protons obtained from neutrons inside a highly evacuated tangential reactor beam tube. Spectroscopy was done outside the reactor shielding by means of an electrostatic condenser and an ion-electron converter detector of the coincidence type. The result, based on 30 measured proton-energy spectra, is  $a = -0.099 \pm 0.011$ , giving  $|G_A/G_V| = 1.250 \pm 0.036$ . Thus a considerable improvement in accuracy concerning the measurement of  $a$  of the free unpolarized neutron has been achieved. The result is in good agreement with the data obtained from polarized neutron decay.

INSTITUT FÜR REAKTORPHYSIK DER TECHNISCHEN HOCHSCHULE GRAZ

1. Determination of the Resonance Self-shielding in Materials  
of Medium Atomic Weight

M.Heindler

To examine, how far the up to now little regarded phenomena of resonance self-shielding in materials of medium atomic weight (Fe, Cr, Ni, Na, ...) are responsible for the discrepancy between theory and experiment with differential dates, respectively for the correspondence of integral dates - evidently caused by a compensation of errors - studies on s-, p- and d-resonances are carried out together with the reactor centres Saclay and Cadarache.

Improvements in regard to the comprehension of the Doppler-broadening in the calculation of the energy-dependent cross sections obtained from the resonance parameter are achieved, and the approximations concerning the computation of self-shielding are examined for their validity. The so obtained self-shielding factors are stated for the element Fe and compared with those used up to now.

\* Institut für Experimentalphysik, Hochschule Linz

2. Measurement of the Cross Sections with the Pile Oscillator Method

W. Ninaus

A measurement system of high sensitivity for the determination of cross sections has been developed in form of a pneumatic pile oscillator, which is to be installed in the central channel of the SAR Graz. With the help of this apparatus the calibration and sensitivity measurements with the  $1/v$  absorber boron have been accomplished.

In the medium S/M range deviations of the measured values from the calculated ones have been found for tungsten (thin slab-shaped samples) at examining the effective resonance integrals\*. By applying the pile oscillator method, a larger S/M interval is to be measured in order to find out by comparison with theoretical results, if errors in the cross sections are responsible for the above mentioned deviations.

3. Measurement of the Prompt Decay Constant in the SAR with the Pulsed Neutron Technique

W. Ninaus

The evaluation of the prompt decay of a thermalized burst of neutrons gives a determination for the prompt decay constant  $\alpha$  in subcritical systems. The pulsed neutron source used here is working after the principle of a pneumatic pile oscillator. The neutron source emits neutrons of the energy of 26 keV. The measured values of  $\alpha$  are corresponding with the values obtained from the Rossi- $\alpha$ -experiments. The prompt decay constant in the pulsed SAR-system is examined by using a one group and a two group diffusion theory.

4. Measurements of Effective Resonance Integrals

F. Siegl

From the materials boron, natural tungsten, tantalum and gold the effective resonance integrals were determined. The experimental measurements were carried out with the pile oscillator method. The theoretical assumption for the interpretation of the experimental results was derived from the energy depending diffusion equation by applying the perturbation theory. Thin hollow cylinders were used as samples.

---

\* H. Heimel, M. Heindler: Effektive Resonanzintegrale von Molybdän, Wolfram und Tantal in ebener Geometrie; Atomkernenergie, 20 (1972)

ANNUAL PROGRESS REPORT TO INDC FROM BELGIAN LABORATORIES  
WORKING IN THE FIELD OF NUCLEAR DATA.

- GHEENT STATE UNIVERSITY
- KATHOLIEKE UNIVERSITEIT LEUVEN
- CEN/SCK MOL







**GHENT STATE UNIVERSITY**

**NUCLEAR PHYSICS LABORATORY**

**LABORATORIUM VOOR KERNFYSICA**

**ANNUAL REPORT 1974**

## INTRODUCTION

*In 1974 the Linear Accelerator of the Nuclear Physics Laboratory of the State University of Ghent has been exploited during more than 3000 hours. At the same time the site was prepared for the installment of two new sections and modulators. It is hoped to have them in operation in 1975.*

*In 1974, work was concentrated on :*

- (1) nuclear fission experiments*
- (2) photonuclear-reaction studies*
- (3) nuclear spectroscopy and positron annihilation studies*
- (4) dosimetry*
- (5) theoretical studies in relation with our experimental programmes.*

*The most important results of this research activity are condensed in the present annual report. For more ample description the reader is referred to the publication list at the end of the report.*

*This research was only possible with the important help of the I.I.K.W. (Interuniversity Institute for Nuclear Sciences, Brussels). We want to thank this Institute and its "Committee for low energy nuclear physics" for this support.*

*Prof. Dr. A. J. Deruytter  
Director of the Nuclear Physics Laboratory.*

Table of Contents

1. Linac Operation
2. Nuclear Fission
  - 2.1. Experimental Arrangements
  - 2.2. Study of the mass distribution for the photofission of  $^{238}\text{U}$  with 25 MeV endpoint bremsstrahlung, for the spontaneous fission of  $^{252}\text{Cf}$  and for the fission of  $^{235}\text{U}$ , bombarded with thermal neutrons
  - 2.3. Determination of the most probable charge ( $Z_p$ ) for the photofission of  $^{238}\text{U}$ , with 25 MeV endpoint bremsstrahlung, for the spontaneous fission of  $^{252}\text{Cf}$  and for the thermal neutron fission of  $^{235}\text{U}$
  - 2.4. Study of the mass- and kinetic energy distribution of the fragments for the photofission of  $^{235}\text{U}$  and  $^{238}\text{U}$  with 25 MeV endpoint bremsstrahlung.
  - 2.5. Study of the binary to ternary fission ratio (B/T) for the spontaneous fission of  $^{252}\text{Cf}$  and the photofission of  $^{235}\text{U}$  with 25 MeV endpoint bremsstrahlung.
3. Photonuclear Reactions
  - 3.1. Introduction
  - 3.2. Experimental study of the  $^{31}\text{P}$  total photoneutron cross section
  - 3.3. Photoproton energy spectra and angular distributions from  $^{12}\text{C}$
  - 3.4. Photoneutron energy spectra from  $^{16}\text{O}$  and  $^2\text{D}$
  - 3.5. Production and acceleration of positrons
4. Nuclear spectroscopy and positron annihilation
  - 4.1. Ge-Ge gamma-gamma coincidence apparatus
  - 4.2. Study of the decay of  $^{147}\text{Pr}$
  - 4.3. Stabilization of the positron annihilation measuring chains
  - 4.4. Positron annihilation in KDP ( $\text{KH}_2\text{PO}_4$ )
  - 4.5. S-factor measurements in glass
  - 4.6. Preliminary experiments and design of a set-up for the measurement of windowed angular correlations of annihilation radiation
  - 4.7. Study of short living isomeric states (milli- and microsec) between the accelerator pulses
5. Dosimetry
  - 5.1. Cavity theory and related experiments
  - 5.2. Thermoluminescent dosimetry and applied cavity theory
  - 5.3. Calorimetry

- 5.4. Beam calibrations
- 5.5. Plastic film dosimeters
- 5.6. Atmospheric pollution of  $^{85}\text{Kr}$

## 6. Theoretical studies

- 6.1. Microscopic structure from (p,p')scattering through isobaric analog resonances
- 6.2. Study of the generator coordinate method
- 6.3. Strutinsky type of calculations for odd-proton Tl and In isotopes
- 6.4. Phase conventions for electromagnetic multipole operators

Publications by members of the Laboratory (published 1974)

Publications in print

Congress or Symposia - Contributions

Doctoral theses at the Rijksuniversiteit-Gent (1974)

## 1. LINAC OPERATION (K.Kiesel)

During the year 1974, the linear electron accelerator of the Physics Laboratory of the State University of Ghent, has been in service for 3.065 hours, distributed as shown in Fig. 1.

Awaiting the rebuilding of the accelerator with new sections and modulators, the machine has been in maximum exploitation with one old section and modulator.

An exploitation of over 3.000 hours poses very serious problems with our restricted number of operators, especially for the night-shifts, and represents an absolute maximum.

Major problems arose with vacuum in the beam-deflection system due to the bad energy-spectrum of the actual section + modulator, resulting in hitting the walls of the vacuum-system and causing outgasing. This problem was very urgent around the vacuum-valves (still using elastomere O-rings).

Two high-power thyratrons had to be replaced (both after about 2.500 hours service).

A major break-down (two weeks in september) was caused by the failure of the electron-gun of the injector (after 2.400 hours service). Due to technical problems, the mounting of the spare cathode caused serious difficulties. The electronics of the injector had to be partly rebuild too.

The new modulator is under construction and almost completed. The first tests under actual high-voltage conditions show an excellent stability of 0,1 % and a pulse-ripple of 0,5 %.

The site for the new sections and modulators is under preparation, especially with a more elaborate cooling-system.

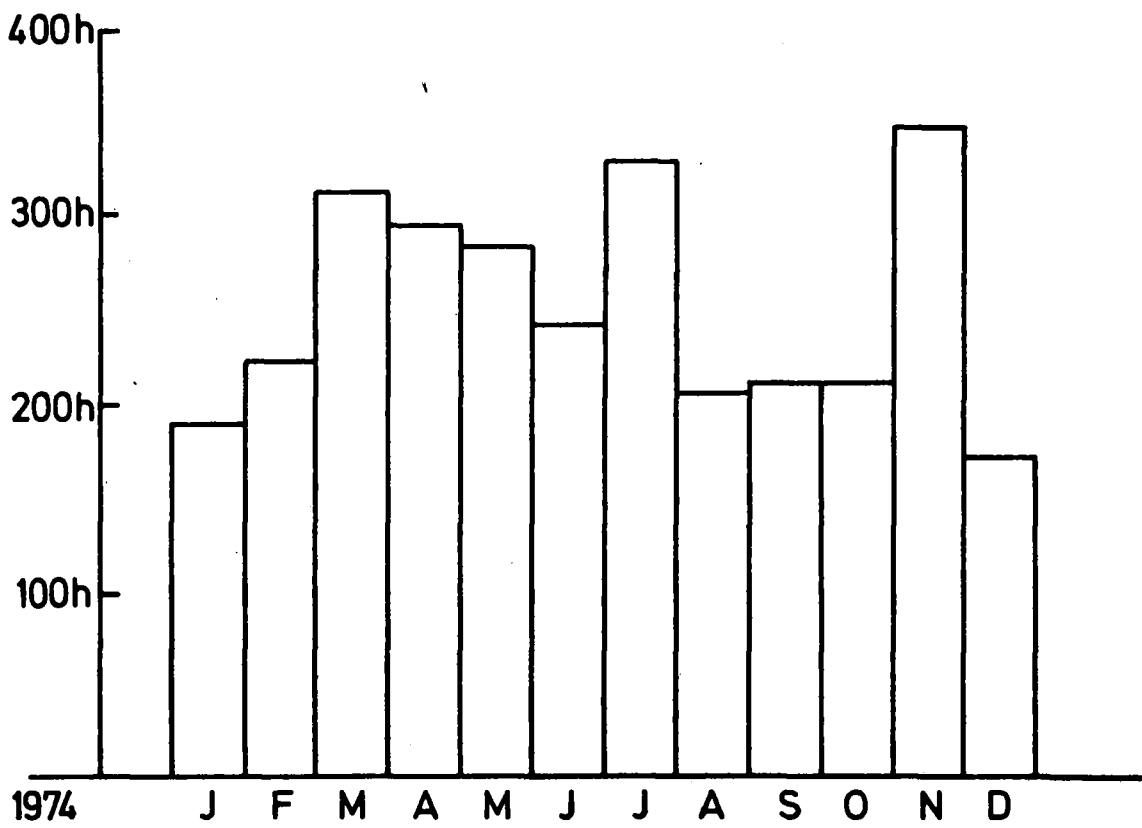


FIG.1: Linac exploitation during 1974.

2. NUCLEAR FISSION : (E. Jacobs, D. De Frenne, A. De Clercq, H. Thierens,  
P. D'Hondt, C. Wagemans\*)

During 1974 the first results concerning photofission studies, on the new deflected beam of the linac of the nuclear physics laboratory, were obtained.

2.1. Experimental Arrangements :

The bremsstrahlung beam, used until now for all photofission experiments, was obtained by sending a deflected electron beam on a 0.5 mm thick W-bremsstrahlungstarget. After passage through the W target, the electrons are stopped in a graphite block.

End 1974 we started the construction of a cleaning magnet in order to deflect the electrons after passage through the bremsstrahlungstarget. After deflection the electrons will be stopped in a large water-tank. Because of the absence of a graphite block behind the bremsstrahlungstarget, we will obtain a cleaner bremsstrahlungsbeam, with relatively more high-energetic  $\gamma$ -rays. This will be of special interest for the photofission studies at different bremsstrahlungsendpoint energies. We expect that the installation of the cleaning magnet will be finished in march 1975.

2.2. Study of the mass distribution for the photofission of  $^{238}\text{U}$  with 25 MeV end point bremsstrahlung, for the spontaneous fission of  $^{252}\text{Cf}$  and for the fission of  $^{235}\text{U}$ , bombarded with thermal neutrons.

These mass distributions are studied using the catcher foil technique. By choosing appropriate irradiation, cooling and measuring times, the yields of 42 masses could be determined for the photofission of  $^{238}\text{U}$  with 25 MeV bremsstrahlung. Practically all the masses are lying on a smooth curve, except for the masses 99, 133, 134 and the valley masses 111 and 113, giving a higher yield than the expected one. On the contrary the yield for mass 142 is lower compared with the surrounding masses. In Fig.2. the mass-distribution for the photofission of  $^{238}\text{U}$  with 25 MeV Bremsstrahlung is shown as an example.

For the determination of those yields, we are using spectroscopic data

-----  
\* N.F.W.O. , University of Gent and S.C.K./C.E.N.

MASS DISTRIBUTION FOR THE PHOTOFISSION OF  
 $^{238}\text{U}$  WITH 25 MeV BREMSSTRAHLUNG.

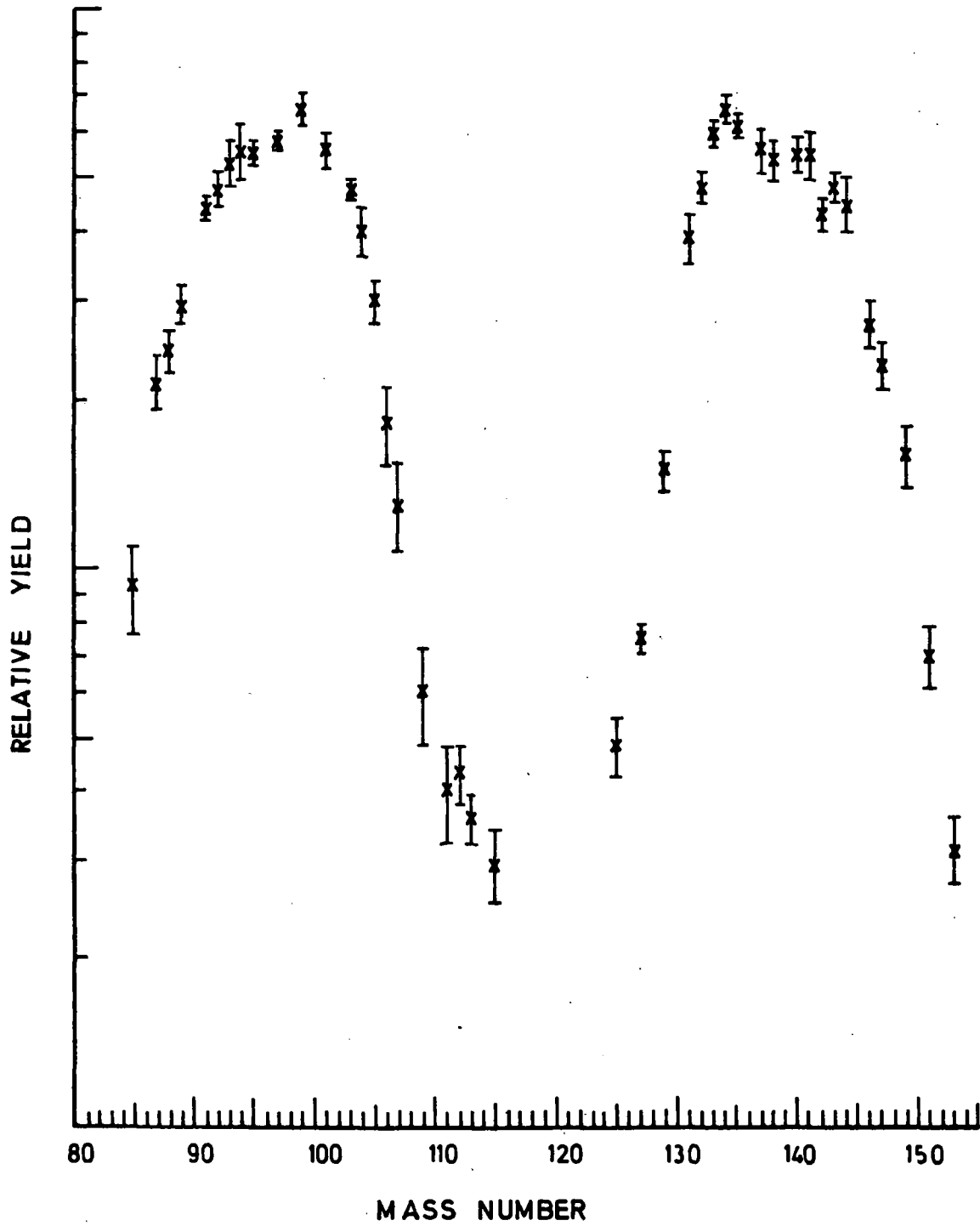


FIG. 2.



from the literature. Except eventually for the masses 133 and 134 we supposed that the deviations should be due to wrong data in the literature. Especially the branching ratios for the isotopes with an important  $\beta$ -branch to the ground-state of the daughter nucleus are not well known.

To control the branching ratios used, or to obtain eventually more accurate values, we have also studied with the same catcher foil method the well-known mass distributions for the spontaneous fission of  $^{252}\text{Cf}$  and for the thermal neutron induced fission of  $^{235}\text{U}$ . The  $^{235}\text{U}$  samples were irradiated at the Belgian High Flux Reactor B.R.L. (S.C.K.-Mol).

From the study of the spontaneous fission of  $^{252}\text{Cf}$  we concluded that the branching ratios from the literature, used for the determination of the yields for the masses 111, 113 and 142 were wrong. By using the branching ratios determined in this way we find yields, for these masses, which are better adjusted to the surrounding masses.

The results from the study of the thermal neutron fission of  $^{235}\text{U}$  are not yet sufficiently analysed to give an answer concerning the masses 99 and 133 - 134.

To determine more accurate yields, especially in the valley region, some experiments were performed in collaboration with Dr. Thielens, to separate some elements (Ag) chemically. It turns out to be rather difficult to find a method to dissolve the Al catcher-foil in a sufficiently short time.

### 2.3. Determination of the most probable charge ( $Z_p$ ) for the photofission of $^{238}\text{U}$ , with 25 MeV endpoint bremsstrahlung, for the spontaneous fission of $^{252}\text{Cf}$ and for the thermal neutron fission of $^{235}\text{U}$ .

Here we are also using the catcher-foil technique. Besides the relative yields for 42 masses, mentioned in 2.2., also independent yields for  $^{131\text{m}}\text{Te}$ ,  $^{131\text{g}}\text{Te}$ ,  $^{132}\text{I}$ ,  $^{134}\text{I}$ ,  $^{135}\text{Xe}$ ,  $^{138}\text{Cs}$  and  $^{140}\text{La}$  were measured for the photofission of  $^{238}\text{U}$ . From these independent yields we can calculate the  $Z_p$  values for the masses 131, 132, 134, 135, 138 and 140, using the P(Z) Gauss-curve of Wahl. (A.C.Wahl, Proceedings of the Symposium on Physics and Chemistry of Fission, Salzburg 1965, Paper SM 60/22).

The obtained  $Z_p$  values are in agreement with the values expected from the U.C.D. (unchanged charge distribution) hypothesis.

For the spontaneous fission of  $^{252}\text{Cf}$  the  $Z_p$  values for the masses

134 and 135 were determined.

The determination of the Zp value for a few masses in the thermal neutron fission of  $^{235}\text{U}$  is under way.

2.4. Study of the mass- and kinetic energy distribution of the fragments for the photofission of  $^{235}\text{U}$  and  $^{238}\text{U}$  with 25 MeV endpoint bremsstrahlung.

For these double-energy measurements with two surface-barrier detectors, a new collimator was constructed. The existing 2-parameter analysis system was extended in such a way that the height of the  $\gamma$ -flash is continuously controlled, and the mean height of the  $\gamma$ -flash is subtracted on-line from the fragment signals. The height of the  $\gamma$ -flash is limited between 0.75 % and 1 % of the fission fragment signal by adjusting the linac beam intensity.

The kinetic energy- and mass distributions for the photofission of  $^{235}\text{U}$  and  $^{238}\text{U}$  with 25 MeV endpoint bremsstrahlung were studied.

The most important characteristics of those mass- and kinetic energy distributions are given in Table 1. The distributions are very analogous for the two isotopes.

TABLE I

Characteristics of the fission induced by 25 MeV end-point bremsstrahlung

Quantity	$^{235}\text{U}$	$^{238}\text{U}$
total		
average kinetic energy $\langle E_k \rangle$	170.2 MeV	170.9 MeV
spread in $\langle E_k \rangle$ $\sigma \langle E_k \rangle$	11.0 MeV	11.2 MeV
average provisional light mass $\langle M_l \rangle$	97.58	99.90
average provisional heavy mass $\langle M_h \rangle$	137.43	138.0
widths of the light and heavy mass distributions $\sigma \langle M_l \rangle = \sigma \langle M_h \rangle$	6.87	6.73
Peak/Valley in the mass distribution	13 $\pm$ 0.5	16 $\pm$ 0.5

The absolute error on  $\langle E_k \rangle$  is estimated to be 1.5 à 2 MeV. It is in the first place due to the error on the thickness of the target material and the VYNS backing of the targets and calibration sources.

The statistical errors on the results are of the order of 0.1%.

One may remark that with increasing total kinetic energy of the fragments, the two peaks in the mass distribution move closer together and the valley is becoming deeper. For extreme high kinetic energy of the fragments, the heavy fragment top is lying practically at mass 132, illustrating the influence of the double magic nucleus  $^{132}\text{Sn}$ . This is clearly illustrated in Fig.3.

### 2.5 Study of the binary to ternary fission ratio (B/T) for the spontaneous fission of $^{252}\text{Cf}$ and the photofission of $^{235}\text{U}$ with 25 MeV endpoint bremsstrahlung.

For the spontaneous fission of  $^{252}\text{Cf}$  the spectrum of the highly energetic ternary  $\alpha$ -particles has been measured. At the same time a value of  $\sim 300$  was found for the B/T ratio. An accurate analysis of these results is under way.

In collaboration with Dr.C.Wagemans tests have been performed to determine B/T ratios and measure spectra of the highly energetic ternary  $\alpha$ -particles for the photofission of a  $500 \mu\text{g}/\text{cm}^2$   $^{235}\text{U}$  target with 25 MeV endpoint bremsstrahlung.

From those preliminary experiments we know that the ternary long range  $\alpha$ -spectrum is deformed by the presence of protons, produced by  $(\gamma, p)$  reactions, especially in the VYNS support of the target. To perform these experiments it will be necessary to use detectors with a smaller area (to reduce the  $\gamma$ -flash), preceded by a  $\Delta E/\Delta x$  detector, to distinguish protons from  $\alpha$ -particles.

$^{235}\text{U}$  N (MASS) EK: 195 - 210 MeV  
FULL SCALE : 300 COUNTS

$^{238}\text{U}$  N (MASS) EK: 195 - 210 MeV  
FULL SCALE : 200 COUNTS.

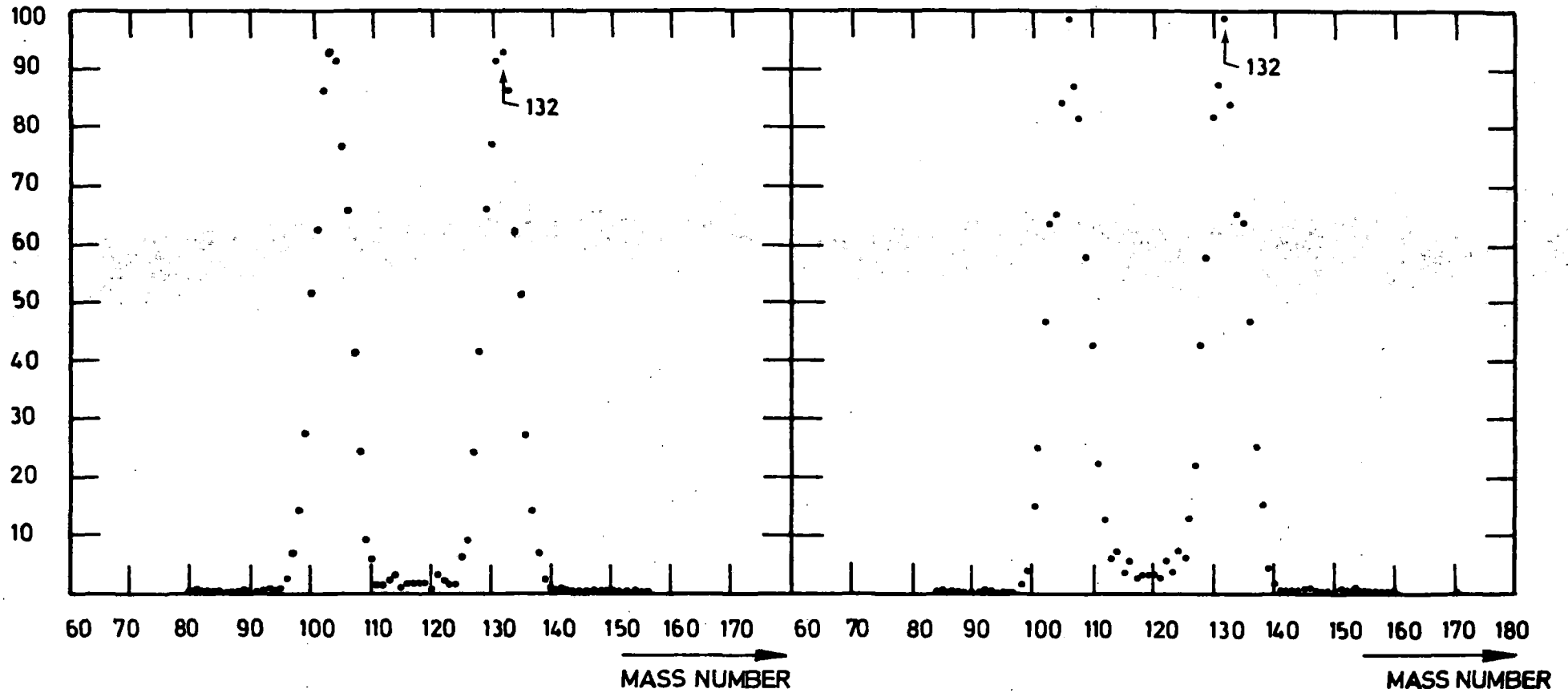


FIG. 3.

### 3. PHOTONUCLEAR REACTIONS

#### 3.1. Introduction

The various experiments which are being performed within the framework of the "Photonuclear Reaction"-project aim at a detailed understanding of the nature of the excitation mechanism that is responsible for the appearance of the giant dipole resonance in nuclei.

During the past few years experimental conditions have been created at this laboratory, which enable us to measure the following quantities, using the bremsstrahlung photon beam from the linear electron accelerator :

1. the total photoneutron cross section
2. The photoproton energy spectra and angular distributions, from which absolute differential cross sections can be derived
3. the photoneutron spectra and absolute differential cross sections.

Below, a short description of the experiments that have been performed with this apparatus is given.

#### 3.2. Experimental study of the $^{31}\text{P}$ total photoneutron cross section

(J.Devos, R.Carchon, H.Ferdinande & R.Van de Vyver)

The photoneutron yield from the  $^{31}\text{P}(\gamma, xn)$  reaction has been measured as a function of bremsstrahlung endpoint energy, in the energy range from threshold (12.3 MeV) to 25 MeV. Several analysis procedures were used to compute the photoneutron cross section from the experimental yield curve. The leading edge of the giant resonance displays an extremely rich fine structure which seems to be characteristic for nuclei in the 1d-2s shell. Our results show in this energy interval a remarkable agreement with the data obtained at Saclay, using a quasi-monochromatic photon beam. This proves that careful measurements which make use of a bremsstrahlung beam, can yield very accurate cross section results in the rising part of the giant dipole resonance, although a sophisticated analysis procedure has to be applied here. It appears that in the discussed energy region, the energy resolution obtained in our experiments is even superior to that obtained in the measurements with monoenergetic gamma-rays.

The results of this work have been published.

#### 3.3. Photoproton energy spectra and angular distributions from $^{12}\text{C}$

(R.Carchon, J.Devos, H.Ferdinande, R.Van de Vyver & E.Van Camp)

The photoproton energy spectra from the  $^{12}\text{C}(\gamma, p)^{11}\text{B}$  reaction have been

measured at 7 angles (from 37° to 143°) simultaneously, using Si(Li)-solid state detectors (3 mm thick), at a bremsstrahlung endpoint energy of 30 MeV. As a target, a polystyrene foil with a thickness of 3.33 mg/cm<sup>2</sup> was taken, which was located at the centre of a specially-constructed reaction chamber; this chamber was heavily shielded with lead while over the beam channels, leading to the detectors, permanent magnets were placed to suppress the effect of scattered gamma-rays and of secondary electrons. To determine the background-spectra, aluminium absorbers (with a thickness of 2mm) were placed in the proton path, right in front of the detectors.

Supposing that only ground state transitions to the residual nucleus occur, the resulting net energy spectra have been converted to absolute differential cross sections by means of a computer programme that explicitly takes account of the energy loss of the protons in the target.

Fitting a sum of Legendre polynomials of the following form

$$\frac{d\sigma}{d\Omega}(E_{\gamma}, \theta) = \sum_{i=0}^4 A_i(E_{\gamma}) \cdot P_i(\cos \theta)$$

to our experimental data, we can derive the angular distribution coefficients. The behaviour of these coefficients as a function of energy, reveals the specific contribution of the various multipoles to the absorption mechanism of photons in the target.

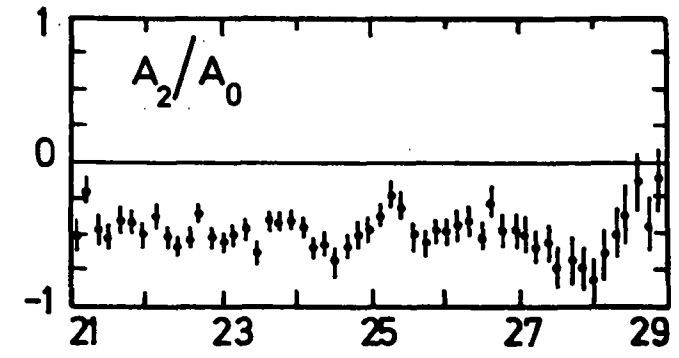
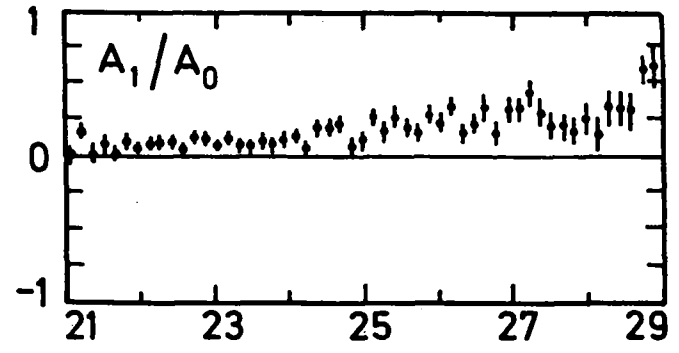
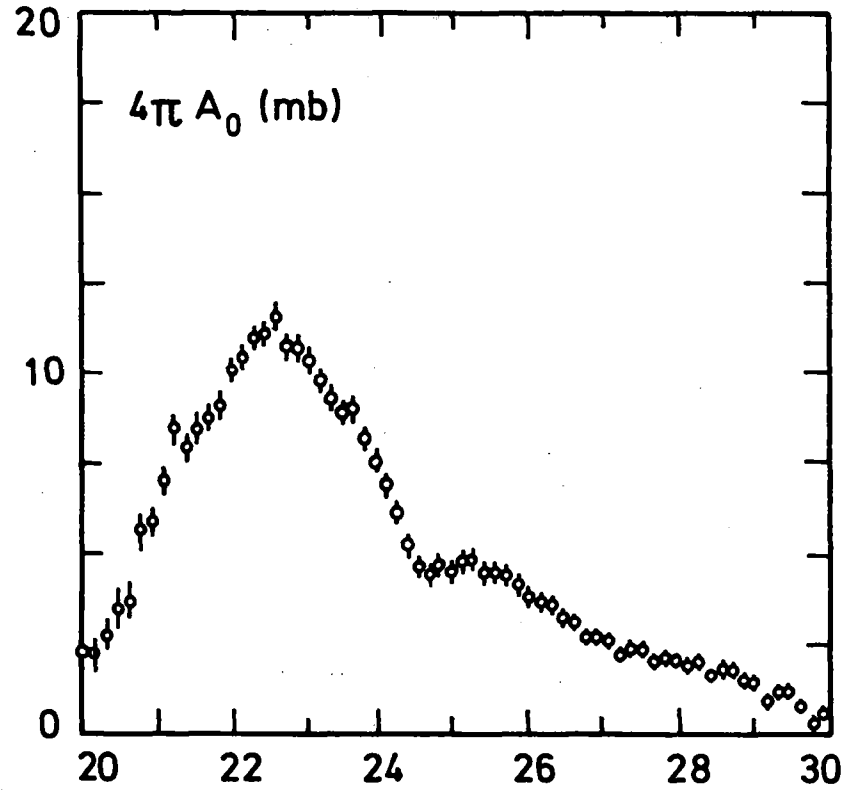
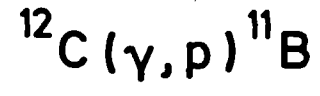
It appears that the  $A_3/A_0$ - and the  $A_4/A_0$ -values are approximately equal to zero in the entire energy range from 20 to 30 MeV, while the  $A_1/A_0$ -coefficient starts at zero but slowly increases with energy to a maximum value of about 0.4. The coefficient  $A_2/A_0$  is negative at all energies and has an average value of about -0.5 ; however, interesting fine structure (at 25.5 MeV) is here observed.

In figure 4 we have plotted the results for the total photoproton cross section ( $4\pi A_0$ ), and for the  $A_1/A_0$ - and  $A_2/A_0$ -coefficients, for a fitting procedure up to  $P_2$ . From our data we can conclude that almost exclusively E1-excitation (with a possible M1 contribution) takes place in the giant resonance region. Our results confirm and complete a recent experiment of Frederick et al. [Phys.Rev. 176(1968)1177], and they show some remarkable points of agreement with a theoretical calculation by Birkholz et al. [Nucl.Phys. A189 (1972) 385]. Our results are now being prepared for publication.

### 3.4 Photoneutron energy spectra from <sup>16</sup>O and <sup>2</sup>D

(J.Devos, R.Van de Vyver, R.Carchon & E.Van Camp)

Neutron spectra can be measured by making use of organic scintillators,



$\rightarrow$   
E $\gamma$  (MeV)

FIG. 4.

such as stilbene or NE213; these materials contain a high concentration of hydrogen nuclei. Neutrons incident upon this material can produce recoil-protons, which create scintillations in the organic material. The light-output of these scintillations is directly related to the energy of the recoil-protons. Analysis of this proton pulseheight distribution yields the incident neutron spectrum.

We have used this type of recoil-proton spectrometer to measure the energy spectrum of the photoneutrons emitted in the  $^{16}\text{O}(\gamma, n)^{15}\text{O}$  reaction, at an angle of  $90^\circ$  and at a bremsstrahlung endpoint energy of 28 MeV. This spectrometer consists essentially of a stilbene crystal with photomultiplier, and of a pulse shape discrimination (PSD) circuit. Pulse shape discrimination is necessary to distinguish between pulses induced by neutrons or by gamma-rays. Supposing that the residual nucleus is left in its ground state we can convert this resulting energy spectrum to an absolute differential cross section. Fig. 5 shows our data; the overall agreement with the results from time-of-flight experiments is very good. However, the relative height of the observed peaks in our cross section seems to correspond better with the results of a total photoneutron cross section measurement, performed with monoenergetic photons.

Moreover, we have applied our spectrometer to measure the photo-neutron energy spectrum from the  $^2\text{D}(\gamma, n)\text{H}$  reaction, again at an angle of  $90^\circ$  and at 20 MeV bremsstrahlung endpoint energy. The theoretical cross section for the two-body break-up in this process is well-known (Partovi); dividing the measured neutron spectrum by this theoretical cross section straightforwardly yields the absolute intensity distribution of the incident bremsstrahlung beam. The photon distribution, obtained in our experiments, is in very good agreement with the theoretical calculations of Schiff and of Bethe & Heitler, performed for very thin radiators. A thick-target computation shows substantial deviations; however, this is to be expected in view of the fact that our experimental set-up contains a very thin Au-foil as a bremsstrahlung converter target. On the other hand, we have now the possibility to check in an absolute way the bremsstrahlung spectrum that is used in most of our photonuclear experiments.

### 3.5. Production and acceleration of positrons.

(R. Van de Vyver, H. Ferdinand & K. Kiesel)

The construction of the long strong solenoid (2500 G), which has to be placed over the Linac section that follows the electron-to-positron converter, has been stopped as the available accelerator sections will be replaced, mid-1975, by new ones which are equipped with suitable focussing coils. The entire positron production and-focussing mechanism has been assembled and is now ready for use. However, the magnetic field pattern (stepped-field configuration) has still to be measured and, eventually, to be corrected.



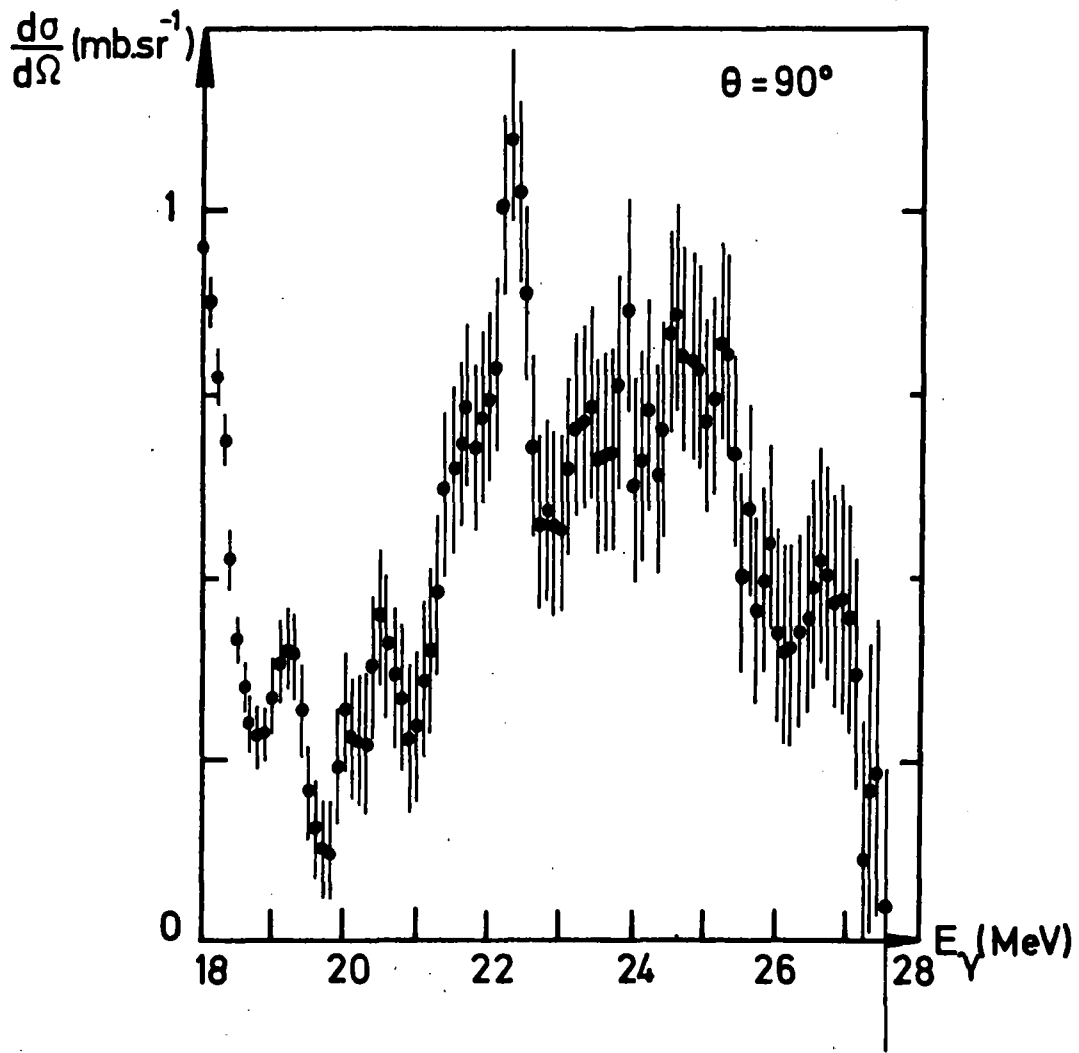
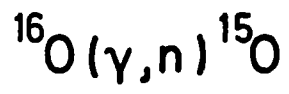


FIG. 5.

4. NUCLEAR SPECTROSCOPY AND POSITRON ANNIHILATION  
M. Dorikens, L. Dorikens-Vanpraet, D. Seghers, C. Dauwe \*  
J. Uyttenhove \*\*

4.1. Ge-Ge gamma-gamma coincidence apparatus.

A double coincidence apparatus with two Ge(Li) detectors was built and tested. In the timing channels extrapolated zero strobes are used. The energy dynamic range covers the region from 70 to 2500 keV. It is possible to record two coincidence measurements simultaneously. The two spectra are routed into different parts of the analyzer memory. This makes direct comparison possible between coincidences measured with a window on a given peak, and coincidences measured with a window directly behind that peak. In this way any chance coincidences and coincidences with underlying Compton distributions are easily recognized.

Fig. 6 shows a block diagram of the set-up. The two Ge(Li) detectors have the same efficiency and dimensions and are mounted on a turntable; consequently the apparatus can eventually be used to perform gamma-gamma angular correlation experiments.

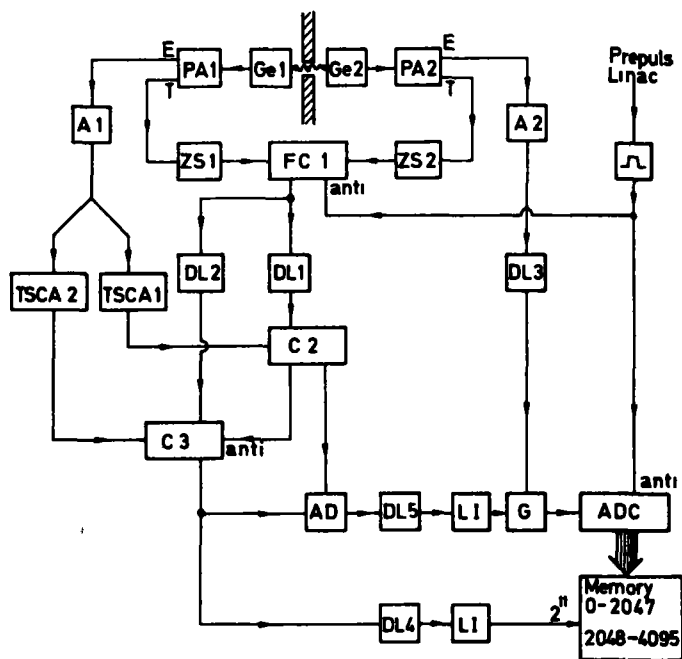
4.2. Study of the decay of  $^{147}\text{Pr}$

The study of  $^{147}\text{Pr}$  is interesting since very little is known about its decay.  $^{147}\text{Pr}$  being a fission product, it is important to have reliable data on the most prominent gamma transitions (energy and intensity). Our  $^{147}\text{Pr}$  sources were prepared by  $(\gamma, p)$  reactions on 95.5% enriched  $^{148}\text{Nd}$ . In this way strong sources are obtained, but many other activities are formed which complicate the spectra considerably. Singles-spectra were taken with different detectors. The low energy range (below 150 keV) was studied with a Low Energy Photon Spectrometer (resolution 600 eV at 122 keV). The medium energy range (150 to 1000 keV) was recorded with a 19cc high resolution Ge(Li) detector (1.4 keV at 514 keV). For the high energy range a 59 cc Ge(Li) detector with high efficiency was used. Fig. 7 shows a singles spectrum taken with this detector. All peaks marked with an energy value belong to the decay of  $^{147}\text{Pr}$ . The peaks marked with an asterisk were used as internal energy calibration points. The unmarked peaks are due to the other activities present in the source (i.e.  $^{147}\text{Nd}$ ,  $^{149}\text{Nd}$ ,  $^{146}\text{Nd}$  etc.).

The decay of each gamma ray was followed. 85 gamma rays having the lifetime of  $^{147}\text{Pr}$  (i.e. 12 min) were found. With 6 of these transitions coincidence spectra were measured. The results of these experiments are summarized in table 2. A tentative level scheme was deduced. It should be confirmed by other coincidence measurements. The experiments are being continued.

\* Laboratorium voor Magnetisme, R.U.G.

\*\* Laboratorium voor Natuurkunde, groep II, R.U.G.



Ge1, Ge2 GeLi detectors, Pb screen  
 ZS1 ZS2 Zero Strobe timing (fast)  
 FC1 Fast Coincidence (100 ns)  
 A1, A2 Main amplifiers  
 TSCA1 Timing single channel analyzer "on the photopeak"  
 TSCA2 " " " " "on the compton"  
 DL1-DL4 Delays, LI Logic Inverter, AD Adder  
 C2-C3 Energy selecting coincidences (200-300 ns)  
 G Linear gate

FIG.6.

Block diagram of the gamma-gamma coincidence apparatus

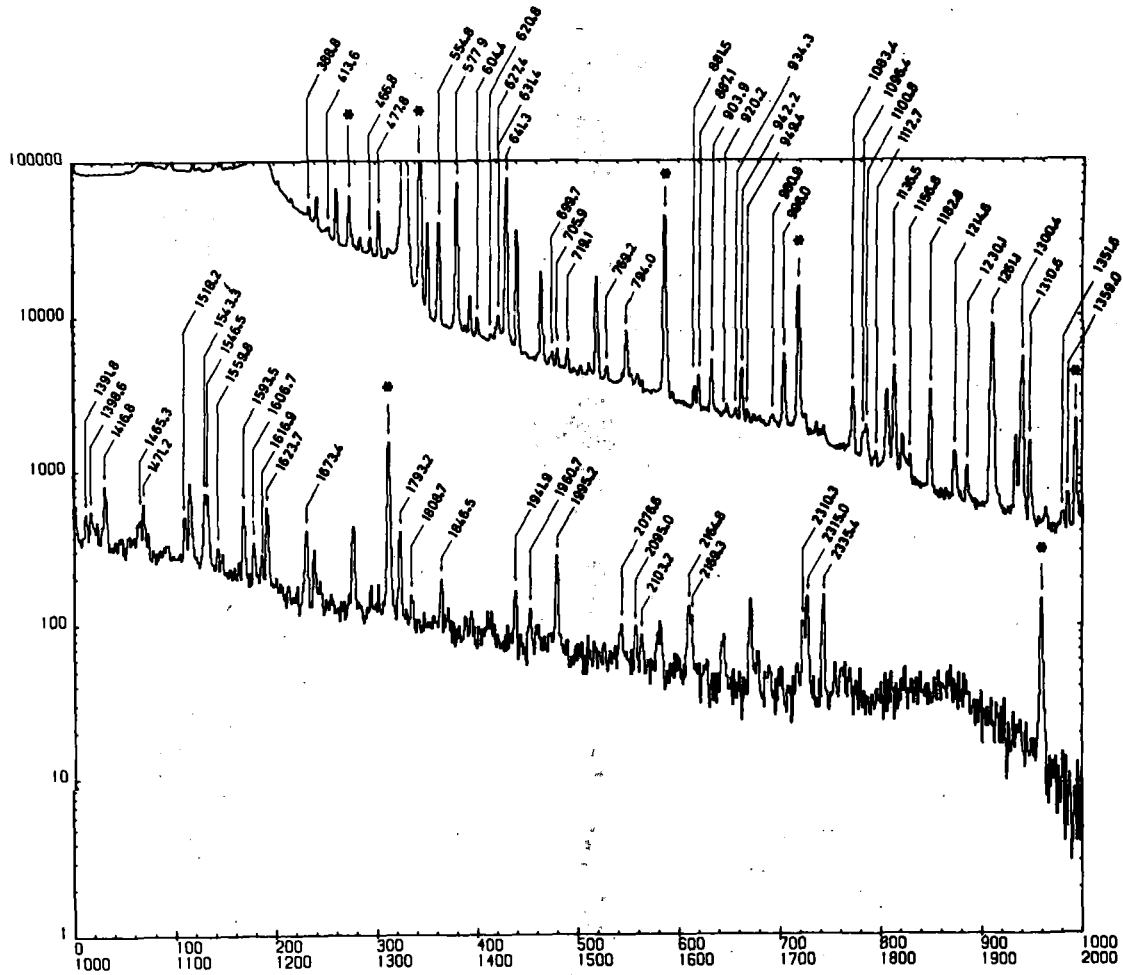


FIG. 7.

Singles-spectrum from  $^{147}\text{Pr}$ , in the high energy region

Table 2

Summary of coincidences measured in  $^{147}\text{Pr}$

Window on E (keV)	Observed coincident gamma energies (KeV)				
78.0	86.6	186.8	328.9	335.7	388.8
	554.8	577.9	641.3		
86.6	100.2	127.9	249.1	328.9	554.8
	577.9				
127.9	86.6	186.8	328.9	335.7	388.8
	554.8	577.9	641.3		
314.6	477.8	627.4	794.0	949.4	996.0
	1083.4				
328.9	78.0	127.9	249.1	335.7	413.6
577.9	78.0	86.6	127.9		

#### 4.3 Stabilization of the positron annihilation measuring chains

a) Stabilization of the S-factor measurements:

The S-factor (=lineform factor) measurements are now equipped with two-point stabilization. For the zero stabilization a  $^{203}\text{Hg}$  source is used. For the gain stabilization an Ortec precision pulser provides the necessary stabilization peak. Actually the stability is 0.5 channel on 1000 over a period of 1 week. Even better stability could be achieved by replacing the  $^{203}\text{Hg}$  source with a second precision pulser. Then the count rate will be better under control, the position of the stabilization peaks can be chosen more favourably in the spectrum and the stabilization is more efficient on a narrow pulser peak.

b) Stabilization of the positron lifetime equipment.

The positron lifetime chain also has two-point stabilization.

By means of a double avalanche pulser, two prompt coincidence peaks are generated, one before and one after the actual lifetime spectrum. They are used respectively for zero and gain stabilization. The necessary signals are introduced into the chain on TPO level, so that the whole chain (with the exception of the photomultipliers) is included in the stabilization process. Temperature stabilization remains necessary for the photomultipliers.

This stabilization system will be published as soon as some complementary experiments have been done. In the last 7 months it has not been possible to perform these and other lifetime measurements due to successive defects of the photomultipliers and photomultiplierbases.

#### 4.4. Positron annihilation in KDP ( $=\text{KH}_2\text{PO}_4$ )

KDP is a ferroelectric material with a large internal electric field. In order to study the influence of this internal field on a positron, S-factors and positron lifetimes were measured at different temperatures, down to below the Curie point (123°K). All measurements gave the same results within the measuring accuracy, so that no conclusions could be drawn.

#### 4.5. S-factor measurements in glass

As a complement to our earlier positron lifetime measurements, S-factors (=annihilation lineshapefactors) were measured in a set of transition-metal ion-doped  $\text{CaO.P}_2\text{O}_5$  glasses. These glasses, mentioned in table 2, were prepared by Dr.A.Paul of the Department of Glass Technology of the University of Sheffield, in cooperation with whom the results of the lifetime measurements were interpreted in terms of a positronium quenching model.

Fig.8 shows the results of the S-factor measurements in function of the intensity of the longest lifetime component. The quenching model alone is insufficient to explain all the aspects of these new data. A combination of "quenching" and "inhibition" model is more satisfactory.

A publication is being prepared.

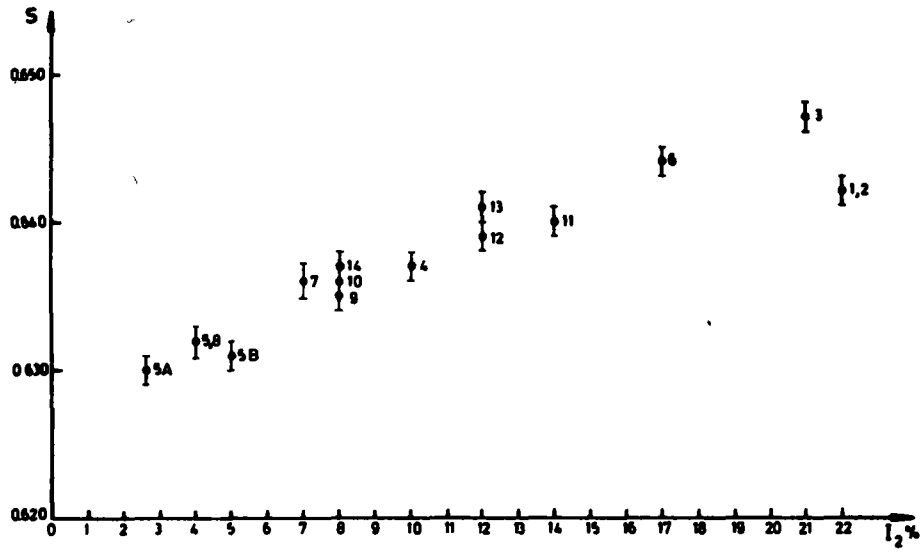


FIG. 8.

S-factor as a function of the intensity of the longest lifetime component, for the various glasses

Table 2

CaO.P<sub>2</sub>O<sub>5</sub> glasses containing various transition-metal ion impurities

Glass number	Concentration of the impurity ion (gm ion per cc x 10 <sup>5</sup> )	Glass number	Concentration of the impurity ion (gm ion per cc x 10 <sup>5</sup> )
1	base glass (no imp.)	7	Cu(I) =37.312 Cu(II) = 0.088
2	Ce(II) =0.714 Ce(IV) =1.070	8	V(total) =33.565 Ce(total) = 8.919
3	Ce(III) =3.570 Ce(IV) =5350	9	Cu(total) =38.401 Ce(total) = 8.919
4	V(V) =0.671 V(IV) =4.697 V(III) =0.671	10	Ti(IV) =33.565
5	V(V) =3.355 V(IV) =23.485 V(III) = 3.355	11	Ni(II) =33.565
6	Mn(II) =14.735	12	Cr(III) =33.565
		13	Co(II) =33.565
		14	Fe(II) =10.070 Fe(III) =23.495



4.6. Preliminary experiments and design of a set-up for the measurement of windowed angular correlations of annihilation radiation.

The new method is a compromise between S-factor measurements with Ge(Li) detectors and angular correlation measurements. The basic idea of the new technique is to measure coincidences between a NaI scintillator on one side, and three plastic scintillators on the other side. The three plastic scintillators define each a geometrical window on the angular correlation curve. Preliminary measurements with an experimental set-up proved that this type of experiments are possible and have sufficient yield with the commercially available positron sources. A permanent set-up was designed and drawn and is now being built.

4.7. Study of short living isomeric states (milli- and microsec) between the accelerator pulses

The study of isomeric states between the bursts of the LINAC is continued. The apparatus has been improved by the use of a new linear measuring chain with a DC coupled Ge(Li) detector. The dead-time after each activation is reduced by using a special preamplifier (60V dynamic range).

The measurements of isomeric states produced by photonuclear reactions on natural Tl ( $^{201m}\text{Tl}$ ,  $^{202m}\text{Tl}$ ,  $^{204m}\text{Tl}$ ) were summarized in a contribution to the "International Conference on Nuclear Structure and Spectroscopy" (Amsterdam 9 - 13 sept 1974).

Fig.9 shows the decay of the 588.0 keV line ( $T_{1/2}=2.1$  ms) in  $^{201m}\text{Tl}$ , near the 595.9 keV  $^{74}\text{Ge}$  line (measured in 175  $\mu\text{s}$  intervals). In the  $^{201m}\text{Tl}$  case, shape isomerism is proposed based on calculations of the total potential energy surfaces and calculations of the lifetimes in a Nilsson model (publication in Nuclear Physics is in press).

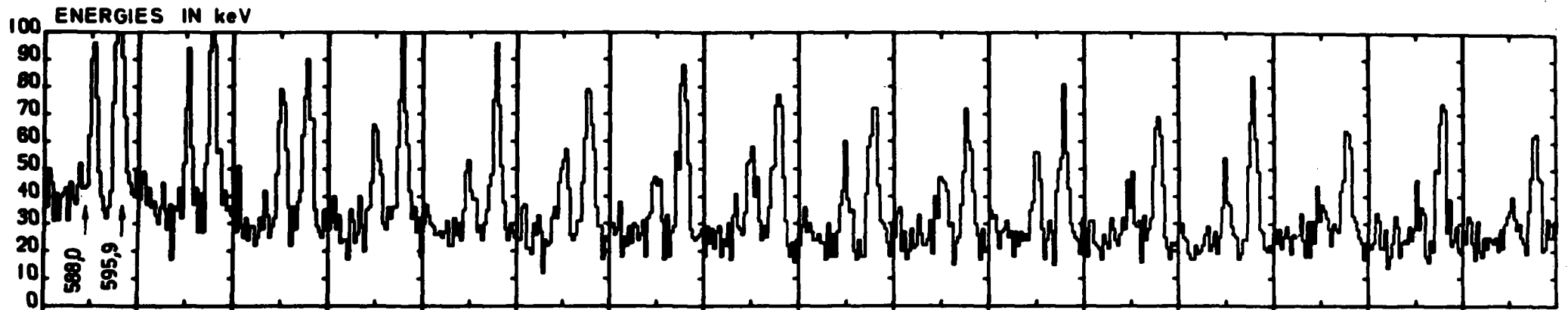


FIG. 9.

Illustration of the decay of the 588.0 keV line ( $T_{1/2}=2.1$  ms) in  $^{201m}\text{Tl}$ .

DOSIMETRY(G. Eggermont, A.Janssens, R.Jacobs\*, G.Thielens,\* E.Cottens,\*\*  
O.Segaert\*,\*\*)

### 5.1. Cavity theory and related experiments

Measuring devices used in dosimetry may be regarded as cavities with a physical composition different from the surrounding medium, for which a correction factor (stopping power ratio) has to be applied. The dosimetry group has developed two complementary models to calculate stopping power ratios. The first model is based upon the calculation of the electron spectrum within the cavity. The model converges to the Spencer-Attix model for small cavities. For large cavities it is erroneous, due to the use of an average for the spectrum of degraded energies. The second model is based upon the calculation of the energy fluence at the interface. For small cavities sizes (as compared to the electron range), this model is not relevant since the inward and outward fluence cancel. Above a cut-off energy the former model is applied.

A computer programme calculates the stopping power ratio as a function of cavity dimension, using both backscattercoefficient and energy as parameters. It applies the theory to experimental situations. Scarce Monte-Carlo data and our TLD experiments yield experimental support for the cavity theory. To investigate the validity of the cavity theory over the entire region of interest, an accurate experimental test is planned. For this purpose the construction of a high-pressure ionisation chamber with different high-Z wall materials is studied. The experiment will be performed with X-rays of 100 to 200 keV<sub>eff</sub>. The design is such to obtain a compromise between maximum sensitivity and minimum systematic error.

### 5.2. Thermoluminescent dosimetry and applied cavity theory

The results of these investigations are laid down in a doctorate thesis, which includes :

- The construction of TLD measuring equipment and experimental results of the energy response of TLD to X-, $\gamma$ -, and electron beams.
- A discussion of earlier cavity theories and a modification of the general theory of Burlin.
- A comparison of cavity theory calculations with experimental results for TLD and cellophane doseimeters.
- A survey of the installed X-, $\gamma$ -, and electron calibration facilities and measurements.

-----  
\* Centrale Dienst voor Fysische Controle - R.U.G.

\*\* Laboratorium voor Natuurkunde (groep II)

### 5.3. Calorimetry

For absolute electron dosimetry at the linac facility an introductory study is made of absorbed dose calorimetry. Carbon construction parts for the planned NBS type calorimeter are made by Gravines, U.K.

### 5.4. Beam calibrations

1) The project of absolute X-ray dosimetry with a free-air ionisation chamber has been postponed due to failing of the Victoreen electronics, at present returned to the U.S.A. Victoreen laboratory.

Due to unfavourable experience with this Victoreen ionisation chamber equipment, the possible errors on the energy-response curves and the lack of a confirmed guarantee by the NBS-authorities with reference to the Victoreen standard, we decided to work out a large calibration programme for ionisation chambers and Fricke solutions. The calibration measurements with  $^{60}\text{Co}$  and 7 X-ray qualities will be performed in the Standard Laboratory of The Netherlands in Bilthoven. A special calibration room is foreseen in the building of the "Centrale Dienst voor Fysische Controle", in construction at present.

#### 2) Monitoring

##### a. 200 kV X-ray machine

The transmission ionisation chamber build in the tube-housing, connected to a home-made integrator, improved the reproducibility.

##### b. 50 kV X-ray machine

A small transmission ionisation chamber is designed.

The construction will be performed by the Physikalische-Technische Werkstätte (PTW), Germany. The electronic equipment will be realised in our laboratory.

#### 3) Linear accelerator

Up to now electron irradiations were monitored by a secondary emission monitor in front of the exit window. The need for stabilised intensity and constant broad beam geometry for the divergent beam requires a control of multiple beam characteristics. A complex transmission chamber has been designed for this purpose and will be installed in front of the phantom. It will also facilitate machine operation and give information on beam intensity, homogeneity and alignment. The chamber consists of segmented aluminised plastic foils as collecting electrodes; it will be constructed by PTW.

### 5.5. Plastic film dosimeters.

Previous research has shown that cellophane films dyed with methyl green, chlorophenol red and malachite green present a radiation sensitive absorption spectrum.

The optical extinction change at the absorption maximum is under certain conditions proportional to the absorbed dose. The radiolytic irreversible degradation of these dyes in solid solution is highly dependent on the presence of sensitizing products.

The extinction change as a result of the properties of dye and sensitizer are studied in more detail.

A precise knowledge of the concentration of both components was necessary to obtain reproducible results and to select the systems with optimal properties. In all the experiments the irradiation sources were a 50 KV X-ray machine, a  $^{60}\text{Co}$  gamma source and the 20 MeV linear electron accelerator. For the most stable systems, doses between 0.1 and 5 Mrad can be determined with a precision of 10%.

### 5.6 Atmospheric pollution of $^{85}\text{Kr}$

A study is done on the atmospheric pollution of the fission fragment  $^{85}\text{Kr}$  released in nuclear energy production. A prognosis of the air concentration and population dose was made up to the next century and compared to other publications. The possibilities of periodical Kr-85 air concentration measurements are studied.

6. THEORETICAL STUDIES (K.Heyde, M.Waroquier and H.Vincx)

6.1 Microscopic structure from (p,p') scattering through isobaric analog resonances (K.Heyde, M.Waroquier, H.Vincx, P.J.Brussaard\*)

During the last year, most of the work performed concerning the generalized neutron particle-hole model in an extended unified-model description has been ended and written up for publication in Nuclear Physics. New extensions, however, have been incorporated and are being studied:

- i) interaction with purely collective degrees of freedom, such as the one-quadrupole one-octupole quintuplet in the doubly-even  $N=82$  nuclei. This extension leads to a substantially better agreement with experiment as well in energy spectra as in angular distributions of inelastically scattered protons. A more specific application has been made in the case of  $^{142}\text{Nd}$ , which is now accepted for publication in Nuclear Physics.
- ii) We have started to study the connection between the spectroscopic factors determined in proton inelastic scattering through isobaric analog resonances and the determination of coefficients of parentage on the one-quadrupole  $2^+$  level. In earlier types of analysis, interference effects have clearly been overlooked, especially when the neutron degrees of freedom do not form a closed shell. Theoretical research concerning this point is being done as well as application to the case of doubly-even Sn isotopes. This point of research continues into 1975.

6.2. Study of the generator coordinate method (H.Vincx)

A study of the generator coordinate method has been performed. To obtain a better knowledge of the method, we participated in the "Generator coordinate seminar" from 16-28 september 1974, organised by Dr.P.Van Leuven and Dr.M. Bouten. As a result of the seminar it seems that application of the method

-----

\* Fysisch Laboratorium, Sorbonnelaan, 4, Utrecht, Nederland

to heavy nuclei can lead to very complicated numerical calculations. A study of the nuclear fission phenomena with the use of the generator coordinate method therefore seems to be too complicated in order to describe the coupling between different excited states.

6.3. Strutinsky type of calculations for odd-proton Tl and In isotopes

(H.Vincx, K.Heyde, in collaboration with J.Uyttenhove\*)

In order to understand measurements of the energy spectra and nuclear lifetimes in the microsecond region as performed by J.Uyttenhove in  $^{201}\text{Tl}$ , we have performed Strutinsky-type calculations for this nucleus. As a result, we observed that by deforming to a slightly oblate shape, a low-lying  $9/2^-$  level can result by thus lowering its excitation energy as compared with the spherical shape. These calculations are in good agreement with the experimental situation. Also lifetime calculations have been performed with pairing taken into account. Analogous calculations have been performed for  $^{115}\text{In}$  where it is shown that by deforming to the prolate shape, a low-lying  $1/2^+$  intrinsic level can be reached and act as the band head for a rotational band. Calculations of retarded E1 transitions, magnetic dipole moments and electric quadrupole moments all support this interpretation.

As a general conclusion we can say that very near to closed shell configuration, coexistence between spherical and deformed states can occur. This phenomenon will also be studied in the  $N=83$ ,  $N=81$  and  $Z=51$  nuclei. Part of this research resulted in a contribution to the Amsterdam conference and an article to be published in Nuclear Physics.

---

\* Laboratorium voor Natuurkunde, groep II, R.U.G.

6.4. Phase conventions for electromagnetic multipole operators.

(M.Waroquier + K.Heyde)

The aim of this work, which has been finished in the beginning of the year 1974, was to draw the attention to the precise formulation of the electromagnetic multipole moments and transition operators.

Their precise structure fixes their transformations under some operations, as time reversal and Hermitian conjugation, and in this way it plays an important role in the properties of their matrix elements. Another point of discussion was the consistent use of a well-defined phase-convention for the angular momentum eigenfunctions and their role in the development of the B.C.S.-formalism.

This review paper is to be published.



PUBLICATIONS BY MEMBERS OF THE LABORATORY (PUBLISHED 1974)

1. Connection between LRA to binary fission cross-section ratio for resonance and Thermal neutron induced fission in  $^{239}\text{Pu}$  and resonance spins.  
A.J. Deruytter, C. Wagemans and W. Becker  
Physics and Chemistry of Fission, IAEA, vol II, p.417-434 (1974).
2. Comparison of the fission characteristics of thermal neutron induced fission of  $^{239}\text{Pu}$  and the spontaneous fission of  $^{240}\text{Pu}$ .  
A.J. Deruytter and G. Wegener-Penning  
Physics and Chemistry of Fission, IAEA, vol II, p.51-63 (1974).
3. Measurement and Normalization of the relative  $^{233}\text{U}$  fission cross-section in the low resonance region.  
A.J. Deruytter and C. Wagemans  
Nucl. Sc. Eng. 54 423-431 (1974) .
4. Redetermination of the half-life of  $^{235}\text{U}$  for  $\alpha$ -emission.  
A.J. Deruytter and G. Wegener-Penning  
Phys. Rev. C10 383-385 (1974).
5. Ratio of the ternary-to-binary fission cross-sections induced by thermal and resonance neutrons in  $^{241}\text{Pu}$ .  
C. Wagemans and A.J. Deruytter  
Nucl. Phys. A234 285-300 (1974).
6. Summary of the consultants meeting on the 2200m/s fission and capture cross-sections of the common fissile nuclides.  
A.J. Deruytter  
Neutron standard reference data, IAEA, p.315-318 (1974).
7. Connections between and common problems for low energy (eV-region) and high-energy (keV to MeV region) precision measurements.  
A.J. Deruytter  
Neutron standard reference data, IAEA, p.341-348 (1974).
8. The Westcott- $g_f$  factor for  $^{239}\text{Pu}$  and its temperature dependence,  
C. Wagemans and A.J. Deruytter  
Ann. Nucl. Sc. Eng. 1 11 (1974).

9. The accurate fission cross-section of  $^{239}\text{Pu}$  from 0.005 eV to 0.1 eV and its reference value at 2200 m/s.  
A.J. Deruytter and W. Becker  
Ann. Nucl. Sc. Eng. 1 311-322 (1974).
  
10. Research at CBNM to improve the accuracy of neutron standard cross-sections.  
A.J. Deruytter  
Proceedings of the All Union Neutron Physics Conference, Kiev, Vol 4, p.26-41 (1974).
  
11. Present and planned work on neutron standard reference data at the CBNM, Euratom.  
A.J. Deruytter and H. Liskien  
Neutron Standard reference data, IAEA, p.11-13 (1974).
  
12. Structure in the giant resonance of  $^{55}\text{Mn}$ .  
R. Carchon, J. Devos, R. Van de Vyver, C. Van Deynse and H. Ferdinande  
Nucl. Phys. A223 416 (1974).
  
13. A data sorting and processing system for photoneutron research.  
H. Tourwé, J. Uyttenhove, R. Van de Vyver  
Nucl. Instr. & Meth. 118 279 (1974).
  
14. Structure in the  $^{31}\text{P}$  photoneutron cross section.  
J. Devos, R. Carchon, H. Ferdinande and R. Van de Vyver  
Z. Physik, 271 391-397 (1974).
  
15. Photoproton angular distribution from  $^{12}\text{C}$ .  
R. Carchon, J. Devos, H. Ferdinande, R. Van de Vyver and E. Van Camp  
Proceedings International Conference Nuclear Structure and Spectroscopy (Amsterdam, Sept. 9-13, 1974) Vol I, p.207 (1974).
  
16. A study on the decay of  $^{81}\text{As}$   
M. C. Chacko, H. Heyde, L. Dorikens-Vanpraet and M. Dorikens  
Z. Physik 266 337 (1974).
  
17. The decay of  $^{75}\text{Ga}$  to levels in  $^{75}\text{Ge}$ .  
M. C. Chacko, L. Dorikens-Vanpraet and M. Dorikens  
Z. Physik 267 359 (1974).

18. Positron Lifetime Measurements in n- and p-type Silicon.  
M. Dorikens, C. Dauwe and L. Dorikens-Vanpraet  
Appl. Phys. 4 271 (1974).
  
19. Analysis of double decay spectra by the SIMPLEX stepping method.  
C. Dauwe, M. Dorikens and L. Dorikens-Vanpraet  
Appl. Phys. 5 45 (1974).
  
20. Positron lifetimes and Lineshape factors in deformed Copper.  
C. Dauwe, M. Dorikens, L. Dorikens-Vanpraet and D. Segers  
Appl. Phys. 5 117 (1974).
  
21. Ortho-Para positronium quenching by transition-metal ions in glass  
A. Paul, R. M. Singru, C. Dauwe, L. Dorikens-Vanpraet and M. Dorikens  
J. Phys. C7 2180 (1974).
  
22. Positron lifetimes in Lithium disilicate glass with different degrees  
of crystallisation  
P. F. James, A. Paul, R. M. Singru, C. Dauwe, L. Dorikens-Vanpraet and M.  
Dorikens  
Phys. Stat. Sol. (B) (1974).
  
23. Caviteitscorrecties in dosimetrie v. X-,  $\gamma$ - en elektronen bundels en de  
invloed op het energieverloop van diverse dosimeters.  
A. Janssens, G. Eggermont, R. Jacobs, G. Thielens and O. Segaert  
Belgisch Tijdschrift voor Radiologie, 56 457-466 (1973).
  
24. Spectrum perturbations and energy deposition models for stopping  
power ratio calculations in general cavity theory.  
A. Janssens, G. Eggermont, R. Jacobs and G. Thielens  
Phys. Med. Biol. 19 619-630 (1974).
  
25. A discussion on the validity of cavity theories and a comparison  
with experimental results.  
G. Eggermont, A. Janssens, R. Jacobs and G. Thielens  
Proceedings of the Fourth Symposium on Microdosimetry, (Verbania  
Pallanza, October 1973), Eur 5122, Vol II, p. 733-754 (1974).
  
26. Nuclear structure of the heavy N=82 isotones  $^{144}\text{Sm}$  and  $^{146}\text{Gd}$   
M. Warquier and K. Heyde  
Z. Physik 268 11-18 (1974).
  
27. Comments on the effective M2 and E3 transition probabilities for the

$1h_{11/2}$  single-quasi proton states.

M.Waroquier and K.Heyde  
Phys.Rev. C10 1548-1550 (1974).

28. Generalized neutron particle-hole states in an extended unified-model.  
K.Heyde, M.Waroquier, H.Vincx and P.J.Brussaard  
Nucl.Phys. A234 216-252 (1974).

PUBLICATIONS IN PRINT

1. Measurement and normalization of the relative neutron induced fission cross-section of  $^{241}\text{Pu}$  in the low resonance region.  
C.Wagemans and A.J.Deruytter  
Ann.Nucl.Sc.Eng.
2. Possible evidence for microsecond shape isomerism in Tl isotopes  
J.Uyttenhove, K.Heyde, H.Vincx and M.Waroquier  
Nucl.Phys.A
3. Note on "Isotropic incident flux in Monte Carlo calculations"  
A.Janssens  
Health Physics
4. Coupling between collective and GNP-H excitations: application to  $^{142}\text{Nd}$   
K.Heyde, M.Waroquier and H.Vincx  
Nucl.Phys.A

CONFERENCE OR SYMPOSIA-CONTRIBUTIONS

-----

1. Algemene wetenschappelijke vergadering B.N.V.-Mons (6-7.6.74)  
Studie van massa- en ladingsdistributies bij fotofissie van  $^{238}\text{U}$   
H.Thierens, D.De Frenne, E.Jacobs and A.De Clercq.
  
2. Algemene wetenschappelijke vergadering B.N.V.-Mons (6-7.6.74)  
Studie van de massa en kinetische energiedistributies bij de fotofissie van  $^{238}\text{U}$   
A.De Clercq, E.Jacobs, D.De Frenne and H.Thierens.
  
3. Algemene wetenschappelijke vergadering B.N.V.-Mons (6-7.6.74)  
Verhouding van de ternaire tot de binaire fissie werkzame doorsneden door thermische en resonantie-neutronen in  $^{241}\text{Pu}$  geïnduceerd  
C.Wagemans and A.J.Deruytter.
  
4. Journées d'Etudes sur la Fission (Cadarache, France, October 1974)  
Expériences de photofission au laboratoire de Physique Nucléaire à Gand  
E.Jacobs, D.De Frenne, A.De Clercq, H.Thierens, P.D.Hondt, A.Deruytter.
  
5. Conf.on Nuclear Structure and High Energy Physics (Glasgow, U.K., March 27-29, 1974) Contribution N35  
Structure in the giant resonance of  $^{31}\text{P}$   
J.Devos, R.Carchon, H.Ferdinande & R.Van de Vyver.
  
6. Algemene wetenschappelijke vergadering B.N.V.(Mons, 6-7 juni 1974) N.P. -9  
Photoproton energy spectra and angular distributions from  $^{12}\text{C}$   
R.Carchon, H.Ferdinande, R.Van de Vyver, J.Devos & E.Van Camp.
  
7. Algemene wetenschappelijke vergadering B.N.V.(Mons, 6-7 juni 1974) N.P.-10  
Structure in het photoneutron cross section of  $^{31}\text{P}$   
H.Ferdinande, J.Devos, R.Carchon & R.Van de Vyver.
  
8. Algemene wetenschappelijke vergadering B.N.V.(Mons, 6-7 juni 1974) N.P.-11  
A photoneutron spectrometer using an organic scintillator  
J.Devos, R.Van de Vyver, H.Ferdinande & R.Carchon.
  
9. Int.Conf.Nuclear Structure and Spectroscopy (Amsterdam, September 9-13, 1974)  
Div.Electron Scattering and Photonuclear Reactions  
Photoproton angular distribution from  $^{12}\text{C}$   
R.Carchon, J.Devos, H.Ferdinande, R.Van de Vyver & E.Van Camp.

10. International Conference on Nuclear Structure and Spectroscopy (Amsterdam 9-13 sept '74)  
Evidence for microsecond shape isomerism in Tl isotopes  
J.Uyttenhove, K.Heyde, H.Vincx and M.Waroquier  
Proceedings Vol.1 p.115 (1974).
11. Algemene Wetenschappelijke Vergadering - Mons (6-6-1974)  
Positronannihilatie als methode voor het onderzoek van Nucleatie en  
Cristallisatie in glas  
C.Dauwe, L.Dorikens-Vanpraet and M.Dorikens.
12. Vosbergenkonferentie (13-16 mei 1974) Vlieland (Nederland)  
Invited talk : Nuclear structure information obtained from proton  
inelastic scattering through isobaric analog resonances  
K.Heyde.
13. International conference on Nuclear Structure and Spectroscopy (Amsterdam 9-13 september 1974)  
Invited talk: Weak coupling, Proceedings of the conference, (eds.H.P.Blok  
and A.E.L.Dieperink) Vol.2, 186-211 (1974).  
K.Heyde.
14. Topical conference on problems of vibrational nuclei, Zagreb, (24-27 sep-  
tember 1974)  
Generalized neutron p-h excitations in a unified model description  
K.Heyde, M.Waroquier and H.Vincx.
15. Topical conference on problems of vibrational nuclei, Zagreb, (24-27 september 1974)  
Interaction between collective and generalized neutron p-h states in the  
doubly-even N=82 nuclei  
M.Waroquier, K.Heyde and H.Vincx.

DOCTORAL THESES AT THE RIJKSUNIVERSITEIT GENT (1974)

1.C.Dauwe

Positronannihilatie in Metalen

2.G.Eggermont

Studie van de geabsorbeerde dosis in caviteiten met behulp van termoluminescente dosimeters en gecalibreerde X-, $\gamma$ -en elektronenbundels



Instituut voor Kern- en Stralingsfysika  
Katholieke Universiteit Leuven  
Celestijnenlaan 200D  
3030 HEVERLEE  
Belgium

Work published in 1974.



1 9 7 4 .

P U B L I K A T I E S .

- 74-1 J.P. LAFAUT. Bepaling van de mengverhouding, E2/M1, van de 123 keV gammastraling van  $^{57}\text{Fe}$  met behulp van de Gamma-gamma Mössbauer Hoekkorrelatie. *Verhandelingen van de Koninklijke Academie voor Wetenschappen, Letteren en Schone Kunsten van België. Klasse der Wetenschappen*, XXXVI, (1974), nr. 131.
- 2 H. PATTYN, G. DUMONT, R. COUSSEMENT, R.E. SILVERANS, E. SCHOETERS, L. VANNESTE. The Hyperfine Field of Xenon Nuclei at lattice sites in Iron. *Journal de Physique*, (1974), p. C1-19.
- 3 F. NAMAVAR, M. ROTS, H. PATTYN, G. DUMONT, R. COUSSEMENT. A Study of the Hyperfine Field of Cesium in Nickel and Iron. *Journal de Physique*, (1974), p. C1-7.
- 4 M. ROTS, R. COUSSEMENT. Time Differential pac on the first Excited State in  $^{129}\text{I}$ . *Journal de Physique*, 1974, p. C1-35.
- 5 G. LANGOUCHE, R. COUSSEMENT, M. VAN ROSSUM, K.P. SCHMIDT. Study of the Quadrupole Interaction of  $^{125}\text{Te}$  and  $^{129}\text{I}$  in Te single crystals by Mössbauer Spectroscopy. *Journal de Physique*, (1974), p. C1-55.
- 6 R. COUSSEMENT, G. DUMONT, G. LANGOUCHE, H. PATTYN, M. ROTS, K.P. SCHMIDT, M. VAN ROSSUM. Implantation of  $^{129\text{m}}\text{Te}$  in Fe and Ni foils and Determination of the Hyperfine Fields. *Journal de Physique*, (1974), p. C1-37.
- 7 K.P. SCHMIDT, M. VAN ROSSUM, A. MEYKENS, G. LANGOUCHE, R. COUSSEMENT. A Mössbauer Study on Pottery of Tureng Tepe II. *Journal de Physique*, (1974), p. C1-105.
- 8 G. LANGOUCHE, M. VAN ROSSUM, K.P. SCHMIDT, R. COUSSEMENT. Quadrupole Interaction of  $^{125}\text{Te}$  and  $^{129}\text{I}$  in polycrystalline Te and in Te single crystals. *Physical Review B*, Vol. 9, nr. 3, (1974).

- 9 R.E. SILVERANS, R. COUSSEMENT, H. PATTYN, E. SCHOETERS, L. VANNESTE. Nuclear Orientation Measurements of the Magnetic Dipole Moments of the  $11/2^-$  Isomeric States in  $^{129}\text{Xe}$ ,  $^{131}\text{Xe}$  and  $^{133}\text{Xe}$ . *Z. Physik* 267, 145-147 (1974).
- 10 J. DE RAEDT, M. ROTS, H. VAN DE VOORDE. Angular Correlation study of  $^{129}\text{I}$  populated in the decay of  $^{129}\text{Te}$ . *Physical Review C*, (1974) Vol. 9, nr. 6.
- 11 G. MAREST, R. HAROUTUNIAN, I. BERKES, M. MEYER. Electromagnetic Properties of low-lying levels of  $^{129}\text{Xe}$ . *Physical Review C*, (1974) Vol. 10, nr. 1.
- 12 M. ROTS, H. VAN DE VOORDE, H. OOMS, F. NAMAVAR, R. COUSSEMENT, J. DE RAEDT. The Angular Correlation of the 459.7 - 27.7 keV  $\gamma$ - $\gamma$ -cascade in  $^{129}\text{I}$  and its Use for a TDPAC. *Z. Physik* 270, 51-54 (1974).
- 13 G. LANGOUCHE, M. VAN ROSSUM, P. BOOLCHAND, A. MEYKENS, R. COUSSEMENT. Observation of a small quadrupole Interaction in  $^{129}\text{IFe}$  Mössbauer Spectra. *Physics Letters, Volume 50A, no. 1, (1974), North-Holland Publishing Company, Amsterdam.*
- 14 R. COUSSEMENT, M. ROTS, G. LANGOUCHE, K.P. SCHMIDT, M. VAN ROSSUM, A. MEYKENS. The Hyperfine Asymmetry Effect. *Gordon and Breach Science Publishers Ltd. (1974), Vol. 6, p. 259-267.*
- 15 G. LHERSONNEAU, J. DE RAEDT, H. VAN DE VOORDE, H. OOMS, M. ROTS, F. NAMAVAR, R. HAROUTUNIAN. Angular Correlation Study of  $^{131}\text{I}$ . *Proceedings. Vol. 1, Contributed Papers. International Conference on Nuclear Structure and Spectroscopy, Amsterdam, september 9-13, 1974.*
- 16 H. HÜBEL, K. FREITAG, E. SCHOETERS, R.E. SILVERANS, L. VANNESTE. Magnetic Moments of the  $I = 23/2^-$  Isomers in  $^{177}\text{Lu}$  and the  $I = 25/2^-$  Isomer in  $^{179}\text{Hf}$ . *Proceedings, Vol. 1, Contributed Papers. International Conference on Nuclear Structure and Spectroscopy. Amsterdam, September 9-13, 1974.*

- 17 K.P. SCHMIDT, M. HUYSE, J. DE RAEDT, G. LANGOUCHE, M. VAN ROSSUM, R. COUSSEMENT. A Computerized Piezoelectric Mössbauer Spectrometer. *Nuclear Instruments and Methods* 120 (1974) 287-291.
- 18 M. VAN ROSSUM, G. LANGOUCHE, H. PATTYN, G. DUMONT, J. ODEURS, A. MEYKENS, P. BOOLCHAND, R. COUSSEMENT. Study of the Magnetic Interaction at  $^{129m}\text{Xe}$  Implanted in Iron. *Journal de Physique*, (1974), p. C6-301.
- 19 R. BOUCHEZ, J.M.D. COEY, R. COUSSEMENT, K.P. SCHMIDT, M. VAN ROSSUM, J. APRAHAMIAN and J. DESHAYES. Mössbauer Study of Firing Conditions used in the Manufacture of the Grey and Red Ware of Tureng-Tepe. *Journal de Physique*, (1974), p. C6-541.

Instituut voor Nucleaire Wetenschappen  
Rijksuniversiteit Gent  
Proeftuinstraat 86  
9000 GENT  
Belgium

Work published in 1974.

1. The total average cross section for the reactions  $^{58}\text{Ni}(n,np)^{57}\text{Co}$   
 $^{58}\text{Ni}(n,pn)^{57}\text{Co}$  and  $^{58}\text{Ni}(n,d)^{57}\text{Co}$  in a fission type reactor  
spectrum.

A. BRUGGEMAN, W. MAENHOUT, J. HOSTE  
Radiochem. Radioanal. Letters, 18 (2), 1974, p 87.

2. A Compilation of Infinite Dilution Resonance Integrals, II.

R. VAN DER LINDEN, F. DE CORTE, J. HOSTE  
Journal of Radioanalyt. Chem., 20 (1974) 695 - 706.

Institut de Physique Nucléaire  
Physique Nucléaire Expérimentale  
Université de Liège  
SART-TILMAN  
4000 LIEGE 1  
Belgium.

Work published in 1974.

1. Application de la méthode de dosage à l'aide des réactions nucléaires pour l'évolution de l'interférence surface masse.  
G. WEBER, L. QUAGLIA.  
J. Radioanal. Chem. 17, (1973), 91-100.
2. Distributions angulaires de la réaction  ${}^7\text{Li}(d,\alpha){}^5\text{He}$  dans une gamme d'énergie incidente variant de 600 à 1250 keV.  
G. ROBAYE, J.M. DELBROUCK-HABARU, H.P. GARNIR, M. HUEZ.  
Bull. Soc. Roy. Sc. Liège n° 11-12, (1973), 598-607.
3. Dispersion en énergie de deutons lors de leur passage à travers la matière. Influence de l'état de surface.  
G. WEBER, L. QUAGLIA - Nucl. Instr. and Meth. 118 (1974), 573-581.
4. Etude des niveaux d'énergie de  ${}^{47}\text{Sc}$  au moyen de la réaction  ${}^{45}\text{Sc}(t,p){}^{47}\text{Sc}$ .  
J.M. DELBROUCK-HABARU, Y. BAUDINET-ROBINET, J. VERVIER.  
Nucl. Phys. A 227, (1974), 257-276.
5. Statistical analysis of intermediate structure.  
Y. BAUDINET-ROBINET, C. MAHAUX  
Phys. Rev. C, 9, (1974), 723-740.
6. Statistical analysis of correlations between partial widths of different channels.  
Y. BAUDINET-ROBINET  
Nucl. Phys. A 222, (1974), 525-536.
7. Bound-states of one nucleon in a Woods - Saxon well from a variational method.  
J.M. DELBROUCK-HABARU, D.M. DUBOIS  
Accepté pour publication : Computer Physics Communications.
8. Etude des différentes possibilités d'exploitation de la distribution en énergie des particules chargées issues de réactions nucléaires produites lors du bombardement de cibles épaisses par des ions légers de faible énergie (0,5 à 2.0 MeV).  
G. WEBER - Thèse de doctorat (1974) P.G.D.

INSTITUT DE PHYSIQUE CORPUSCULAIRE  
UNIVERSITE CATHOLIQUE DE LOUVAIN  
Chemin du Cyclotron 2  
1348 LOUVAIN-LA-NEUVE (Belgium)

ACTIVITIES IN 1974

PROG. 1. : ANALYSES D'EXPERIENCES AU CYCLOTRON D'HEVERLEE

- 1.1. Niveaux de spin élevés dans  $^{50}\text{Ni}$  et  $^{58}\text{Co}$   
Y. EL MASRI, J. VERVIER

PROG. 2. : EXPERIENCES AU CYCLOTRON ISOCHRONE

- 2.1. Mise en évidence d'un terme I.L dans la diffusion élastique de particules alpha  
M. BOSMAN, P. LELEUX, P. MACQ, J.P. MEULDERS, C. PIRART
- 2.2. Mise au point d'un faisceau de neutrons polarisés de 25 à 50 MeV
- 2.3. Mise au point d'un polarimètre à helium liquide pour neutrons  
M. BOSMAN, P. LELEUX, P. LIPNIK, P. MACQ, J.P. MEULDERS, C. PIRART, G. VALENDUC
- 2.4. Mesure de la dépolarisation de neutrons dans la diffusion élastique sur deutons
- 2.5. Production de faisceaux de neutrons rapides monocinétiques  
M. BOSMAN, P. LELEUX, P. LIPNIK, P. MACQ, J.P. MEULDERS, C. PIRART, G. VALENDUC
- 2.6. Etude de l'interaction faible par des mesures de corrélation directionnelle beta-gamma dans la triade  $A = 20$   
J. DEUTSCH, D. FAVART, R. PRIEELS, N. ROLIN, B. VAN OYSTAEYEN
- 2.7. Etude des réactions  $^{12}\text{C}(p, ^3\text{He})^{10}\text{B}$ ,  $^{12}\text{C}(p, ^4\text{He})^9\text{B}$  et  $^{12}\text{C}(p, t)^{10}\text{C}$  à 75 MeV  
T. DELBAR, G. GREGOIRE, J. LEGA, D. ROEGIERS, C. VERBEKE, P. WASTYN

PROG. 3. : EXPERIENCES A L'ACCELERATEUR DE VAN DE GRAAFF

- 3.1. Taux de désintégration beta du niveau isomérique  $0^-$  de  $^{16}\text{N}$   
L. PALFFY, J. DEUTSCH, L. GRENACS, J. LEHMANN
- 3.2. Résonance magnétique nucléaire sur le noyau  $^{12}\text{B}$  implanté dans divers milieux  
A. POSSOZ, D. FAVART, L. GRENACS, J. LEHMANN, D. MEDA, L. PALFFY, M. STEELS
- 3.3. Effets quadrupolaires dans la résonance magnétique nucléaire  
P. DESCHEPPER



- 3.4. Etude expérimentale de la symétrie-G dans la désintégration beta des noyaux miroirs A = 12

M. STEELS, L. GRENACS, J. LEHMANN, L. PALFFY, A. POSSOZ

PROG. 4. : COLLABORATIONS INTERNATIONALES

- 4.1. Mesure systématique de diffusion élastique d'alpha en fonction de E, Z et A  
R. CEULENEER, F. MICHEL, M. BOSMAN, J. LEGA, P. LELEUX, P. MACQ, J.P. MEULDERS, C. PIRART
- 4.2. Etude de la réaction  $^{12}\text{C}(p,px)$  à EP = 75 MeV
- 4.3. Hélicité du muon négatif dans la désintégration du pion  
T. DELBAR, G. GREGOIRE, J.LEGA, J.Y. GROSSIORD, A. GUICHARD, M. GUSAKOW, J.P. PIZZI
- 4.4. Mesure de la polarisation moyenne et longitudinale de  $^{12}\text{B}$  issue de la réaction  $\mu^- + ^{12}\text{C} \rightarrow \nu_{\mu} + ^{12}\text{B}$   
A. POSSOZ, D. FAVART, L. GRENACS, J. LEHMANN, P. MACQ, D. MEDA, L. PALFFY, M. STEELS, J. JULIEN, C. SAMOUR
- 4.5. Photoproduction de pions près du seuil sur  $\text{Li}^6$ ,  $\text{C}^{12}$  et  $\text{N}^{14}$
- 4.6. Photoproduction de pions neutres sur noyaux  
J. DEUTSCH, D. FAVART, R. PRIEELS, B. VAN OYSTAEYEN, G. AUDIT, N. DE BOTTON, J.L. FAURE, C. SCHUHL, G. TAMAS, C. TZARA
- 4.7. Continuation des travaux sur  $^{156}\text{Dy}$ ; Niveaux de spin élevé dans  $^{178}\text{Os}$ ,  $^{162}\text{Er}$ ,  $^{168}\text{Hf}$ , par les réactions ( $\text{N}^{14}$ ,  $5n\gamma$ ) et ( $p, 4n\gamma$ )  
Y. EL MASRI, J.M. FERTE, R. JANSSENS, C. MICHEL, P. MONSEU, J. STEYAERT, J. VERVIER

PROG. 5. : EXPERIENCES AU SYNCHROCYCLOTRON DU CERN

- 5.1. Mesure de précision du taux de capture partiel  $\text{Li}^6 - \text{He}^6$  de muons g.s.  
J. DEUTSCH, D. FAVART, P. LIPNIK, P. MACQ, R. PRIEELS
- 5.2. Recherche du mode d'absorption inconnu pion  $\rightarrow$  2 gamma de pions sur noyaux  
J. DEUTSCH, D. FAVART, P. LELEUX, P. LIPNIK, P. MACQ, R. PRIEELS

PROG. 6. : COLLABORATION PLURIDISCIPLINAIRE

- 6.1. Utilisation de la spectrométrie gamma à la localisation en profondeur d'organes  
G. HOFFELT, J. DEUTSCH, D. FAVART, R. PRIEELS
- 6.2. Production de radioisotopes à usage radio-diagnostique  
J. DEUTSCH, M. COGNEAU, R. GILLET
- 6.3. Mise au point d'un faisceau intense de neutrons rapides en vue d'applications radiobiologiques  
J.P. MEULDERS, P. LELEUX, P. MACQ, C. PIRART, G. VALENDUC, A. WAMBERSIE



C.E.N./S.C.K. MOL

Annual Progress Report 1974 in the Field  
of Nuclear Data.

---

Experimental Nuclear Physics

- Neutron Spectrometry p. 63
- Fission Physics and Chemistry p. 70
- Nuclear Spectroscopy p. 76

Theoretical Nuclear Physics p. 82

Integral Neutron Cross Section Measurements p. 85

Appendix I (Publications) p. 88

Appendix II (Colloquia, Seminars, Symposia) p. 91



NUCLEAR PHYSICS

1. EXPERIMENTAL NUCLEAR PHYSICS

1.1. NEUTRON SPECTROMETRY

(Joint SCK/CEN-CBNM(Euratom)-RUCA neutron cross-section programme. Contract Euratom-SCK/CEN N° 002/66/12 - PG PG B/Av. n° 2)

Total cross-section of  $^{226}\text{Ra}$

H. CEULEMANS

In the Progress Report for 1973 some preliminary data and conclusions were given concerning the neutron resonances in  $^{226}\text{Ra}$ . During the past year, the statistical accuracy of the data, especially the thick-sample data, was increased. This was done by repeatedly cycling the sample and a reference cadmium screen, in and out of the neutron beam at the Linac of CBNM. The stability of the apparatus was regularly checked and proved to be very good. The data taking extended over several months.

The Ra sample was positioned inside the shielded room surrounding the Linac target at a distance of 3 m from the neutron source. The detector ( $^3\text{He}$  gas scintillator) was at a distance of 29.73 m. The burst width was usually 20 ns and the detector timing channel width varied in four zones between 40 ns and 320 ns. The neutron energy was calibrated by using the Cd resonances.

The results obtained from the data with the  $5.9\text{E}-3$  atom/barn sample are shown in Table 1. Taking into account the resonance at 0.539 eV, which was analysed before, the experimental average spacing is :  $\bar{D} = 27.5$  eV.

It is likely that at higher energy, especially in the neighbourhood of the strong resonances, a few small ones with  $\Gamma_n^0 \approx 1 \text{ m eV}^{1/2}$  have been missed. The corrected value would then be  $\bar{D} \text{ (est.)} = 25 \pm 2.5 \text{ eV}$  which is substantially less than the previously obtained value of 42.3 eV and more in accordance with the systematics of comparable neighbouring nuclei ( $^{232}\text{Th}$ ,  $^{238}\text{U}$ ).

The neutron widths (see table I) were obtained by shape analysis of the resonances and assuming a gamma width of 30 meV as obtained from an accurate shape analysis of the 0.539 eV resonance. For the Doppler width a temperature of 290°K was assumed and for the (Gaussian) resolution width,  $\Delta E/E$  was 0.0016 for the fixed term. The choice of these constants influences the results to an extent which is different for each resonance. This influence has been checked however and the fluctuations quoted take into account variations of the constants within reasonable limits and the quality of the fit to the experimental data.

The neutron strength in this region is  $S_0 = (1.37 \pm 0.3)E^{-4}$  if a fractional fluctuation of (number of resonances) $^{-1/2}$  is assumed.

Table I

$E_o$ (eV) Value $\pm$ Fluct.	$\Gamma_n$ (meV)* Value $\pm$ Fluct.	$r_n^o$ (m.eV <sup>1/2</sup> ) Value $\pm$ Fluct.
24.25 $\pm$ 0.01	0.016 $\pm$ 0.002	0.0032 $\pm$ 0.0004
39.14 $\pm$ 0.01	0.07 $\pm$ 0.02	0.011 $\pm$ 0.003
39.72 $\pm$ 0.01	0.42 $\pm$ 0.04	0.085 $\pm$ 0.008
55.53 $\pm$ 0.01	6.4 $\pm$ 0.6	0.86 $\pm$ 0.08
80.45 $\pm$ 0.04	0.15 $\pm$ 0.02	0.017 $\pm$ 0.002
88.16 $\pm$ 0.02	27.0 $\pm$ 2.0	2.9 $\pm$ 0.2
154.6 $\pm$ 0.1	1.65 $\pm$ 0.3	0.13 $\pm$ 0.02
217.5 $\pm$ 0.1	2.4 $\pm$ 0.5	0.16 $\pm$ 0.03
236.5 $\pm$ 0.1	187. $\pm$ 20.	12.2 $\pm$ 1.3
261.9 $\pm$ 0.1	15. $\pm$ 3.	0.9 $\pm$ 0.2
290.3 $\pm$ 0.1	180. $\pm$ 20.	10.6 $\pm$ 1.2
328.0 $\pm$ 0.1	134. $\pm$ 15.	7.4 $\pm$ 0.8
346.6 $\pm$ 0.1	250. $\pm$ 25.	13.4 $\pm$ 1.3
375.9 $\pm$ 0.1	95. $\pm$ 10.	4.9 $\pm$ 0.5
396.8 $\pm$ 0.1	240. $\pm$ 25.	12.0 $\pm$ 1.3
460.1 $\pm$ 0.2	23.7 $\pm$ 3.	1.1 $\pm$ 0.15
470.8 $\pm$ 0.2	17. $\pm$ 2.	0.8 $\pm$ 0.1
481.7 $\pm$ 0.2	7.7 $\pm$ 2.	0.35 $\pm$ 0.1
522.2 $\pm$ 0.2	83. $\pm$ 10.	3.6 $\pm$ 0.4

\* In the analysis a value of  $\Gamma_\gamma = 30$  meV has been assumed. There is a correlation between this assumed value and the result obtained for  $\Gamma_n$ .

Resonance parameters of  $^{236}\text{U}$  ; Final results.

L. MEWISSEN, F. POORTMANS, G. ROHR<sup>\*</sup>, J.P. THEOBALD<sup>\*</sup>,  
G. VANPRAET<sup>\*\*</sup>, H. WEIGMANN<sup>\*</sup>

Some additional analysis-work on the  $^{236}\text{U}$  data was made, mainly to find out how much possible systematic errors would influence the results. The final results are the following :

- mean level spacing after correction of missed levels :

$$\bar{D} = 15.2 \pm 0.5 \text{ eV}$$

- s-wave neutron strength function :

$$S_0 = (1.05 \pm 0.14) 10^{-4}$$

- mean total capture width :

$$\Gamma_{\gamma} = [23.0 \pm 0.3 \text{ (stat)} \pm 1.5 \text{ (syst.)}] \text{ meV.}$$

The estimated systematic error of about 7 percent on the mean capture width is due to uncertainties in the sample thickness, the flux measurement in the capture experiments, the multiple scattering corrections and the base-line determination in the area analysis. All these sources of possible uncertainties, except the sample thickness, are more or less dependent on neutron energy. In fact a slight increase in the  $\Gamma_{\gamma}$  values with increasing energy was noticed, as well as a correlation between  $\Gamma_n$  and  $\Gamma_{\gamma}$  (correlation coefficient = 0.239 for 57 resonances). These effects are probably due to one or more of the experimental errors mentioned above.

---

\* CBNM, Euratom, Geel

\*\* R.U.C. Antwerpen



Resonance Parameters of  $^{238}\text{U}$

F. POORTMANS, L. MEWISSEN, G. ROHR\*, T. van der VEEN\*, G. VANPRAET\*\*,  
H. WEIGMANN\*, J. WINTER\*

Scattering cross-section experiments have been done below 1.2 keV with 4 samples, respectively  $1.312 \cdot 10^{-5}$  at/b,  $5.527 \cdot 10^{-5}$  at/b,  $1.004 \cdot 10^{-3}$  at/b and  $1.099 \cdot 10^{-2}$  at/b. The measurements were performed on a 30 meter flightpath station using the  $^3\text{He}$  high pressure gaseous scintillator detector system. The thinnest samples are 10 to 100 times thinner than those used in previous partial cross-section measurements in other laboratories so that possible errors on the corrections for multiple scattering effects are minimized. The total systematic error is not larger than 3% and the statistical error is within 1% for strong resonances and 10 % for weaker ones. The data are partly analysed for the two thinnest samples and preliminary results were communicated at the "Specialists Meeting on Resonance Parameters of Fertile Nuclei" held at Saclay, May 20-22, 1974.

A new series of transmission experiments with samples cooled at liquid nitrogen temperature will be started very soon.

Capture cross-sections experiments. A first run using a  $\text{C}_6\text{F}_6$  gamma detector covering the energy range from 20 eV to 1.8 keV and using a thick sample ( $6.32 \cdot 10^{-3}$  at/b) is being analysed. The aim of this present analysis is twofold :

a) determination of a precise value of the p-wave strength function by an area analysis of the smaller resonance in combination with resonance parity assignments,

---

\* CBNM, Euratom, Geel  
\*\* R.U.C. Antwerpen

b) information on the coupling conditions in sub-barrier fission of  $^{238}\text{U}$  and resonance parities from the measured gross shape of the  $\gamma$ -ray spectrum.

Further capture cross-section experiments on thinner samples will be started soon.

Resonance parameters of  $^{237}\text{Np}$

A. ANGELETTI<sup>+</sup>, L. MEWISSEN, F. POORTMANS, G. ROHR<sup>\*</sup>,  
T. van der VEEN<sup>\*</sup>, G. VANPRAET<sup>\*\*</sup>, H. WEIGMANN<sup>\*</sup>

Transmission experiments : the analysis is completed up to 50 eV for all three sample thicknesses : ( $1.68 \cdot 10^{-3}$  g/cm<sup>2</sup>,  $5.23 \cdot 10^{-3}$  g/cm<sup>2</sup>,  $2.32 \cdot 10^{-2}$  g/cm<sup>2</sup>). The data obtained with the 3 g sample ( $5.23 \cdot 10^{-3}$  g/cm<sup>2</sup>) yielded neutron widths for 128 resonances between 50 eV and 204 eV as a result of an area analysis. For some of these levels the analysis of the runs with other sample thicknesses will be necessary.

Scattering experiments : the analysis of the scattering data (up to  $\sim 200$  eV) is still in progress.

Capture experiments : neutron widths for 110 resonances have now been evaluated up to 100 eV neutron energy.

Combined analysis of the results of total and partial cross section experiments will be performed after completion of the partial analysis to obtain the resonance parameter set.

---

+ Euratom-fellow  
\* CBNM, Euratom, Geel  
\*\* R.U.C. Antwerpen

Neutron Cross Section Measurements on  $^{93}\text{Nb}$ .

L. MEWISSEN, F. POORTMANS, J. WINTER\*, G. ROHR\*, H. WEIGMANN\*

Neutron scattering cross section measurements have been performed on  $^{93}\text{Nb}$  using the  $^3\text{He}$  gaseous scintillator detector system at a 30 meter flight path. Data were taken for two samples ( $4.25 \cdot 10^{-3}$  at/b and  $1.267 \cdot 10^{-2}$  at/b) in an energy range between 60 eV and 4 keV. The neutron beam diameter was decreased to 4 cm so that the time-of-flight resolution was sufficiently good to resolve most of the resonances in this energy range. The data reduction is finished, the analysis will be done later. Total and capture cross section measurements are planned for early 1975.

Resonance Parameters of  $^{240}\text{Pu}$

H. WEIGMANN\*, G. ROHR\*, F. POORTMANS

An evaluation of the resonance parameters of  $^{240}\text{Pu}$  has been presented at the "Specialists Meeting on Resonance Parameters of Fertile Nuclei and  $^{239}\text{Pu}$ " held at Saclay, May 20-22, 1974. It includes a review of the status of experimental data on  $^{240}\text{Pu}$  resonance parameters as well as some statistical tests and recommendations, particularly with respect to average parameters.

Two parameter data acquisition system for capture measurements

L. MEWISSEN

A new diagnostic programme, run on the H.P. 2115 A Computer revealed a hardware error in the A.M.C. disc. Due to difficulties in the maintenance by the factory, it was decided to use only one half of the storage capacity. The diagnostic confirmed for this part of the disc, the same error rate as found earlier, i.e. 1 for  $10^{10}$  bits. So we have modified the two parameter programme to measure the time-of-flight spectrum of the incoming neutrons, together with the energy spectrum of the prompt  $\gamma$ -rays emitted after capture. It now can yield 16 pulseheight spectra, of 4096 channels each.

---

\* C.B.N.M. Euratom, Geel.

## 1.2. FISSION PHYSICS AND CHEMISTRY

### Identification of short-lived Ru isotopes produced in thermal neutron fission of $^{235}\text{U}$

P. FETTWEIS , P. del MARMOL

Short lived Ru-isotopes produced in the thermal neutron fission of  $^{235}\text{U}$  have been chemically separated from the other fission products as volatile  $\text{RuO}_4$ . Successive  $\gamma$ -ray spectra were taken by means of Ge(Li)-detectors. The isotope  $^{110}\text{Ru}$  could be definitively identified ( $T_{1/2} = 16$  s), the observed  $\gamma$ -rays have been assigned to the various Ru isotopes ( $A = 107$  to  $110$ ) or to their daughter elements on the basis of their half-lives, intensity ratios and known level properties. Partial decay schemes have been constructed and a final report is being written.

### Fission barrier of $^{185}\text{Re}$

P. del MARMOL, F. HANAPPE\* and M. BERLANGER\*

The fission cross section  $\sigma_f$  measurements for the  $^{181}\text{Ta}(\alpha, f)$  reaction, using the cyclotron of Louvain-la-Neuve, have been ended for  $\alpha$ -energies between 28.5 and 140 MeV.

From the total cross section  $\sigma_t$  calculated following the optical model, one finds the ratio of the reduced widths for fission and neutron emission :

$$\sigma_f/\sigma_t \sim \Gamma_f/\Gamma_n$$

As  $\Gamma_f/\Gamma_n = f(B_f, B_n, a_f, a_n)$  where  $B_f$  is the fission barrier of  $^{185}\text{Re}$ ,  $B_n$  the neutron binding energy of the daughter nucleus and  $a_f$  and  $a_n$  the level density parameters of the deformed nucleus at critical deformation and of the residual nucleus after emission of a neutrons, respectively, one can obtain an estimation of  $B_f$ . Preliminary results of this analysis show that  $B_f$  is close to 23 MeV.

In spite of having a 2 mm diameter collimator, the beam was not sufficiently defined to obtain precise results as regards the angular distribution of fission products.

---

\* I.I.S.N. bursar.

A few measurements will be done to compare the parameters obtained in the preceding experiments with those from the reaction  $^{184}\text{W} + \text{p}$  yielding the same compound nucleus  $^{185}\text{Re}$ .

JOINT SCK/CEN-CBNM (EURATOM) STUDIES IN FISSION PHYSICS AND STANDARDS.

(Contract EUR/C/4146/67 f)

Ratio of the ternary (LRA) to binary fission cross section induced by resonance neutrons in  $^{241}\text{Pu}$

C. WAGEMANS\*, A.J. DERUYTTER\*\*

The results of this study were published (Nucl. Phys. A234, 285, 1974) with the following abstract :

The ternary-to binary fission cross-section ratio (T/B) was determined for  $^{241}\text{Pu}$  for neutron induced fission in the energy region from 0.01 eV to 50 eV. The ternary and binary fission time-of-flight spectra were recorded at a 8.1 m flightpath at the CBNM Linac with a bank of four large gold-silicon surface-barrier detectors viewing a  $1 \text{ mg/cm}^2$   $^{241}\text{Pu}$  target. The ternary alpha pulse-height spectrum in the neutron energy region of interest was checked continuously. From the time-of-flight spectra the ratios of the areas of the strongest resonances in ternary and in binary fission were calculated; in the neutron energy region from 0.01 to 0.5 eV ratios were calculated for 18 zones throughout the spectrum. In the energy region from 1 to 50 eV the T/B ratio varies significantly from resonance to resonance, allowing a classification into a "high" and a "low" group. Although the statistical accuracy is poorer in the region below 1 eV we deduce from these T/B data that the 0.260 eV resonance probably belongs to the "high" group and also that there is only a slight difference between the T/B value at 0.260 eV and at thermal energy. We correlate these T/B values with the resonance spin  $J$  in terms of the channel theory of fission.

---

\* NFWO, aangesteld navorser, Rijksuniversiteit Gent and SCK/CEN

\*\* I.N.W., R.U. Gent

The emission of long-range  $\alpha$ -particels in the thermal neutron induced fission of  $^{233}\text{U}$ ,  $^{235}\text{U}$  and  $^{239}\text{Pu}$ .

C. WAGEMANS<sup>\*</sup>, A.J. DERUYTTER<sup>\*\*</sup>

The yields of the long-range  $\alpha$ -particles (LRA) in the thermal neutron induced fission of  $^{233}\text{U}$ ,  $^{235}\text{U}$ , and  $^{239}\text{Pu}$  have been determined relative to the corresponding binary fission yield. The measurements were performed with surface barrier detectors on a well-thermalized beam of the BR2 reactor having a cadmium ratio of 30 to 1. We obtained for  $^{233}\text{U}$ ,  $^{235}\text{U}$  and  $^{239}\text{Pu}$  binary-to-LRA ratios the values  $485 \pm 20$ ,  $615 \pm 20$  and  $475 \pm 20$ , respectively. For the same isotopes the following binary-to-ternary ratios were found:  $460 \pm 25$ ,  $530 \pm 20$  and  $420 \pm 25$ , resp. Some of the discrepancies between the published data were explained and experimental indications for  $^{235}\text{U}$  (n, $\alpha$ )- and  $^{239}\text{Pu}$  (n, $\alpha$ )- reactions are present. Finally the ternary fission yield was correlated with the symmetric fission yield, with the excitation energy available just above the fission barrier and with the  $\alpha$ -clustering inside the nucleus, following a suggestion by N. Carjan (T.H. Darmstadt, on leave from I.F.A., Bucarest).

Fission Fragment Kinetic Energy and Mass Distribution for  $^{235}\text{U}$

C. WAGEMANS<sup>\*</sup>, H. WEIGMANN<sup>\*\*\*</sup>, G. WEGENER-PENNING<sup>\*\*\*\*</sup>

A three parameter data acquisition system has been built up based on a Tridac (Intertechnique) 16K memory system, two Northern Scientific 8K ADC's and a home made time-coder. For the fission fragment detection two large ( $2000 \text{ mm}^2$ ) Ortec surface-barrier detectors with their appropriate electronics were used. This apparatus allows the detection of correlated fission fragment pulse-heights ( $E_1$ ,  $E_2$ ) in a  $128 \times 128$  channels matrix, and this for four predetermined neutron energy intervals.

The aim of the present experiment is to investigate the fission fragment kinetic energy- and mass-distributions for the resonance neutron induced fission of  $^{235}\text{U}$ . Reliable resonance spin-values (J) are available now for this isotope and hence it will be possible to look for correlations

---

<sup>\*</sup> NFWO, aangesteld navorsers, R.U. Gent and SCK/CEN  
<sup>\*\*</sup> I.N.W., R.U. Gent  
<sup>\*\*\*</sup> C.B.N.M., Euratom, Geel  
<sup>\*\*\*\*</sup> IWONL, R.U. Gent and SCK/CEN

of  $J$  with  $\bar{E}_K$  (mean total fission fragment kinetic energy) and the symmetric-to-asymmetric fission yield.

Measurements were already performed in which  $E_1$  and  $E_2$  were detected for four predetermined groups of  $J = 4$  resonances : 7 - 12 eV; 15 - 17 eV; 19 - 21 eV; 31 - 35 eV. Similar measurements are underway for four  $J = 3$  resonances : 12.4 eV; 13.5 - 15 eV; 18 eV; 24 - 26 eV. Furthermore a data analysis program has been adapted to these measurements and is operational now on the IBM 370 computer.

Measurement and Normalization of Neutron Induced Fission Cross-Sections in the Resonance Region

C. WAGEMANS <sup>\*</sup>, A.J. DERUYTTER <sup>\*\*</sup>

$^{233}\text{U}$  : The results of these measurements were published (Nucl. Sc. Eng. 54, p. 423, 1974).

$^{241}\text{Pu}$  : These measurements complete a series of experiments and evaluations of the low energy neutron induced fission cross-sections of the four common fissile isotopes and of their normalizations. All the measurements were performed at the same 8 m flightpath using the same basic apparatus. The fission cross-section was obtained via a direct comparison of the fission rate and the  $^{10}\text{B}$  (n, $\alpha$ )-rate detected with surface barrier detectors placed on both sides of a back-to-back  $^{241}\text{Pu}$ - $^{10}\text{B}$  foil. The background, which was very low, was determined by the black resonance technique. The measurements are finished and analysed. The relative fission cross-section curve obtained was normalized at 0.0253 eV to  $\sigma_f$  (2200 m/s) =  $1019 \pm 8$  i.e. the value recommended in "The 3rd IAEA Review of the 2200 m/s and 20°C Maxwellian neutron data for  $^{233,235}\text{U}$  and  $^{239,241}\text{Pu}$ " (H. LEMMEL et al., to be published). The important low-energy part of this curve is shown in fig. 1. Several fission and resonance integrals are calculated from the normalized  $\sigma_f$ -curve and compared with other results. A suitable fission integral is proposed for further normalization purposes :

$$\int_{12.0 \text{ eV}}^{20.0 \text{ eV}} \sigma_f(E) dE = (1368 \pm 13) \text{ b. eV}$$

\* NFWO, aangesteld navorsers, R.U. Gent and SCK/CEN  
\*\* I.N.W., R.U. Gent

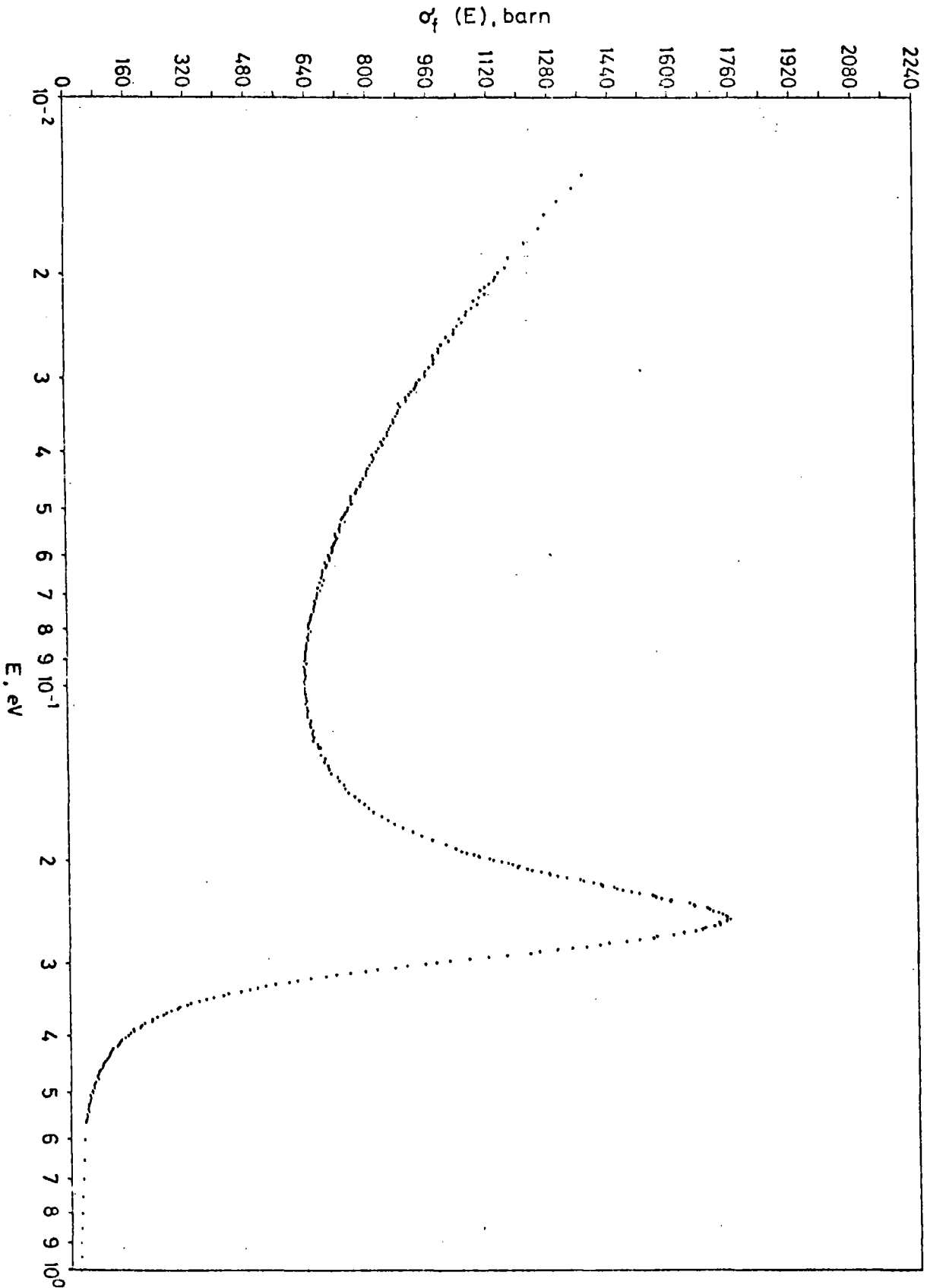


Fig. 1: Fission cross-section of  $^{241}\text{Pu}$  between 0.01 and 10 eV neutron energy.



Neutron Induced Fission Cross-Section of  $^{235}\text{U}$  in the Energy Region  
5 eV - 30 keV

C. WAGEMANS\*

These measurements are the logical extension towards higher energies of the previously published absolute fission cross-section measurements at 2200 m/s (Journ. Nucl. Eng., 27, p. 645, 1973) and of the measurements in the energy region 0.01 eV - 20 eV (Journ. Nucl. Eng., 25, p. 263, 1971). The latter result were normalized to the first one. The aim of the present experiment is to obtain accurate fission integrals in the high energy region carefully normalized to the previously mentioned results. The measurements were performed at a 30 m flightpath of the Linac under similar conditions as the above mentioned experiment i.e. the fission rate and the neutron spectrum were measured simultaneously with surface barrier detectors on each side of a back-to-back  $^{235}\text{U}$  and  $^{10}\text{B}$  layer. The fission cross-section data from thermal up to 30 keV will be available soon. Integration of these data in well defined parts of this energy range yields accurate normalization integrals. The integrals might be useful for the renormalization of published data and the reduction of discrepancies between them.

The temperature dependence of the Westcott  $g_f$ -factor for  $^{239}\text{Pu}$  and  
 $^{241}\text{Pu}$

C. WAGEMANS\*, A.J. DERUYTTER\*\*

The Westcott  $g_f$ -factor, which is important for the physics of thermal reactors, was calculated using our recent accurate fission cross-section data for  $^{239}\text{Pu}$  and  $^{241}\text{Pu}$ .

For  $^{239}\text{Pu}$  it yielded :  $g_f(20.44\text{ }^\circ\text{C}) = 1.053 \pm 0.003$  and for  $^{241}\text{Pu}$  we obtained :  $g_f(20.44\text{ }^\circ\text{C}) = 1.046 \pm 0.006$ . For both isotopes the temperature dependence of  $g_f$  was calculated in the temperature range 0 °C - 1000 °C and compared with previous results. The results for  $^{239}\text{Pu}$  were published (Ann. Nucl. Sc. Eng. 1, vol. 11, 1974) and those for  $^{241}\text{Pu}$  will appear soon in Ann. of Nucl. Sc. & Engn.

\* NFWO, Aangesteld navorser, R.U. Gent and SCK/CEN

\*\* I.N.W., R.U. Gent

Scattering of Fission Fragments

A.J. DERUYTTER \*, G. WEGENER-PENNING \*\*

The back scattering of fission fragments by several solid surfaces, covering a wide range of Z-values, was studied.

With the present experimental set-up it was possible to measure the angular distribution and the energy of the scattered fragments.

Preliminary results show :

- most of the fragments are scattered under low angles (75% of the fragments were detected between 0.5 ° and 10 °)
- the average energy of the scattered fragments is about 30% of their initial energy.
- the scattering intensity is strongly Z-dependent : it is about 10 times stronger for Au than for C.

1.3. NUCLEAR SPECTROSCOPY

Neutron capture  $\gamma$ -rays studied with Ge(Li) detectors

P. FETTWEIS, J. DEHAES \*\*\*

In the frame of the Association Contract ULB-IRE-CEN/SCK it has been decided to equip the thermal and epithermal (25 keV) neutron beam (R5) with an angular correlation table in order to study perturbed and ordinary angular correlations. The technical study is in progress.

Properties of  $^{235m}\text{U}$

M. NEVE de MEVERGNIES, P. del MARMOL

The measurements of the effect of the oxidation state of U on the isomeric half-life were ended and the final results published (Phys. Lett. 49B, 428, 1974)

---

\* I.N.W., R.U. Gent

\*\* IWONL, R.U. Gent and SCK/CEN

\*\*\* U.L.B., Brussels

Decay of  $^{90m}\text{Nb}$

P. FETTWEIS, A. MEYKENS <sup>\*</sup>, M. NEVE de MEVERGNIES, J. VERVIER <sup>\*\*</sup>

The accurate measurement of the half-life (about 20 sec.) of the 2.4 keV isomeric transition in  $^{90}\text{Nb}$  was started successfully. As mentioned in the Annual Scientific Report 1973, the isomer was produced by the  $^{90}\text{Zr}$  (p,n) reaction, using a 10 MeV proton beam of the Cyclotron of Louvain-la-Neuve. The target is a thin ( $50 \mu\text{g}/\text{cm}^2$ ) Zr deposit on a  $200 \mu\text{g}/\text{cm}^2$  carbon backing. The  $^{90m}\text{Nb}$  reaction product escapes from the target and penetrates in a metallic catcher foil in order to search for a perturbation of the isomeric half-life when  $^{90m}\text{Nb}$  is implanted in various metallic foils. After each irradiation, the catcher foil, is transferred mechanically in front of a well-shielded Ge(Li) detector, and the decay of the 122 keV line, which is in cascade with the isomeric transition is followed either in a multi-spectra mode or in a multi-scaler mode. With a 1  $\mu\text{A}$  proton beam, the 122 keV peak has an initial intensity of about  $10^3$  counts/sec, thus the summation of some 50 irradiations can, in principle, yield a statistical accuracy well below 1%. Data have been collected with Zr, Hf, Ta, W and Au catchers. To avoid systematic errors, the procedure for analysing the data is currently being studied carefully. Additional measurements on Nb, Ir and Pt catchers are planned.

JOINT KUL-SCK/CEN PROGRAMME

Neutron capture gamma ray studies

P. VAN ASSCHE, J.M. VAN DEN CRUYCE <sup>\*\*\*</sup>, G. VANDENPUT <sup>\*\*\*\*</sup>,  
L. JACOBS <sup>\*\*\*\*</sup>

With the availability of the results (obtained recently elsewhere) from two-dimensional Ge(Li)- Ge(Li) coincidence and angular correlation measurements and from single-neutron transfer reactions leading to  $^{151}\text{Sm}$ , a new impetus has been given to the nuclear structure study of this transitional nucleus at low energy and to the interpretation of our  $^{150}\text{Sm}$  (n, $\gamma$ ) data.

---

<sup>\*</sup> I.K.S., K.U. Leuven  
<sup>\*\*</sup> U.C.L., Louvain-La-Neuve  
<sup>\*\*\*</sup> Assistent, K.U. Leuven  
<sup>\*\*\*\*</sup> I.I.K.W.-bursaal, K.U. Leuven

A vast number of spins and parities of excited levels have been fairly well established and sufficient evidence has been provided to believe that even this weakly deformed nucleus can be described by a Nilsson model, albeit a very perturbed one. The single-particle states of an axially symmetric non-spherical harmonic oscillator potential are calculated at a deformation  $\delta$  of 0.16 approximately, with spin-orbit coupling and  $l^2$  term parameters of 0.0637 and 0.42 resp.. Pairing correlations in the intrinsic state are taken into account through a ECS-calculation (blocking included) resulting in quasi-particle energies and pairing factors for the reduction of single-particle matrix elements. In this basis the Coriolis interaction matrix is numerically diagonalised by the Givens - Householder method for real symmetric matrices. Only small energy shifts have been applied to some band heads of the rotational bands to obtain a better agreement with experimental energy levels. Calculated branching ratios, multipole mixings, lifetimes and magnetic moments have been compared with the available experimental data.

#### Diffracting crystals

The collaboration with Dr. M. Hart of the Bristol University (U.K.), concerning the study of diffracting crystals for use in the bent crystal  $\gamma$ -diffractometer has been continued.

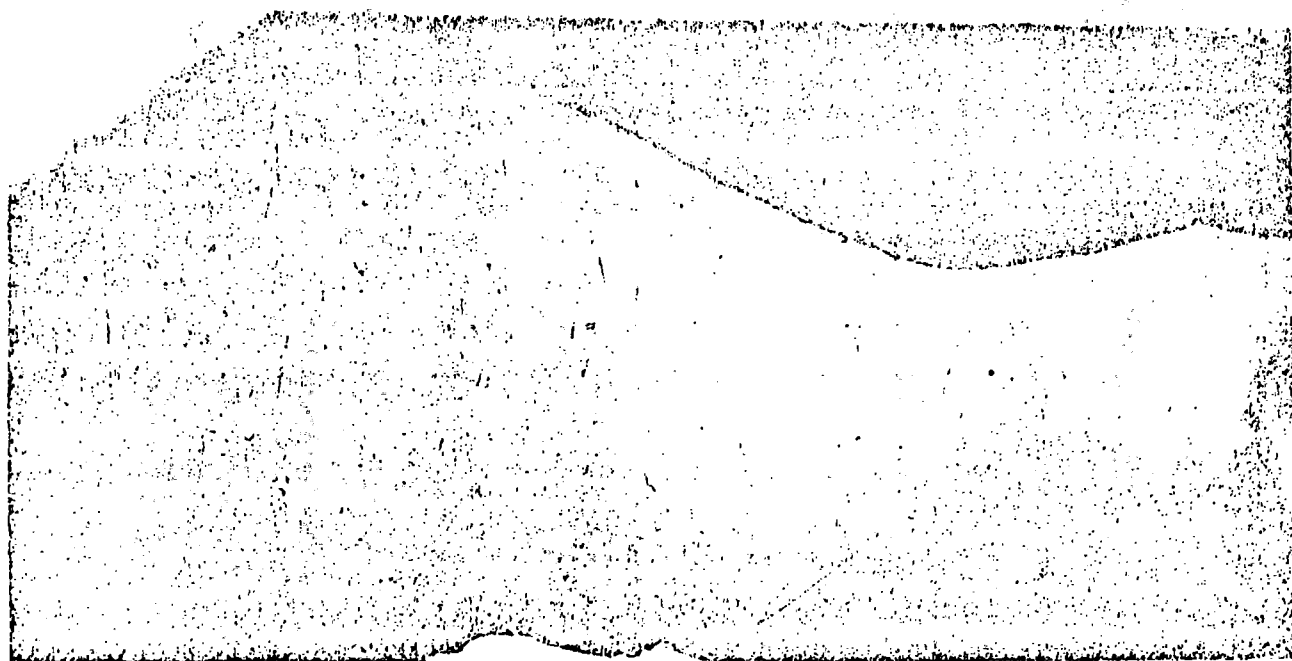
Topographical tests with specific X-rays have been carried out, mainly on Si-single crystals but also on  $\alpha$ -quartz and Ge. From Lang's topographical technique with transmission geometry and double diffraction images with transmission and reflection geometry, one could conclude that the large ( $\phi \gg 75$  mm) Si-crystals from Métallurgie Hoboken were dislocation free and very homogenous ( $\leq 1$  sec of arc over a large area)

From a topographical point of view Si looked more promising than  $\alpha$ -quartz, where large misorientations of the order of 1 sec of arc could be detected (see fig. 2 )

Si-crystals have been cut in orthogonal, oblique and longitudinal directions with respect to the growth axis  $\langle 111 \rangle$ .

In order to exploit fully the intrinsic perfection of the crystal, the elastic bending of the crystal slabs should also be very precise. Therefore the crystals have also been tested after bending, by means of

Fig. 2.



Double diffraction topograph ( $\text{Cu K}\alpha_1$  on  $(3\bar{3}1)$  Si,  $(30\bar{3}2)$  quartz) in Bragg-reflection of an  $\alpha$ -quartz for use in a  $\gamma$ -diffractometer. The intensity-difference is a measure of a misorientation of  $\sim 1$  sec of arc in the toplayer of the crystal.

a double diffraction set-up. This leads to "Zebra patterns", giving information about the uniformity of the bending. The results have been compared when the crystal was bent with the help of cylindrically grinded clamping blocs or with two opposite bending-moments at the far ends of the crystal slab.

#### 1.4. INSTRUMENTATION

P. D'HOGHE, E. MIES, L. VANSTEEELANDT

##### Neutron spectrometry

A Tally lineprinter model 132 was added to the existing equipment of the HP 2115 A computer.

For the equipment of the 2108 microprocessor a study was started to connect several peripherals on the 9 input and output channels.

##### Fission

A 4-input mixer-routersystem has been tested, it operates now together with a 400 channelanalyser.

The study of the construction of a new apparatus for fission experiments at the UCL Cyclotron at Louvain-la-Neuve has been started. The study of a one-meter diameter reaction chamber has been finished. Several parts such as the sample changer and supporting tripod were assembled.

##### Nuclear spectroscopy

##### Ge(Li) spectrometry

To increase the flexibility of the HP 2114 B computer the study of a CAMAC system was started. With this system the user can always modify and extend his equipment and the corresponding software. A power supply and a unit to display the dataway operations were tested. Also a manual crate controller was constructed which will be used as a tester for the different CAMAC devices under design.

The study of the mechanical construction of a coincidence apparatus for  $\gamma$ - $\gamma$ -angular correlation measurements on neutron capture gamma rays (Joint CEN/SCK-ULB Programme) has been started. As a horizontal beam

(R5 or R1 of BR2) has to be used the two Ge(Li)-detectors with their cooling dewars must move in a vertical plane. The dewars thus limit the maximum angle of rotation of the detectors.

#### Diffraction Spectrometer

The final assembly of the Bent Crystal Diffraction Spectrometer at BR2 was started, and the various parts of the T2-T5 in-pile components were ready to be introduced in the BR2 in September. After the reactor stop, and after removing the beam-shutters, a water leak between the beam-tube and the reactor shielding was observed. The mounting of the spectrometer parts was stopped, and it was decided first to repair this leak during the following long stop of BR2 early in 1975.

The spectrometer itself has been moved from Louvain-la-Neuve, and mounted for several tests in the BR1 reactor building.

#### Properties of $^{90}\text{Nb}^m$

For the study of  $^{90}\text{Nb}^m$  at the UCL Cyclotron, the ten-position sample changer has been tested and mounted at the Cyclotron. It has been completed with a support and shielding for a Ge(Li) detector.

## 2. THEORETICAL NUCLEAR PHYSICS

### A projected Hartree-Fock calculation in intermediate coupling for $^{12}\text{C}$

M. BOUTEN <sup>\*</sup>, M.-C. BOUTEN

Previous projected Hartree-Fock (PHF) calculations for  $^{12}\text{C}$  in the LS-coupling limit generally yielded too low excitation energies for the 2+ and 4+ levels of the ground state band. It was surmised that this defect had to be attributed to the neglect of non-central forces. In order to test this idea, we have carried out a PHF calculation in intermediate coupling for  $^{12}\text{C}$  using the method described previously for  $^{10}\text{B}$ . The non-central Hamiltonian was diagonalised in the space spanned by the PHF functions corresponding to the partitions  $[444]$ ,  $[4431]$  and  $[4422]$ . The calculation becomes quite involved due to the complicated structure of some intrinsic states. The results confirm the expectation: the 2+ and 4+ levels move up with increasing spin-orbit strength and come at about the experimental value for a strength of 5 MeV. The calculation also yields higher excited levels with low J values. However, they come out too high as compared to experiment. It can be seen that this defect is due to the too large L/K ratio of the Volkov force, L and K being the radial integrals which determine the force in the p-shell. Slightly better results are obtained with the realistic Yale potential. In fact, in order to improve the results, one should try to construct a force with good saturation properties for variational calculations and at the same time, a L/K ratio which would bring down the excited partitions.

Electromagnetic transitions probabilities were calculated with the wave functions of the ground state band. These transitions appear to be not very sensitive to the presence of non-central forces. They depend essentially on the deformation of the central field and are slightly decreasing functions of the degree of spin-orbit coupling. The results are quite satisfactory. For the modified Volkov force and a spin orbit strength of 5 MeV, we obtain in unit  $e^2 \text{fm}^4$

	PHF	SM	Exp
B(E2 ; 2+ → 0+ )	7.81	3.09	8.4
B(E2 ; 4+ → 2+ )	8.02	2.87	

Results with the Yale potential are similar.

\* Limburgs Universitair Centrum, Hasselt.



K-Bands in  $^{10}\text{B}$

M. BOUTEN <sup>\*</sup>, M-C. BOUTEN

In order to remove the discrepancies mentioned in the previous Annual Report for  $^{10}\text{B}$ , some test calculations were carried out. The results suggest that the order of the two K-bands could probably be brought into agreement with experiment if the intrinsic states are allowed to become triaxial. To settle this question definitely, however, will require some quite extensive calculation.

Form factors for electron scattering in  $^{10}\text{B}$  and  $^{12}\text{C}$

M. BOUTEN <sup>\*</sup>, M-C. BOUTEN

The wave functions obtained for the ground state and low-lying excited states in  $^{10}\text{B}$  and  $^{12}\text{C}$  have been tested by calculating form factors for elastic and inelastic electron scattering.

In  $^{12}\text{C}$ , the results are quite satisfactory for the elastic and for the inelastic form factors of the lowest 2+ and 4+ states. The only disagreement occurs in the  $0+ \rightarrow 2+$  transition for  $q^2$  greater than  $6 \text{ fm}^{-2}$ . In that region, although the order of magnitude of the results is acceptable the shape of the experimental curve remains unexplained.

In  $^{10}\text{B}$ , comparison with experimental data is only possible for elastic scattering. Good agreement is also obtained here.

The dependence of our results on the force used was also studied. We found that the results obtained with the realistic Yale potential are not very different from those obtained with a modified Volkov force.

New rotational structure in light nuclei

F. ARICKX <sup>\*\*</sup>, M. BOUTEN <sup>\*</sup>, P. VAN LEUVEN <sup>\*\*</sup>

Configuration Interaction calculations on  $^8\text{Be}$ , taking into account  $0\hbar\omega$ ,  $2\hbar\omega$  and  $4\hbar\omega$  shell model configurations, reveal a new kind of classification of the energy levels. Whereas in the simple shell-model picture each configuration produces truncated rotational bands  $[\text{SU}(3)]$ , after configuration mixing we obtain families of continuing rotational

---

\* LUC. Hasselt  
\*\* RUC. Antwerp

bands. The classification in families gives rise to a new quantum number whose physical origin remains to be found.

Theory and Application of the Generator Coordinate Method

M. BOUTEN <sup>\*</sup>, L. LATHOUWERS <sup>\*\*</sup>, P. VAN LEUVEN <sup>\*\*</sup>

From the theoretical point of view the question of complex generator coordinates and the natural expansion of kernels in the Hill-Wheeler equation has been studied.

The method has also been applied to the non-adiabatic vibrations of the  $H_2^+$ -molecular ion. On this example some numerical aspects of the method could be tested.

The work as a whole is a fine example of cross-fertilisation between nuclear and molecular physics.

International Seminar on Generator Coordinates in nuclear Physics

M. BOUTEN <sup>\*</sup>, P. VAN LEUVEN <sup>\*\*</sup>

From 16.9.74 till 28.9.74 an international seminar on the Generator Coordinate Method (GCM) has been organized at SCK/CEN. About 20 specialists in this field from 5 different countries have participated. The meeting consisted of two parts : Part 1, where the results obtained in the respective Institutes during the past 2 years were presented and Part 2, where, open problems were discussed by separate working groups. The proceedings are being prepared and will be published.

---

<sup>\*</sup> LUC, Hasselt

<sup>\*\*</sup> RUC. Antwerpen

### 3. Integral Neutron Cross Section Measurements

#### Integral cross section measurements in the thermal neutron induced uranium-235 fission spectrum (A. Fabry)

Fission spectra are generated by means of two types of source-detector configurations, exposed in the 1 meter diameter spherical cavity of the vertical graphite thermal column of the BR1 reactor :

1) coaxial disc arrangements : detector foils are centered in a cadmium box which is sandwiched between two thin uranium-235 discs (whose separation distance can be systematically changed). This assembly, patterned according to a NBS design, is well suited for radiometric fission yield measurements and for the determination of absolute activation cross sections, even for capture reactions. It has been used in cooperation with the SEIBERSDORF, IAEA, Laboratory (A. FABRY, K.H. CZOCK - Report INDC (IAE) - 005/G, 1974).

2) cylindrical source arrangements : the exposure zone is within a vertical, 1 mm thick, 2 meter long co-extruded cadmium tube (the diameter of which can be changed), around which a thin uranium-235 fission source (of variable length) is wrapped, at cavity center.

This assembly is ideal for accurate fission chamber experiments and for activation cross section determinations for threshold reactions ; it is amenable to helium generation rate measurements in  $^{10}\text{B}$  and  $^6\text{Li}$ .

It has been used in particular to fulfill the WRENDA 74 priority 1 request for an accurate determination of the uranium-238 to uranium-235 integral fission cross section ratio, in cooperation with NBS and using three different types of fission chambers.

(A. FABRY, J.A. GRUNDL, C. EISENHAUER - "Fundamental integral cross section ratio measurements on the thermal-neutron-induced uranium-235 fission neutron spectrum" - Nuclear Cross Section and Technology Conference, March 1975).

The most recent experimental data obtained in the U-235 fission spectrum are compared in table I to the predictions from the

ENDF/BIV dosimetry file, accepting the NBS evaluation for the differential measurements of the fission spectrum shape (J.A. GRUNDL, C. EISENHAUER - "Fission spectrum neutrons for cross section validation and neutron flux transfer" - Nuclear Cross Section and Technology Conference, March 1975). Though there is a trend for some discrepancy between differential and integral data, it is believed, to mostly lie within uncertainties of differential data ; these cannot be propagated reliably, partly because there is no satisfactory error file yet.

TABLE I. - INTEGRAL CROSS SECTIONS IN THE THERMAL-NEUTRON-INDUCED URANIUM-235 FISSION NEUTRON SPECTRUM :  
COMPARISON OF RECENT MEASUREMENTS WITH PREDICTIONS FROM DIFFERENTIAL DATA

Reaction, i	$\bar{\sigma}(i, \chi_{25})$			$\bar{\sigma}(i, \chi_{25})/\bar{\sigma}_{n.f.}(^{235}\text{U}, \chi_{25})$		
	Predicted <sup>(a)</sup>	Measured	Ratio	Predicted <sup>(a)</sup>	Measured	Ratio
$^{235}\text{U}(n, f)$	1243.2	1204 (+ 2.5%) <sup>(b)</sup>	0.968	1	1	1
$^{239}\text{Pu}(n, f)$	1782.0	1812 (+ 3.4%)	1.017	1.433	1.505 (+ 2.2%)	1.050
$^{237}\text{Np}(n, f)$	1319.0	1329 (+ 3.9%)	1.008	1.061	1.104 (+ 3%)	1.040
$^{103}\text{Rh}(n, n')^{103m}\text{Rh}$	710	735.7 (+ 4.7%)	1.036	0.5711	0.611 (+ 4%)	1.070
$^{115}\text{In}(n, n')^{115m}\text{In}$	181.3 <sup>(c)</sup>	189.5 (+ 3.9%)	1.045	0.1458 <sup>(c)</sup>	0.1574 (+ 3%)	1.080
$^{238}\text{U}(n, f)$	294.7	305.5 (+ 3.2%)	1.037	0.2370	0.2538 (+ 2%)	1.071
$^{58}\text{Ni}(n, p)^{58g,m}\text{Co}$	101.3	108.7 (+ 4.7%)	1.073	0.08148	0.0903 (+ 4%)	1.108
$^{32}\text{S}(n, p)^{32}\text{P}$	63.72	66.4 (+ 5.6%)	1.042	0.05125	0.05515 (+ 5%)	1.075
$^{54}\text{Fe}(n, p)^{54}\text{Mn}$	77.49	79.4 (+ 5.6%)	1.025	0.06233	0.06595 (+ 5%)	1.058
$^{56}\text{Fe}(n, p)^{56}\text{Mn}$	1.080	1.029 (+ 5.6%)	0.953	0.0008687	0.000855 (+ 5%)	0.984
$^{27}\text{Al}(n, \alpha)^{24}\text{Na}$	0.725	0.700 (+ 5.6%)	0.963	0.0005832	0.000581 (+ 5%)	0.994

- (a) NBS evaluation for  $\chi_{25}(E)$  [J.A. GRUNDL, C.M. EISENHAUER - Nuclear Cross Sections and Technology Conference, paper DB-6, March 1975 ], ENDF/B IV for  $\sigma_i(E)$  except in the case of rhodium [J.P. BUTLER, D.C. SANTRY - Neutron Cross Sections and Technology Conference, vol. 2 p 803-810 (1968)] .
- (b)  $^{252}\text{Cf}$  experiment [H.T. HEATON II et al. - Nuclear Cross Sections and Technology Conference, March 1975 ]: change of  $\bar{\sigma}$  between  $^{252}\text{Cf}$  and  $^{235}\text{U}$  fission spectra is computed to be less than 0.15% is accounted for only by increasing the uncertainty.
- (c) ENDF/B IV data rescaled to be consistent with a branching ratio of 45.9% (radiation intensity per decay) for the  $^{115m}\text{In}$  336.2 keV gamma ray, as accepted in interpreting the integral measurements.

APPENDIX I  
PUBLICATIONS

NUCLEAR PHYSICS

- Configuration mixing in  $^8\text{Be}$  and the quadrupole force  
F. ARICKX, M. BOUTEN and P. VAN LEUVEN  
Proceedings of the International Conference on Nuclear Structure and Spectroscopy, Amsterdam, September 9-13, 1974  
Edited by M.P. Blok and A.E.L. Dieperink, Vol. 1, p. 56.
- Intermediate coupling in the deformed shell model  
M. BOUTEN and M-C. BOUTEN  
Proceedings of the International Conference on Nuclear Structure and Spectroscopy, Amsterdam, September 1974, Vol. 1, p. 57
- A PHF calculation in intermediate coupling for light nuclei  
M. BOUTEN, M-C. BOUTEN  
Czech. J. Phys. B24, 1277 (1974)
- Energy Shifts of Ground-State Rotational bands in  $^8\text{Be}$  and  $^9\text{Be}$   
M. BOUTEN and M-C. BOUTEN  
Lett. al Nuovo Cimento 10, 161 (1974)
- Intermediate-coupling calculation for  $^{10}\text{B}$  in a projected Hartree-Fock basis  
M. BOUTEN and M-C. BOUTEN  
Nuclear Physics A228, 314 (1974)
- Extension of Elliott's projection technique to compact semisimple groups  
M. BOUTEN, D. HAENTJENS and P. VAN LEUVEN  
Physica 73, 585 (1974)
- Two exactly soluble models as a test of the hermitian operator method  
M. BOUTEN, P. VAN LEUVEN, M. MIHAJLOVIC and M. ROSINA  
Nuclear Physics A221, 173 (1974)
- Analysis of neutron resonances in  $^{143}\text{Nd}$   
H. CEULEMANS  
Proceedings of the tripartite symposium on "Nuclear Physics with thermal and resonance energy neutrons", Petten, May 22-25, 1973, Report RCN.203, p. 219.
- Connection between LRA to binary fission cross-sections ratio for resonance and thermal neutron induced fission in  $^{239}\text{Pu}$  and resonance spins  
A. DERUYTTER, C. WAGEMANS  
Physics and Chemistry of Fission - 1973, IAEA, Vienna, Vol. II, p. 417 (1974)
- Comparison of the fission characteristics of thermal-neutron-induced fission of  $^{239}\text{Pu}$  and the spontaneous fission of  $^{240}\text{Pu}$   
A. DERUYTTER, G. WEGENER-PENNING  
Physics and Chemistry of Fission - 1973, IAEA, Vienna, Vol. II, p. 51 (1974)
- Measurement and normalization of the relative  $^{233}\text{U}$  fission cross section in the low resonance region  
A. DERUYTTER, C. WAGEMANS  
Nucl. Sci. & Engn., 54, 423-431 (1974)
- Redetermination of the half-life of  $^{235}\text{U}$  for  $\alpha$ -emission  
A. DERUYTTER, G. WEGENER-PENNING  
Phys. Rev. C, 10, 383 (1974)

APPENDIX I (continued)

An extension of Wong's theory for complex generator coordinates

L. LATHOUWERS

Nuclear Physics A228, 125 (1974)

Cross section measurements on  $^{236}\text{U}$  below 2 keV

L. MEVISSSEN, F. POORTMANS, G. ROHR, J. THEOBALD, G. VANPRAET, H. WEIGMANN, R. WERZ

Proceedings of the tripartite symposium on "Nuclear Physics with thermal and resonance energy neutrons", Petten 1973, Report RCN 203, p. 279.

Effect of the oxidation state on the half-life of  $^{235\text{m}}\text{U}$

M. NEVE de MEVERGNIES, P. del MARMOL

Phys. Lett., 49B, 428 (1974)

Neutron resonance parameters of  $^{242}\text{Pu}$

F. POORTMANS, G. ROHR, J. THEOBALD, H. WEIGMANN, G. VANPRAET

Proceedings of the tripartite symposium on "Nuclear Physics with thermal and resonance energy neutrons", Petten 1973, Report RCN 203, p. 113

Neutron multiplicity measurements on resolved fission resonances of  $^{235}\text{U}$  and  $^{239}\text{Pu}$

J. THEOBALD, J. WARTENA, H. WEIGMANN, R. WERZ, F. POORTMANS

Proceedings of the tripartite symposium on "Nuclear Physics with thermal and resonance energy neutrons", Petten 1973, Report RCN 203, p. 100

The mass distribution of neutron induced fission for  $^{239}\text{Pu}$  at the 0.297 eV resonance

P. VAN ASSCHE, G. VANDENPUT, L. JACOBS, J.M. VAN DEN CRUYCE, R. SILVERANS

Proceedings of the tripartite symposium on "Nuclear Physics with thermal and resonance energy neutrons", Petten 1973, Report RCN 203, p. 95

Rotational structure of the doubly odd deformed  $^{182}\text{Ta}$  nucleus

J.M. VAN DEN CRUYCE, G. VANDENPUT, L. JACOBS, P. VAN ASSCHE et al.

Proceedings of the tripartite symposium on "Nuclear Physics with thermal and resonance energy neutrons", Petten 1973, Report RCN 203, p. 57

Ternary to binary fission ratio for neutron induced fission in  $^{239}\text{Pu}$  in the energy region 0.02 eV - 50 eV

C. WAGEMANS, A. DERUYTTER

Proceedings of the tripartite symposium on "Nuclear Physics with thermal and resonance energy neutrons", Petten 1973, Report RCN 203, p. 147

Ratio of the ternary-to-binary fission cross sections induced by thermal and resonance neutrons in  $^{241}\text{Pu}$

C. WAGEMANS, A. DERUYTTER

Nuclear Physics A234, 285-300 (1974)

The Westcott  $g_f$ -factor for  $^{239}\text{Pu}$  and its temperature dependence

C. WAGEMANS, A. DERUYTTER

Ann. of Nucl. Sci. & Eng., 1, 11 (1974)

APPENDIX I (continued)

Comparison of the thermal neutron induced fission of  $^{239}\text{Pu}$  and the spontaneous fission of  $^{240}\text{Pu}$

G. WEGENER-PENNING, A. DERUYTTER

Proceedings of the tripartite symposium on "Nuclear Physics with thermal and resonance energy neutrons", Petten 1973, Report RCN 203, p. 135

SOLID STATE PHYSICS

A device for the preparation of composite crystal samples

E. LEGRAND, S. HAUTECLER, L. VANSTEEELANDT

Nucl. Instr. Methods 120, 197-198 (1974)

Dispersion of acoustical magnons and phonons in  $\text{Mn}_{1.7}\text{Fe}_{1.3}\text{O}_4$

D. SCHEERLINCK, W. WEGENER, S. HAUTECLER, U. BRABERS

Solid State Commun. 15, 1529-1533 (1974)

Inelastic neutron scattering by cerium hydrides

I. Experimental

P. VORDERWISCH, S. HAUTECLER

Phys. Stat. Sol. (b) 64, 495-501 (1974)

II. Lattice dynamical approach

P. VORDERWISCH, S. HAUTECLER, H. DECKERS

Phys. Stat. Sol. (b) 65, 171-180 (1974)

III. Localized vibrations of interstitial hydrogen in the f.c.c.  $\text{CeH}_2$  lattice

P. VORDERWISCH, S. HAUTECLER

Phys. Stat. Sol. (b) 66, 595-606 (1974)

Inelastic neutron scattering study of acoustical magnons in  $\text{MnFe}_2\text{O}_4$

W. WEGENER, D. SCHEERLINCK, E. LEGRAND, S. HAUTECLER, U. BRABERS

Solid state Commun. 15, 345-349 (1974)



APPENDIX II

COLLOQUIA, SEMINARS and SYMPOSIA

Kernforschungsanlage Jülich, 14.1.1974

- The study of the doubly-odd deformed  $^{182}\text{Ta}$  nucleus by (m,n) reactions  
P. VAN ASSCHE

Technische Hogeschool Eindhoven, Afdeling der Technische Natuurkunde,  
Eindhoven, 9.4.1974

- Study of magnetic interactions in some spinels by neutron inelastic scattering  
S. HAUTECLER

Université Libre de Bruxelles, Faculté des Sciences Appliquées, Bruxelles,  
3.5.1974

- Détermination des interactions magnétiques dans des spinelles par diffusion inélastique de neutrons thermiques  
S. HAUTECLER

Seminar on Inelastic Scattering of Neutrons U.I.A., Antwerpen, 8.5.1974

- Acoustical magnons in  $\text{Mn}_{1.7}\text{Fe}_{1.3}\text{O}_4$   
D. SCHEERLINCK, W. WEGENER
- Rotational motions of some molecules encaged in  $\text{D}_2\text{O}$  clathrates  
J. VANDERHAEGHEN, W. WEGENER

Vosbergen Konferentie, Vlieland, Nederland, 13-16.5.1974

- A new method for collective states  
P. VAN LEUVEN

Specialist Meeting on Resonance Parameters of fertile nuclei and  $^{239}\text{Pu}$ ,  
Saclay, 20-22.5.1974

- Conclusions of Sessions on Resonance Parameters of fertile Nuclei  
H. CEULEMANS
- The low energy neutron induced fission cross-section of  $^{239}\text{Pu}$  and the temperature dependence of the Westcott  $g_f$ -factor  
C. WAGEMANS, A.J. DERUYTTER
- Neutron scattering cross section measurements on  $^{238}\text{U}$  in the resolved energy range  
F. POORTMANS, L. MEWISSEN, G. ROHR, G. VANPRAET, H. WEIGMANN
- A review of  $^{240}\text{Pu}$  resonance parameter data  
H. WEIGMANN, G. ROHR, F. POORTMANS
- Neutron cross section measurements on  $^{236}\text{U}$  below 2 keV  
L. MEWISSEN, F. POORTMANS, J. THEOBALD, H. WEIGMANN, G. VANPRAET
- Investigations of resonance neutron capture in  $^{238}\text{U}$   
H. WEIGMANN, G. ROHR, F. POORTMANS, L. MEWISSEN, G. VANPRAET

Université Catholique de Louvain, Louvain-la-Neuve, 27.5.1974

- The Generator Coordinate method for molecular vibrations  
L. LATHOUWERS

APPENDIX II (continued)

Symposium on "Theory of lightest nuclei", Liblice, Czechoslovakia,  
29-31.5.1974

- A PHF calculation in intermediate coupling for light nuclei  
M. BOUTEN, M-C. BOUTEN

Kvantkemiska Gruppen, Universitet Uppsala, Uppsala, Sweden, 5.6.1974

- Generator Coordinates  
P. VAN LEUVEN

Réunion Scientifique Générale de la Société Belge de Physique -  
Algemene Wetenschappelijke Vergadering van de Belgische Natuurkundige  
Vereniging, Mons, 6-7.6.1974

- Spin waves in  $Mn_{1.7}Fe_{1.3}O_4$  spinel from inelastic neutron scattering  
D. SCHEERLINCK, W. WEGENER, U. BRABERS, E. LEGRAND, S. HAUTECLER
- Localized vibrations of interstitial hydrogen in  $CeH_2$   
S. HAUTECLER, P. VORDERWISCH
- Neutron resonance parameters of  $^{236}U$   
L. MEWISSEN, F. POORTMANS, G. ROHR, J. THEOBALD, H. WEIGMANN, G. VANPRAET
- Resonantie-structuur in  $^{226}Ra + n$   
H. CEULEMANS
- Configuration interaction in  $^8Be$   
F. ARICKX
- Etude des isotopes de fission du Ru de court temps de vie  
P. FEITWEIS, P. del MARMOL
- Verhouding van de ternaire tot de binaire fissiewerkzame doorsneden  
door thermische en resonantieneutronen in  $^{241}Pu$  geïnduceerd  
C. WAGEMANS, A.J. DERUYTTER

Conference on capture  $\gamma$ -ray studies, Petten 2-6.9.1974

- Neutron resonance capture investigations as a means of studying the  
coupling conditions in sub-barrier fission  
H. WEIGMANN, G. ROHR, T. VAN DER VEEN, G. VANPRAET
- Experimental developments in  $(n, \gamma)$  spectroscopy  
P. VAN ASSCHE

International conference on nuclear structure and spectroscopy,  
Amsterdam, 9-13.9.1974

- Intermediate coupling in the deformed shell model  
M. BOUTEN, M-C. BOUTEN
- Configuration mixing in  $^8Be$  and the quadruple force  
F. ARICKX, M. BOUTEN, P. VAN LEUVEN

International seminar on generator coordinates in nuclear physics, Mol,  
15-28.9.1974

- Natural expansion of the intrinsic generator wave function  
L. LATHOUWERS

- 93 -  
APPENDIX II (continued)

- Complex generator coordinates  
L. LATHOUWERS
- Generator coordinates as an approximation to Shell model: rotational structure in  $^8\text{Be}$   
F. ARICKX

Journées d'Etudes sur la fission, Cadarache, 21-23.10.1974

- Is the ternary fission yield for neutron induced fission correlated with the resonance spin?  
C. WAGENIANS



PROGRESS REPORT to I. N. D. C.

from GREECE

July, 1975

Edited by

S. Dritsa

N. R. C. "Democritos"

Athens, Greece



## 1. NEUTRON CAPTURE GAMMA-RAY SPECTROSCOPY

S. Dritsa, O.A. Wasson\*

The iron filter facility installed in the No. 2 channel of the 5 MW Demokritos<sup>1</sup> reactor has been further developed, in order to improve the purity of the 24 keV neutron beam. Additional shielding - heavily borated paraffin block on the reactor face - to reduce the epithermal background was installed. The 24 keV neutron flux measured is  $5 \times 10^5$  n/cm<sup>2</sup> sec.

A Ge(Li) detector of 40 cm<sup>3</sup> active volume with a FWHM resolution of 2 keV at 1.33 MeV and a 4096 multichannel analyzer with gain stabilization are used for the recording of spectra.

24 keV neutron capture gamma-ray spectra were obtained for natural samples of W and Nb and the analysis is in progress.

An attempt is being made to measure the total neutron capture cross section of Al at 24 keV. There are several difficulties to be overcome as there is a lot of aluminum near the detector to cause background but the Al presents the advantages of low neutron scattering cross section at 24 keV and an intense 1.78 MeV decay  $\gamma$ -ray with a 2.3 min. half-life. Preliminary measurements indicated that the problems are manageable. The cross section measurements are to be supplemented by measurements of the prompt neutron capture gamma-ray spectrum of aluminum.

---

\* Permanent address : National Bureau of Standards, Washington D. C.

## 2. TANDEM ACCELERATOR LABORATORY N. R. C. "DEMOKRITOS"

### 2.1. INVESTIGATION OF THE $^{16}\text{O} (^{16}\text{O}, \alpha) ^{28}\text{Si}$ REACTION

J. D. Fox\*, G. Vourvopoulos, S. Kosionides.

The excitation function of elastically scattered  $^{16}\text{O}$  on  $^{16}\text{O}$  shows some structure which was attributed to quasi-molecular states. In order to clarify this question the excitation function of the reaction  $^{16}\text{O} (^{16}\text{O}, \alpha) ^{28}\text{Si}$  was measured for  $\alpha$ 's leading to the ground and first excited states of  $^{28}\text{Si}$ . The energy of  $^{16}\text{O}$  was varied from 17 to 32 MeV in steps of 200 keV. The cross section shows strong fluctuations and transitions of the relative phase of  $\alpha_0$  and  $\alpha_1$ . Quantitative analysis of the data is in progress.

---

\* Permanent Address : Florida State University.

### 2.2 GAMMA-GAMMA DIRECTIONAL CORRELATIONS IN $^{69}\text{Ga}$ .

T. Paradellis, A. Xenoulis, C.A. Kalfas

Employing a Ge(Li)-NaI (Tl) detector system, gamma-gamma directional correlations for nine cascades in  $^{69}\text{Ga}$  have been measured. The result of the present measurements combined with other existing data allowed the adoption of a  $5/2^-$  spin and parity for the 1106.4 keV level, and a  $7/2^-$  for the 1336.1 and 1487.5 keV levels. A tentative  $7/2^-$  spin and parity has been adopted for 1923.1 keV level. Mixing ratios have been determined for six transitions. The data obtained was utilized to extract M1 and E2 reduced transition probabilities. A comparison of the experimental data was made with the predictions of the one particle-core and three particles-core coupling models.

### 2.3 TRANSITIONAL NUCLEI : $^{150}\text{Sm}$ FROM THE DECAY OF $^{150}\text{Pm}$

C. A. Kalfas, A. Xenoulis and T. Paradellis.

Gamma-gamma directional correlation techniques employing a Ge(Li)-NaI(Tl) system were used to investigate the de-excitation mechanism



and character of several states in  $^{150}\text{Sm}$ , following the decay of  $^{150}\text{Pm}$ . Spins of certain levels and multipole mixing ratios of transitions from the quadrupole and octupole quasi-vibrational bands were determined. The experimental mixing ratio values are compared with the theoretical prediction of Kumar and with corresponding values in neighbouring nuclei.

#### 2.4 HEAVY ION REACTIONS

A. D. Panagiotou<sup>\*</sup>, G. Vourvopoulos, E. Kosionides, P. Kakanis  
E. Gazis, N. Xiromeritis.

The heavy ion programme utilizes beams of  $^{16}\text{O}$ ,  $^{12}\text{C}$  and  $^{14}\text{N}$ , presently available from the T 11/25 Tandem Accelerator. As a sample, beams of 40 MeV  $^{16}\text{O}^{+7}$ , with intensity of about 100 nA analyzed, is mentioned. The research programme consists of :

a) Transfer Reactions,    b) Mass Measurements.

Employing a detector telescope consisting of  $\Delta E(9 \mu)$ ,  $E(50 \mu)$  and anticoincidence ( $100 \mu$ ) detectors preliminary angular distributions of the reactions ( $^{16}\text{O}$ ,  $^{20}\text{Ne}$ ) and ( $^{16}\text{O}$ ,  $^{12}\text{C}$ ) on  $^{16}\text{O}$  and  $^{28}\text{Si}$  targets, were obtained. Detailed angular distributions of the above reactions with a number of  $\beta$ -type nuclei from  $^{12}\text{C}$  to  $^{40}\text{Ca}$  as targets are planned.

For the Mass Measurements reactions such as ( $^{18}\text{O}$ , 2p) on light targets are employed. At present the method is under test and development.

---

\* N. R. C. "Demokritos" and University of Athens.

#### 2.5 ELECTROMAGNETIC PROPERTIES OF STATES IN $^{92}\text{Mo}$

##### FROM THE $^{92}\text{Mo}(p, p', \gamma)$ REACTION<sup>†</sup>

C. T. Papadopoulos<sup>\*</sup>, A. G. Hartas<sup>\*</sup> and P. A. Assimakopoulos<sup>\*</sup>  
G. Andritsopoulos<sup>\*\*</sup> and N. H. Gangas<sup>\*\*</sup>

Levels in  $^{92}\text{Mo}$  were studied through the  $^{92}\text{Mo}(p, p', \gamma)$  reaction at incident proton energies  $E_p = 7.0, 7.6$  and  $8.5$  MeV. Singles  $\gamma$ -ray spectra

were obtained with a Ge (Li) detector at angles of observation  $\Theta_{\gamma} = 0^{\circ}$ ,  $30^{\circ}$ ,  $55^{\circ}$ ,  $70^{\circ}$ ,  $90^{\circ}$  and  $125^{\circ}$ .

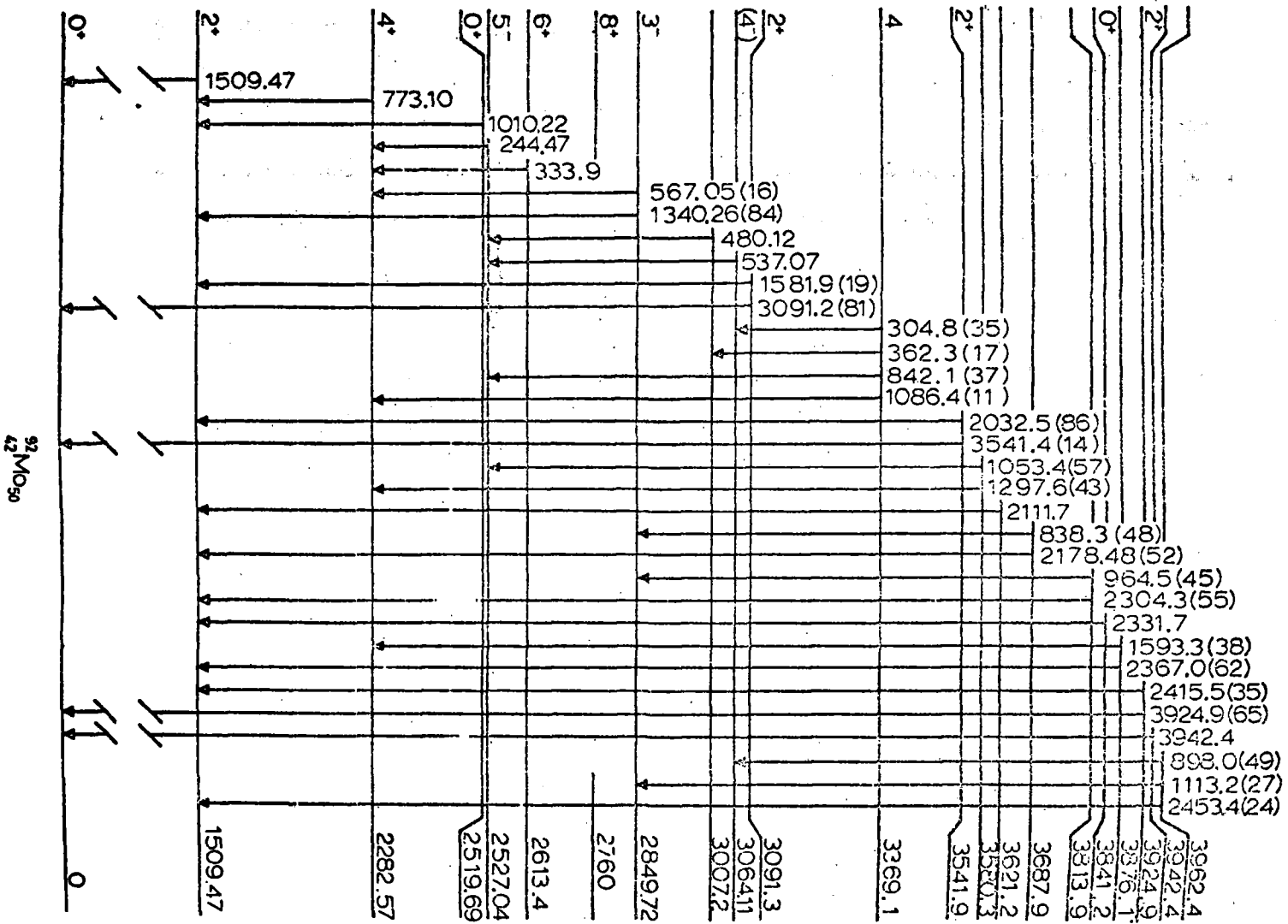
Level and transition energies were extracted from the  $\Theta_{\gamma} = 90^{\circ}$  spectra with an accuracy better than  $\pm 0.5$  keV. Branching ratios were extracted from the  $\Theta_{\gamma} = 55^{\circ}$  spectra. For transitions demonstrating an energy shift with respect to the angle of observation, the corresponding lifetime of the state was determined through the Doppler Shift Attenuation Method. The analysis of angular distributions yielded multipole mixing ratios and  $J^{\pi}$  values for several states. The properties of states in  $^{92}\text{Mo}$ , determined in present work are shown in the figure. The experimental information obtained in this work was employed to calculate reduced transition probabilities. The properties of low lying states in  $^{92}\text{Mo}$  strongly indicate that this nucleus may be described in the framework of the shell model by considering simple configurations of four protons occupying the  $p_{1/2}$  and  $g_{9/2}$  orbitals outside an inert  $^{88}\text{Sr}$  core.

---

+ Work submitted to Nuclear Physics A.

\* N. R. C. "Demokritos" and Ioannina University

\*\* Ioannina University, Ioannina Greece.





PROGRESS REPORT TO NEANDC  
FROM SPAIN

September 1975

Compiled by  
F. Manero  
Junta de Energía Nuclear  
Madrid



PREFACE

This document contains information of a preliminary or private nature and should be used with discretion. Its contents may not be quoted, abstracted or transmitted to libraries without the explicit permission of the originator.

CONTENTS

	<u>Page</u>
1. JUNTA DE ENERGIA NUCLEAR, MADRID .....	
2. UNIVERSIDAD COMPLUTENSE, MADRID	
Facultad de Ciencias .....	
3. UNIVERSIDAD AUTONOMA DE MADRID	
Departamento de Física Teórica .....	
4. INSTITUTO DE FISICA CORPUSCULAR. VALENCIA.....	
5. UNIVERSIDAD DE VALLADOLID	
Departamento de Física Fundamental ... ..	
6. UNIVERSIDAD DE ZARAGOZA	
Facultad de Ciencias. Departamento de Física	
Atómica y Nuclear .....	

## 1. JUNTA DE ENERGIA NUCLEAR.

### 1.1. Experimental determination of $X_L$ - ray intensities in Th, U and Pb.

L. González and E. Vañó.

By means of the excitation of thin samples of uranium, thorium and lead with an  $^{241}\text{Am}$  ring-source of 30 mCi, the  $X_L$ -ray spectra of these elements have been measured. As spectrometer a  $0.37\text{ cm}^3$  flat Ge(Li) detector was used.

The  $X_L$ -ray spectra were obtained by subtracting from the excitation spectra the americium source background measured in the same geometrical conditions.

The measured intensities were compared with the theoretical calculations of Scofield and the following intensity relationships obtained:

$L_3M_{4,5}/L_3M_1$  of 18.4, 20.7 and 23.2 for U, Th and Pb respectively;  $L_3M_{4,5}/L_3N_{4,5}$  of 4.1 and 3.5 for U and Th;  $L_2M_4/L_2N_4$  of 4.9 and 5.5 for U and Th;  $L_2M_4/L_2O_4$  of 9.6 and 19 for U and Th and  $L_2M_4/(L_2N_4 + L_2O_4)$  of 7.0 for Pb.

### 1.2. Application of the $\gamma$ -Xray coincidence technique to the measurement of $L_2/L_3$ vacancy relationships due to internal conversion.

E. Vañó and L. González.

The use of the  $\gamma$  -Xray coincidence technique for the determination of vacancy relationships in certain atomic subshells, due to gamma transitions, is studied..

The method is used to study the  $^{232}\text{Th}$ , by measuring the coincidence spectra of the  $X_K$ - and  $X_L$ -rays with the transitions of 143, 163, 185 and 205 KeV.

From the measured intensities the  $L_2/L_3$  vacancy relationships were determined by using the theoretical emission rates of Scofield and the fluorescence factors of McGuire.



### 1.3. Application of the rotational model to the calculation of neutron cross-sections.

J.A. Cabrera Jimenez and R. Martín Garcia.

A nuclear rotational model has been used for the calculation of neutron cross-sections and angular distributions.

An interaction Hamiltonian, with a potential which generalizes the ordinary optical model is used. This Hamiltonian leads in the calculation of the matrix elements between rotational states and deformed nuclei to a set of coupled equations, which are solved by the ECIS method (Equations Couplées en Iteration Séquentielle) of Raynal. A numerical program was developed which gives the elastic cross sections and their angular distributions for fast neutron reactions on deformed nuclei. The program has been used for the study of the particular case of e-e nuclei with a  $2^+$  first excited state.

### 1.4. Analysis of a non-local optical model.

R. Martín Garcia and J.A. Cabrera Jimenez.

An analysis has been made of an optical model with non-local potentials, suitable for the study of fast neutron interactions with non-deformed nuclei of  $A \geq 50$ , in the energy range of  $0.1 \text{ MeV} < E < 5 \text{ MeV}$ .

A numerical program in FORTRAN V is being developed to solve the Schrödinger equation for each partial wave, in which the potential is an integral operator with complex core and L-S interaction.

- 1.5. Comparison of the experimental results of the level scheme of  $^{22}\text{Na}$  and the theoretical predictions of the unified model.

J. Fernandez

The collective model with strong coupling describes well the static and dynamic properties of deformed nuclei, and its great success in the description of the "collective" properties of nuclei with  $19 \leq A \leq 25$  presents a big interest, not only from the experimental point of view but also from the theoretical one. In particular, the nucleus  $^{22}\text{Na}$ , which seems to be the most deformed nucleus in this region constitutes a case of utmost interest.

Therefore, and taking into account that  $^{22}\text{Na}$  is an auto-conjugated nucleus, an analysis was carried out of this nucleus in which a comparison is made of the experimental values of some levels of  $^{22}\text{Na}$ , with the theoretical predictions of the collective model and the isospin selection rules, and a possible interpretation is given for the experimental results in the frame of the shell model theory.

## 2. UNIVERSIDAD COMPLUTENSE. MADRID

Facultad de Ciencias.

### 2.1. Determination of the total cross section of some elements for 0.511 MeV photons

Carlos Willmott.

The atomic total cross sections of carbon, magnesium, aluminium, titanium, iron, copper, molybdenum, cadmium, tungsten, lead and uranium for gamma rays of 511 KeV incident energy were measured by means of coincidences detection between the photons of the annihilation radiation.

### 2.2. Liquid scintillator detector behaviour.

M. Ortiz Ramis and J. Campos.

The de-excitation curves of some scintillator materials in solution in the presence of oxygen are been measured for  $\alpha$  -and  $\beta$  particles and  $\gamma$  -rays excitation. The experimental results have been compared with theories based in a kinetic treatment which take into account several hypothesis for the molecules of solute and solvent in those liquids.

### 3. UNIVERSIDAD AUTONOMA DE MADRID

Departamento de Física Teórica.

#### 3.1. Microscopic description of giant multipole resonances in nuclei.

S. Krewald(\*) and J. Sánchez-Dehesa

Giant resonances of a higher multipolarity than the well-known dipole resonance have been detected experimentally in the last two years. Because of this interest, a study was made of the giant resonance region of different nuclei (O, Pb, . . .) within the framework of the higher RPA theory.

The main characteristics of the treatment are the following:

i) It takes into account the biggest part of the 2p-2h excitations, which come from the coupling of low-lying collective states of the core to the single-particle states in the neighbouring odd nuclei.

ii) The RPA calculations include single-particle orbitals in two major shells above and two below the Fermi surface.

iii) It is used the density dependent delta-force proposed by Migdal with parameters fitted in the Pb region to electromagnetic properties.

#### 3.2. Influence of configuration mixture in the Nolen and Schiffer anomaly.

A. Poves and J.M.G. Gómez.

The mass difference between the mirror nuclei  $^{41}\text{Sc}$  and  $^{41}\text{Ca}$  was calculated by using the shell model in the isospin formalism. The use of the effective inte-

---

(\*) Institut für Kernphysik.-Kernforschungsanlage, Jülich

raction proposed by Zucker for the d - f shell gives place to a mixture of excitations  $3p-2h$ , which represents for the ground state of these nuclei about 28 % of the wave function.

By using the principal components of the wave function the discrepancy in the mass difference between the theoretical and experimental values is reduced in about 20 %.

### 3.3. Energetic shift between isobars and possible dependence of the charge on nuclear forces.

J.M.G. Gómez and J. Sesma.

The energy differences between analogue states in a long series of isobar pairs in the region  $A = 34-54$  are calculated. The calculations are of microscopic type, inside de framework of the shell model, and carried out with several hypothesis for the interactions.

The results, based in charge independent nuclear forces with pure Coulomb interaction, agree very well with the experimental values, except for some states  $J = 0 T = 1$ . It is found that if we take into account small corrections, such as the magnetic interactions between nucleons, the agreement is considerably improved. It is discussed also the possible relationship of the small discrepancies between theory and experimental results on the violations of the nuclear forces charge simmetry.

#### 4. INSTITUTO DE FISICA CORPUSCULAR, VALENCIA

##### 4.1. Elastic scattering of 25 MeV alpha particles on several nuclei in the region $A = 50 - 70$ .

J. Alabau, E. Casal, A. García, T. Picazo, J.B.A. England<sup>+</sup>, G.J. Pyle<sup>+</sup> and P.M. Rolph<sup>+</sup>

The differential elastic scattering cross-sections for 25 MeV alpha particles have been measured for a total of 18 different nuclei in the region of  $A=50-70$ . The corresponding angular distributions were analysed according to the interaction optical model. In particular, the dependence of the values of the respective parameters on the mass number of the target nuclei was studied, as well as the possible characterization of the found results in relationship with the strong absorption radius and the values for the real potential and its derivative for such distance.

##### 4.2. Inelastic scattering of 25 MeV alpha particles on $^{51}\text{V}$ , $^{52}\text{Cr}$ , $^{53}\text{Cr}$ and $^{54}\text{Fe}$ .

J. Alabau, E. Casal, A. García and J.B.A. England<sup>+</sup>.

The analysis of spectra obtained in the interaction of a beam of 25 MeV alpha particles with the nuclei  $^{51}\text{V}$ ,  $^{52}\text{Cr}$ ,  $^{53}\text{Cr}$  and  $^{54}\text{Fe}$  has allowed to identify, together with the maxima of the elastic scattering process, several peaks originated by inelastic scattering of the  $\alpha$ -particles on the lower excited states of such nuclei. The corresponding angular distributions of the experimental differential cross sections have been analyzed by making use of coupled channel theory.

---

<sup>+</sup> Physics Department, University of Birmingham.

4.3. Study of the reaction  ${}^9\text{Be}({}^3\text{He}, p){}^{11}\text{B}$  at 5.0 MeV. Experimental values.

J.L. Ferrero, A. García, J.C. Pacheco, B. Bilwes<sup>††</sup> and R. Bilwes<sup>††</sup>.

The angular distributions for the reaction  ${}^9\text{Be}({}^3\text{He}, p){}^{10}\text{B}$  at 5.0 MeV have been measured for the 10 lower excited states of  ${}^{11}\text{B}$ , by means of photonuclear plates associated to a magnetic single-channel spectrometer and solid state detectors. The measured angular distributions are compared with those obtained by other authors at neighbouring energies, and a change in the interaction mechanism with the incident particle energy has been shown. In fact, while at lower energies the compound nucleus contribution is the strongest one, this contribution changes with increasing incident energy, so that at higher energies the direct interaction process is dominant (two-nucleons stripping).

4.4. Analysis of the input channel of the  ${}^9\text{Be}({}^3\text{He}, p){}^{11}\text{B}$  reaction at 5.0 MeV, according to the optical model.

J.L. Ferrero, A. García, J.C. Pacheco, B. Bilwes<sup>††</sup> and R. Bilwes<sup>††</sup>.

The input channel of the  ${}^9\text{Be}({}^3\text{He}, p){}^{10}\text{B}$  reaction was studied by means of the measurement of the elastic scattering of 5 MeV  ${}^3\text{He}$  particles on  ${}^9\text{Be}$ . The angular distribution was analysed in the framework of the interaction optical model with independent geometries for the real and imaginary parts of the potential. A particular attention was given to the ambiguities which present the real parameters of the model.

The result of this analysis is compared with that obtained for the values of other authors at neighbouring energies.

---

<sup>††</sup> Laboratoire des Basses Energies. CRN Strasbourg.

## 5. UNIVERSIDAD DE VALLADOLID

Departamento de Física Fundamental.

### 5.1. Analysis of the $^{19}\text{F}(p, \alpha)^{16}\text{O}$ reaction between 1,5 and 3.8 MeV.

C. Casanova and L. Marquez.

The differential cross sections of the  $^{19}\text{F}(p, \alpha)^{16}\text{O}$  reaction were measured at the incident proton energies of  $E_p = 1.5, 2.0, 3.0$  and  $3.8$  MeV. The experimental values have been analyzed by means of the Hauser-Feshbach statistical theory in order to deduce the level density values of the compound nucleus  $^{20}\text{Ne}$ .

### 5.2. Measurement of the multipolar mixture coefficient of the transition $2_2 \rightarrow 2_1$ of $^{62}\text{Ni}$ .

J.L. Casanova, M<sup>a</sup> L. Sanchez and J. Casanova.

By means of the  $\gamma - \gamma$  angular correlation method, the multipolar mixture ratio  $E_2/M_1$  for the gamma transition between the  $2_2 \rightarrow 2_1$  levels of the e-e nucleus  $^{62}\text{Ni}$  was measured. The obtained value was

$$\delta_{2_2 \rightarrow 2_1} = -2.7 \begin{matrix} +1.8 \\ -1.2 \end{matrix}$$

The measured value is in good agreement with the prediction of the shell model, supposing a nuclear-nuclear interaction of type MSDI.



6. UNIVERSIDAD DE ZARAGOZA.

Facultad de Ciencias. Departamento de Física Atómica y Nuclear.

6.1. Spin, multipolarities and mixture ratios determination for some excited levels of  $^{210}\text{Po}$ .

A. Morales, J. Morales, R. Nuñez-Lagos and M. Pló.

By making use of a  $^{226}\text{Ra}$  source of 10  $\mu\text{Ci}$  and of angular correlation techniques the values of the spin, gamma transition multipolarities and mixture ratios of some excited levels of  $^{214}\text{Po}$  have been determined.



NEANDC (OR) - 142 "L"  
INDC (SWT) - 008/L

PROGRESS REPORT TO NEANDC  
FROM SWITZERLAND

June 1975

T. Hürlimann

Swiss Federal Institute for Reactor Research  
Würenlingen

NOT FOR PUBLICATION



PREFACE

This document contains information of a preliminary or private nature and should be used with discretion. Its contents may not be quoted, abstracted, or transmitted to libraries without the explicit permission of the originator.

CONTENTS

	page
I. Institut de Physique, Université de Neuchâtel	120
II. Institut de Physique, Université de Fribourg	124
III. Physik-Institut der Universität Zurich	126
IV. Laboratorium für Kernphysik, Eidg. Technische Hochschule, Zürich	128
V. Eidg. Institut für Reaktorforschung, Würenlingen	134

I. Institut de Physique, Université de Neuchâtel

---

(Dir.: Prof. Jean Rossel)

1.  $D(\vec{n} \vec{n})$  elastic scattering at low energy

M. Ahmed<sup>†</sup>, D. Bovet, P. Châtelain, S. Jaccard<sup>††</sup>,  
R. Viennet and J. Weber

The depolarization factor  $D(\theta)$  at  $E_n = 2.45$  MeV has been measured at the Lab. angles:  $30^\circ$ ,  $40^\circ$ ,  $55^\circ$ ,  $70^\circ$ ,  $90^\circ$ . The data processing is in progress. The experimental set up has been described elsewhere {1}.

A phase shift analysis has been performed at 2.45 MeV, fitting the differential cross section data of Seagrave {2} as well as our complete set of measurements of the polarisation  $P(\theta)$  and our two preliminary results of  $D(\theta)$  {1}. The analysis was done for two distinct situations:

- a) Mixing parameters and J-degenerate phase shifts
- b) Splitting of the quartet phase shifts.

The angular distribution of the Wolfenstein's parameters predicted by these two kinds of analysis do not show any significant differences.

An ERA analysis below the deuteron break-up threshold, in the framework of the diagonal-J degenerate model is in progress.

A fast neutron-gamma discriminator {2} is being tested which should be included in our experimental set-up.

A sophisticated supra-conducting magnetic system is also under test. It will be used in the near future in the measurements of the Wolfenstein's parameters.

<sup>†</sup> Present address: Birmingham University, England

<sup>††</sup> Present address: TRIUMF, Columbia University, Vancouver, Canada

References

- {1} S. Jaccard, thèse, Université de Neuchâtel 1972
- {2} Seagrave et al. Phys. Rev. 105 (1957) 1816
- {3} P. Betz et al. Nucl. Instr. Meth. 119 (1974) 199

2. Study of three models for the quasifree scattering of two neutrons in the  $d(n,nn)p$  reaction\*

E. Bovet and F. Foroughi

We have made a systematic study of n-n quasi-free scattering in the  $d(n,nn)p$  reaction, with the aid of three models: the impulse approximation, the Cahill model {1} and the Ebenhöh Code {2}. We have obtained interesting results. For example, the "Chew-Low Plot" for all three models is a straight line, while the Cahill model satisfies the Treiman-Yang {3} criterion and gives a considerable improvement in the absolute value of the differential cross-section, over that obtained with the impulse approximation.

References

- {1} R. T. Cahill, Phys. Lett. 49B (1974) 150
- {2} W. Ebenhöh, Nucl. Phys. A191 (1972) 97
- {3} S. B. Treiman and C. N. Yang, Phys. Rev. Lett. 8 (1962) 140

\* An article has been submitted to H. P. A. for publication

3. Checking the alignment of a scattering chamber and measuring angular resolution with the aid of a position sensitive detector\*

E. Bovet, F. Foroughi, G. Pauletta, C. Nussbaum and S. Tchiguir<sup>†</sup>

In the non relativistic case, the relation between the coincidence angles of two elastically scattered particles does not depend on the incident energy. For relativistic energies such as are obtained from a cyclotron, there is a weak correction in the angle. For example the variation is of the order of  $0.01^{\circ}/\text{MeV}$  for elastic scattering of 70 to 80 MeV protons on deuterium. Consequently, the energy of the incident beam need not be known accurately.

Two signals are obtained from our surface barrier position sensitive detector (SBPSD); one proportional to the energy  $E$  deposited in the detector and the other to  $E \cdot X$ , where  $X$  is the distance from one end of the detector at which the particle is incident. The ratio  $X$  of these two signals is independent of  $E$ . Thick targets and a beam having a poor energy resolution can therefore be used, and this leads to an important reduction in the machine time. It should also be noted that since it is not necessary to stop the particles in the SBPSD, a thin SBPSD can be used.

In order to check the alignment of a scattering chamber with respect to the beam direction, or to measure the angular resolution of a detector mounted at an angle  $\theta_b$ , one centres a SBPSD at an angle  $\theta_a$  (where  $\theta_a$  and  $\theta_b$  correspond to the coincidence angles). Signals from the SBPSD are passed if they are in coincidence with those from the detector, and  $X$  is obtained as described above. The angular displacement of the chamber axis from the beam direction is directly related to the mean value of  $X$ , and the angular resolution of the detector at  $\theta_b$  to the width of the  $X$  distribution. It should be noted that one should not use particles of the same mass because, in the non-relativistic case, their angular separation is always  $90^{\circ}$  and therefore does not depend on the direction of the incident beam, while at relativistic energies, the dependence is slight.

<sup>†</sup>On leave from the Moscow Physical Engineering Institute



The angular resolution depends on the defocalisation of the beam. Thus this method also represents a good way of finding the compromise between good focalisation and beam current best suited to ones particular requirements. It has been used successfully for our scattering chamber {1} at SIN (Swiss Institute for Nuclear Research) with a proton beam and a deuterated polyethylene target.

References

- {1} J. E. Durisch, W. Neumann, J. Rossel, NIM 80, (1970) 1

II. Institut de Physique, Université de Fribourg

---

(Dir.: Prof. Dr. O. Huber)

Study of the  $^{191}\text{Ir}(n,\gamma)$  and  $^{193}\text{Ir}(n,\gamma)$   
reactions with a curved crystal spectrometer\*

W. Beer, J.-C. Dousse, J. Kern, A. Raemy and W. Schwitz

The thermal capture gamma rays from the  $^{191}\text{Ir}(n,\gamma)$ ,  $^{193}\text{Ir}(n,\gamma)$  and  $^{\text{nat}}\text{Ir}(n,\gamma)$  reactions have been observed with the Fribourg curved crystal spectrometer of DuMond type {1}. The targets were placed in the tangential through-tube of the reactor SAPHIR in Würenlingen.

The gamma rays from the above reactions had been previously observed with semiconductor detectors by Krüger et al. {2} and by the present authors in the energy range 40 - 600 keV. It was obvious from the spectra that many peaks were unresolved. A new measurement with a spectrometer of higher energy resolution was thus felt necessary. Fig. 1 shows two portions of the same spectrum observed with a Ge(Li) detector of good resolution and with the crystal spectrometer.

In fig. 2 are compared three spectra from the above reactions, showing how the lines can be assigned to one or the other isotope. About 100 transitions have been observed in  $^{194}\text{Ir}$  and over 200 in  $^{192}\text{Ir}$ . For the more intense peaks an energy precision of the order of one eV has been achieved. Most lines have been observed in several orders of reflection. The number of orders at which a particular line can be seen is limited by the decreasing crystal reflectivity with increasing order of reflection.

References

- {1} O. Piller, W. Beer and J. Kern, Nucl. Instr. Meth. 107 (1973) 61  
{2} H. Krüger, H. Hanle, M. Koriath and K. Stelzer  
Nucl. Phys. A 169 (1971) 363

\* Work supported in part by the Fonds National Suisse de la Recherche Scientifique

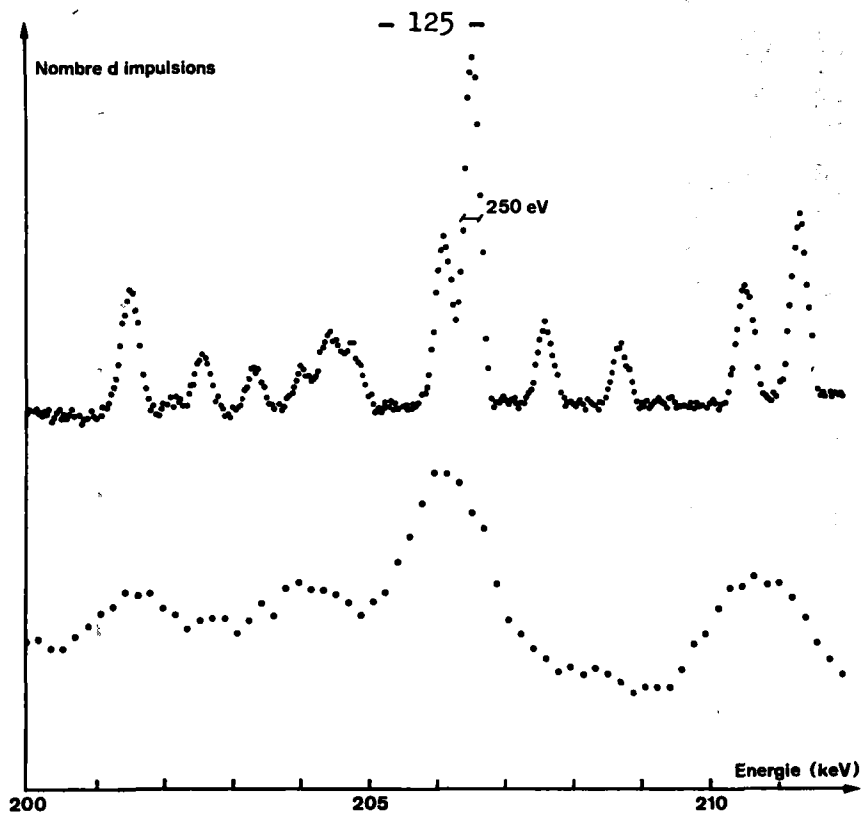


Fig. 1: Comparison of two portions of the  $^{nat}\text{Ir}(n,\gamma)$  spectrum observed with a  $2.4 \text{ cm}^3$  Ge(Li) diode (lower spectrum) and with the curved crystal spectrometer (upper spectrum) in 2<sup>nd</sup> order of reflection.

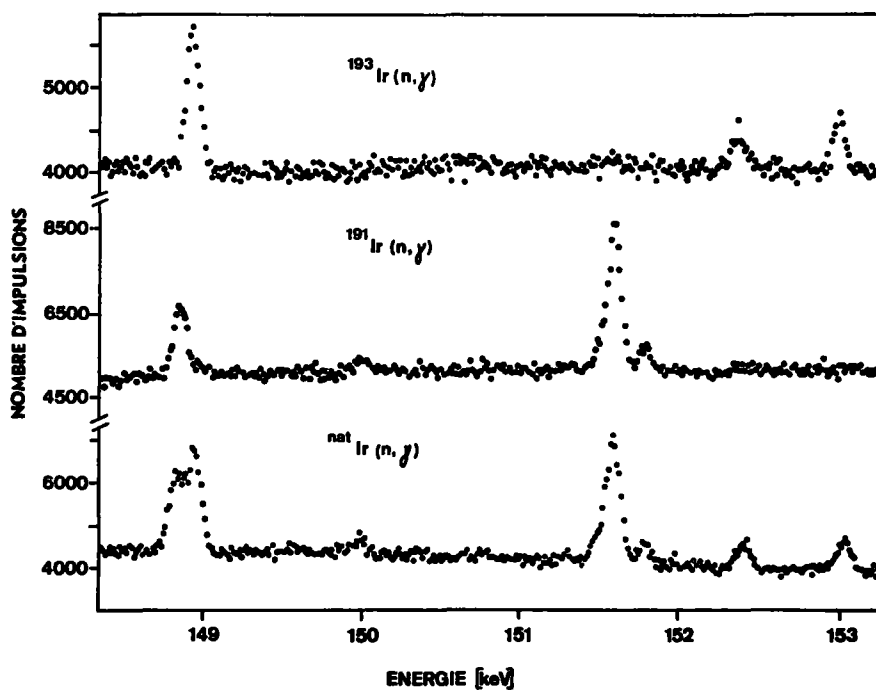


Fig. 2: Three portions of the  $^{191}\text{Ir}(n,\gamma)$ ,  $^{193}\text{Ir}(n,\gamma)$  and  $^{nat}\text{Ir}(n,\gamma)$  spectra observed in 3<sup>rd</sup> order of reflection.

III. Physik-Institut der Universität Zürich

(Dir.: Prof. Dr. Verena Meyer)

Elastic and inelastic scattering of protons from  $^{54}\text{Fe}$

H. Brändle, V. Meyer, M. Salzmann

The cross sections for elastic and inelastic scattering of protons from  $^{54}\text{Fe}$  leading to the compound nucleus  $^{55}\text{Co}$  have been measured at proton energies between 3.1 and 4.4 MeV at angles of  $90^\circ$ ,  $125^\circ$ ,  $141^\circ$  and  $165^\circ$  with respect to the beam. The results for  $165^\circ$  are shown in fig. 1, together with an R-matrix fit. The resonant levels, their elastic and inelastic widths are given in table 1.

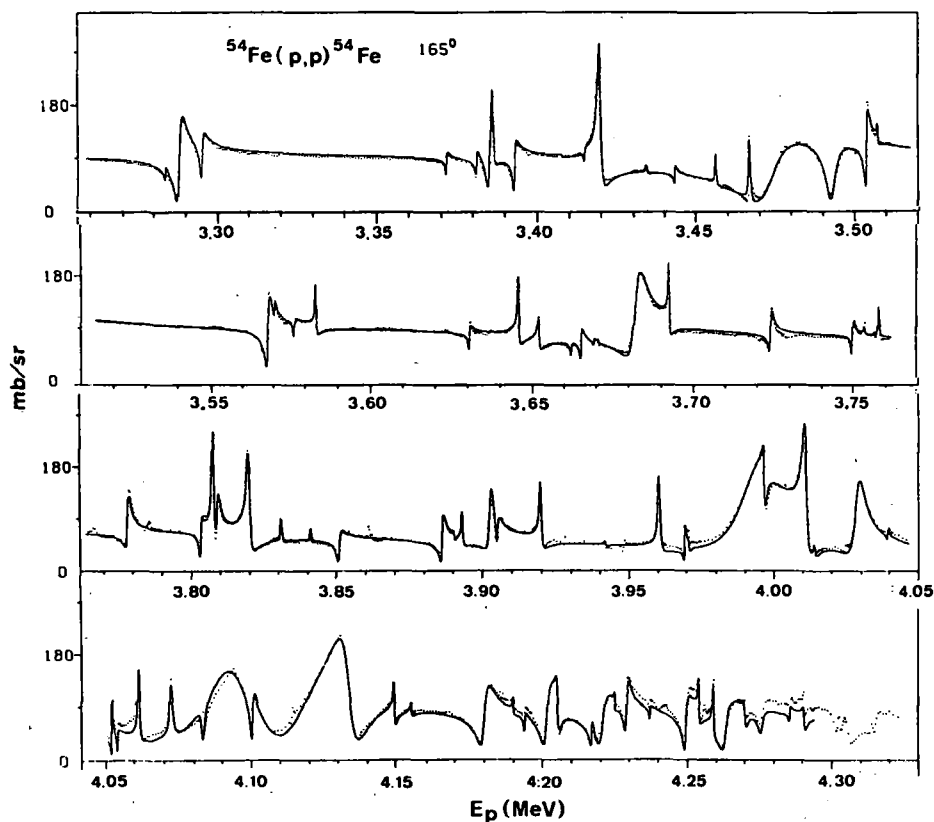


Fig. 1: Elastic scattering cross section at  $\theta_{\text{lab}} = 165^\circ$ . The solid curve is a fit to the data with the parameters given in table 1.

Table 1

$^{54}\text{Fe}(p,p)$  and  $^{54}\text{Fe}(p,p')$  resonance parameters

$E_p^{\text{lab}}$ (MeV)	$l_p$	$J^\pi$	$\Gamma_p$ (eV)	$\gamma_p^2$ (keV)	$\Gamma_{p'}$ (eV)	$\gamma_{p'}^2$ (keV)	$E_p^{\text{lab}}$ (MeV)	$l_p$	$J^\pi$	$\Gamma_p$ (eV)	$\gamma_p^2$ (keV)	$\Gamma_{p'}$ (eV)	$\gamma_{p'}^2$ (keV)
3.2834	1		60	0.36			3.9420	2	(3/2 <sup>+</sup> )	30	0.22	10	1.49
3.2876	1	3/2 <sub>-</sub>	1400	8.31	30	11.03	3.9481						
3.2948	1	1/2 <sub>-</sub>	500	2.93			3.9603	2	5/2 <sup>+</sup>	500	3.50	30	0.43
3.3715	1	3/2 <sub>+</sub>	100	0.52			3.9693	1	(3/2 <sub>+</sub> )	150	0.34		
3.3810	0	1/2 <sub>-</sub>	170	0.46			3.9710	2	(5/2 <sub>+</sub> )	100	0.69	150	2.12
3.3846	1	1/2 <sub>+</sub>	1100	5.57			3.9894	0	1/2 <sub>+</sub>	20000	26.66		
3.3861	2	5/2 <sub>+</sub>	300	5.36			3.9968	2	3/2 <sub>+</sub>	400	2.66	10	0.13
3.3927	1	3/2 <sub>-</sub>	350	1.75	100	22.78	4.0109	2	5/2 <sub>+</sub>	1300	8.49	120	1.53
3.4147	1	(3/2 <sub>+</sub> )	60	0.29			4.0141	2	(3/2 <sub>+</sub> )	200	1.30	70	0.88
3.4195	2	5/2 <sub>+</sub>	750	12.95	10	0.86	4.0244						
3.4342	2	(5/2 <sub>-</sub> )	20	0.31			4.0254						
3.4432	1	3/2 <sub>+</sub>	95	0.44			4.0282	0	1/2 <sub>+</sub>	3800	4.88		
3.4561	2	(5/2 <sub>+</sub> )	50	0.78			4.0392	0	1/2 <sub>+</sub>	50	0.06	10	1.11
3.4667	(2)	(5/2 <sub>+</sub> )	200	3.08	30	25.60	4.0524	1	3/2 <sub>-</sub>	200	0.42	10	0.25
3.4724	1	1/2 <sub>-</sub>	14000	61.57			4.0543	1	(1/2 <sub>-</sub> )	160	0.33	30	0.73
3.4930	1	1/2 <sub>-</sub>	3600	15.39			4.0615	2	5/2 <sub>+</sub>	400	2.44	10	0.11
3.5036	1	3/2 <sub>+</sub>	350	1.47	15	2.16	4.0726	2	5/2 <sub>+</sub>	750	4.50	90	0.98
3.5072	2	(5/2 <sub>-</sub> )	60	0.86	10	0.61	4.0834	2	5/2 <sub>+</sub>	400	2.37	400	39.26
3.5663	1	(1/2 <sub>-</sub> )	50	0.19	15	1.70	4.0850	0	1/2 <sub>+</sub>	25000	30.47		
3.5678	1	3/2 <sub>-</sub>	600	2.30	15	1.69	4.1005	1	3/2 <sub>-</sub>	500	0.99	35	0.76
3.5700	0	1/2 <sub>+</sub>	80	0.17	40	22.19	4.1210	0	1/2 <sub>+</sub>	30000	35.39		
3.5764	1	3/2 <sub>-</sub>	60	0.23	25	2.51	4.1340	2	5/2 <sub>+</sub>	6000	33.22	200	1.89
3.5831	2	(5/2 <sub>+</sub> )	140	1.76	5	0.23	4.1497	2	(5/2 <sub>+</sub> )	180	0.98	80	6.52
3.6308	1	3/2 <sub>+</sub>	110	0.39	15	1.34	4.1556	2	(5/2 <sub>+</sub> )	40	0.22	20	1.61
3.6459	2	5/2 <sub>+</sub>	220	2.49	25	0.93	4.1805	0	1/2 <sub>-</sub>	2600	2.91		
3.6524	2	3/2 <sub>+</sub>	220	2.46	10	0.36	4.1904	2	(5/2 <sub>-</sub> )	40	0.21	10	0.08
3.6623	1	(1/2 <sub>-</sub> )	120	0.40			4.1943	1	3/2 <sub>-</sub>	100	0.18	40	0.69
3.6654	1	3/2 <sub>-</sub>	160	0.53	20	1.58	4.2018	0	1/2 <sub>+</sub>	2500	2.75		
3.6694	1	3/2 <sub>+</sub>	30	0.10	5	0.39	4.2055	2	3/2 <sub>-</sub>	600	3.03	120	0.97
3.6707	2	(3/2 <sub>+</sub> )	15	0.16	3	1.13	4.2172	1	(3/2 <sub>-</sub> )	250	0.44	20	0.33
3.6820	0	1/2 <sub>+</sub>	3800	7.03			4.2206	1	1/2 <sub>-</sub>	3300	5.78		
3.6928	2	5/2 <sub>+</sub>	220	2.31	15	0.48	4.2252	2	(3/2 <sub>+</sub> )	100	0.49	15	0.12
3.7244	0	1/2 <sub>-</sub>	300	0.53			4.2292	0	1/2 <sub>+</sub>	700	0.75		
3.7497	1	3/2 <sub>-</sub>	700	2.09			4.2372	1	3/2	50	0.09	25	0.39
3.7499	2	5/2 <sub>+</sub>	400	3.83	15	0.40	4.2432						
3.7537	3	(5/2 <sub>-</sub> )	10	0.55	20	1.18	4.2496	1	3/2 <sub>-</sub>	800	1.36	220	3.32
3.7581	3	(5/2 <sub>+</sub> )	25	1.37	40	2.32	4.2542	2	(5/2 <sub>+</sub> )	170	0.81	60	0.44
3.7782	0	1/2 <sub>+</sub>	800	1.33	90	23.02	4.2592	2	(5/2 <sub>-</sub> )	200	0.95	50	3.04
3.8032	1	3/2 <sub>+</sub>	400	1.12	100	5.03	4.2632	1	1/2 <sub>-</sub>	3000	5.04		
3.8076	2	5/2 <sub>-</sub>	500	4.33	50	1.11	4.2703	2	(3/2 <sub>+</sub> )	200	0.93	400	2.81
3.8090	1	3/2 <sub>-</sub>	800	2.22	80	3.95	4.2757	1	1/2 <sub>-</sub>	700	1.16	900	12.82
3.8198	2	5/2 <sub>+</sub>	800	6.88	80	1.72	4.2856	0	1/2 <sub>+</sub>	100	0.10	60	0.34
3.8311	3	(7/2 <sub>-</sub> )	30	1.44	50	2.31	4.2907	2	(3/2 <sub>+</sub> )	180	0.82	200	11.26
3.8412	3	(7/2 <sub>-</sub> )	15	0.71	30	1.34	4.3024						
3.8509	1	1/2	900	2.37			4.3051						
3.8611							4.3142						
3.8624							4.4132	0	1/2 <sub>+</sub>	2500	2.32		
3.8861	1	3/2 <sub>-</sub>	600	1.51	60	2.34	4.461	0	1/2 <sub>+</sub>	2000	1.79		
3.8903	2	(5/2 <sub>+</sub> )	30	0.23	50	0.88	4.526	0	1/2 <sub>+</sub>	2400	2.04		
3.8931	2	(5/2 <sub>+</sub> )	150	1.16	35	0.61	4.576	0	1/2 <sub>+</sub>	1500	1.25		
3.9023	0	1/2 <sub>-</sub>	1700	2.47			4.671	0	1/2 <sub>+</sub>	20000	15.53		
3.9049	1	1/2 <sub>-</sub>	500	1.23	30	1.11	4.748	0	1/2 <sub>+</sub>	1500	1.12		
3.9199	2	(5/2 <sub>+</sub> )	350	2.60	50	7.99	4.83	0	1/2 <sub>+</sub>	50000	34.32		

IV.                   Laboratorium für Kernphysik, Eidg. Technische Hochschule, Zürich

---

(Dir.: Prof. Dr. J. Lang)

Investigation of the  $^2\text{H}(\vec{d},p)^3\text{H}$  reaction with polarized deuterons

W. Gruebler, P. A. Schmelzbach, V. König, R. Risler and  
D. O. Boerma

For several years the reaction  $^2\text{H}(\vec{d},p)^3\text{H}$  has been among the favourite reactions used in investigating the  $^4\text{He}$  nucleus. Not only the cross section, but also the polarization of the outgoing protons have been measured over a wide energy range {1}. The production of polarized deuterons by polarized ion sources has permitted this reaction to be studied in more detail. A series of analysing power measurements have been performed at low energy up to about 0.5 MeV by the Basle group {2}, Franz and Fick {3}, and Ad'yasevich et al. {4}. Measurements in the energy range between 3 and 11.5 MeV have been performed some time ago {5} in this laboratory. The analysis in {5} suffers from the fact that between 0.5 and 3.0 MeV no analysing power data were available. The installation of a more powerful polarized ion source at the 12 MeV EN-tandem accelerator made it possible to measure the necessary data in the energy range between 1.0 and 3.0 MeV. At these low energies the transmission through the accelerator was quite low, but the target current was still sufficiently high (a few n A). Measurements of the differential cross section  $\sigma_0$ , the vector analysing power  $iT_{11}$ , and the three tensor analysing powers  $T_{20}$ ,  $T_{21}$ , and  $T_{22}$  have been carried out in energy steps of 0.5 MeV.

The experimental method and the general procedure for measuring the vector and tensor analysing powers of nuclear reactions with the polarized deuteron beam has been discussed in previous papers {6}. The Madison convention {7} has been used in the representation of the tensor components  $T_{kq}$ .

The results of the differential cross section measurements are shown in fig. 1. The vector and tensor analysing powers are represented in figs. 2

and 3. For comparison, the result of ref. [2] at 0.46 MeV is shown too. In all three figures most of the statistical errors are smaller than the dots; the solid lines are the result of a Legendre polynomial analysis.

The results of analysing the differential cross section data in term of Legendre polynomials can be used to calculate the total cross section at the various energies measured. The results are represented in fig. 4. The open circles at lower energy are from [8]; the results at higher energy are from [5]. At 3 MeV the results of the analysis of the present data and of [5] are shown. A curve has been drawn by hand through the dots representing the data.

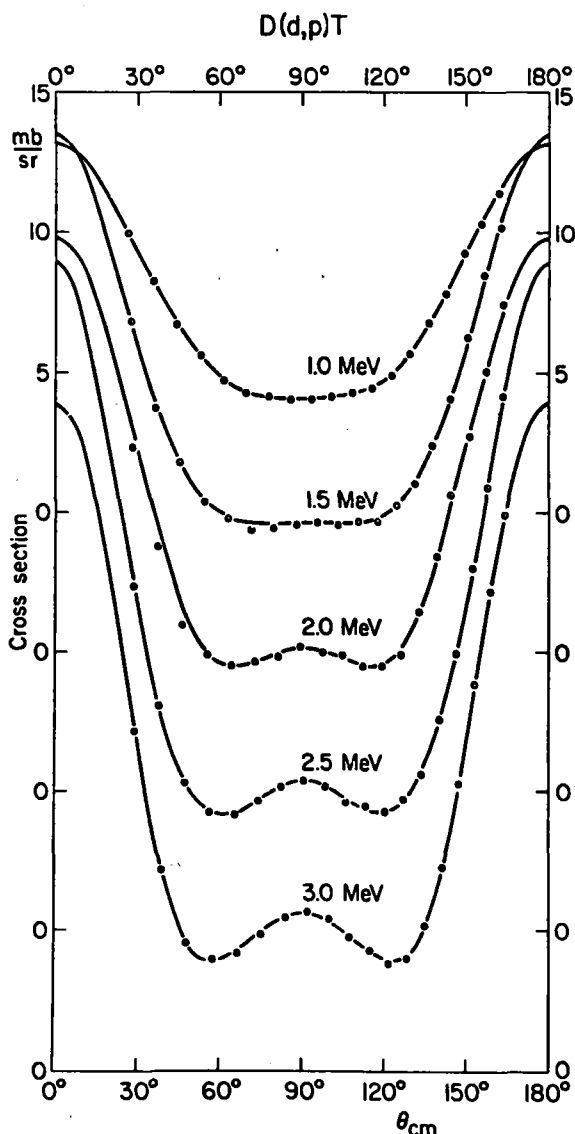


Fig. 1: Angular distributions of the cross section for the  ${}^2\text{H}(d,p){}^3\text{H}$  reaction. The dots are larger than the statistical error. The solid lines are Legendre polynomial fits.

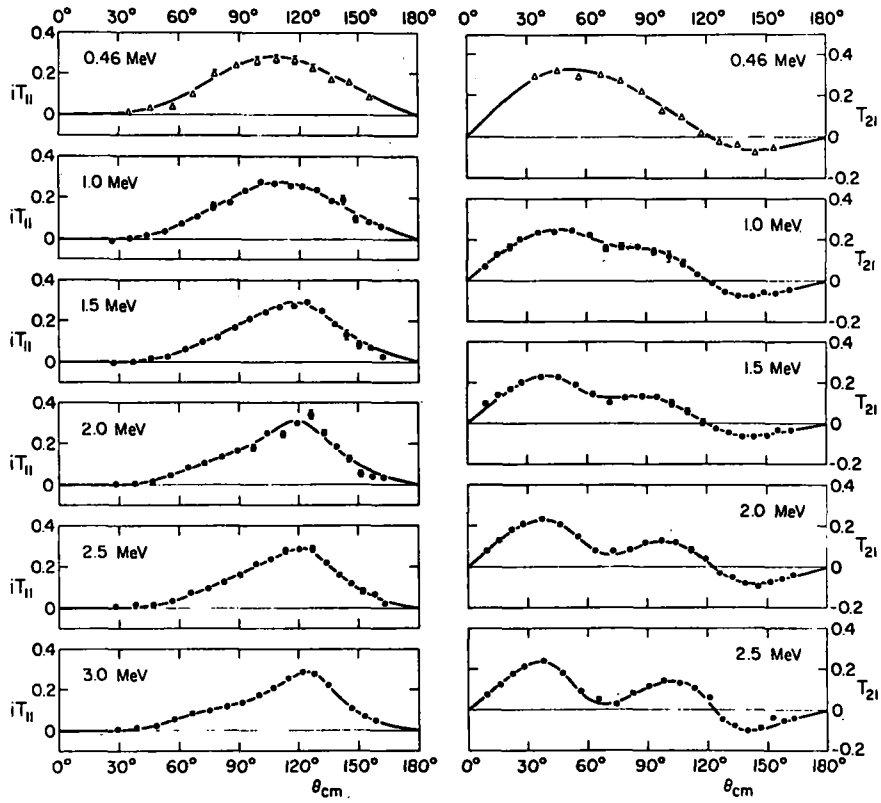


Fig. 2: The analysing powers  $iT_{11}$  and  $T_{21}$  between 0.46 and 3.0 MeV. Where no error bars are shown the statistical error is smaller than the dots. The solid lines are Legendre polynomial fits. The results at 0.46 MeV are from ref. [2].

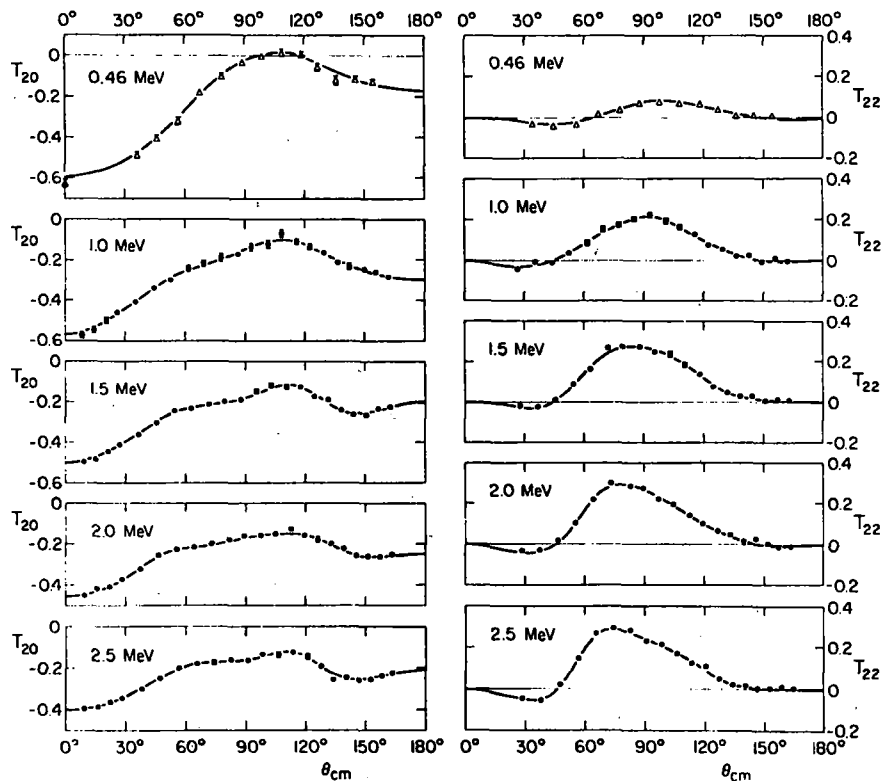


Fig. 3: The tensor analysing powers  $T_{20}$  and  $T_{22}$  between 0.46 and 2.5 MeV. Where no error bars are shown the statistical error is smaller than the dots. The solid lines are Legendre polynomial fits. The results at 0.46 MeV are from ref. [2].



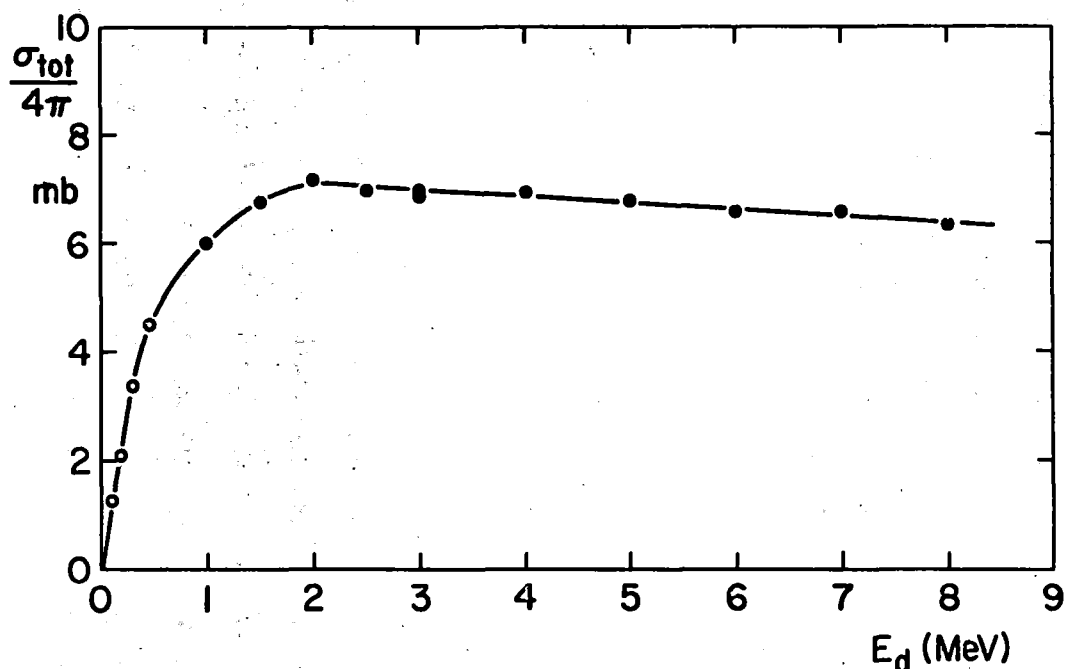


Fig. 4: Total cross section  $\sigma_T/4\pi$  of the  ${}^2\text{H}(d,p){}^3\text{H}$  reaction. The open circles are from ref. {8}; the results at energies higher than 3 MeV are from ref. {5}.

The normalized Legendre polynomial coefficients {5}

$$d_{kq}(L) = \frac{4\pi \lambda^2 a_{kq}(L)}{\sigma_{tot}} = \frac{a_{kq}(L)}{a_{00}(0)}$$

are presented as a function of the incident deuteron energy in fig. 5. The dots are the results of the calculations; the solid lines are drawn by hand for the sake of clarity. The size of the dots are in all cases larger than or equal to the error found in the fit. Legendre coefficients which are too small to appear different from zero at all energies on the scale used in fig. 5 are not shown. At low energy the results of the Basle group {2} and at energies higher than 2.5 MeV the results of {5} are indicated. The most prominent variation in the value of the coefficients occurs in the energy range up to about 3 MeV. The present experimental data were needed to determine the behaviour in this energy range quantitatively. A search for one or more resonances in  ${}^4\text{He}$  in this energy region, as well as the assignment of spin and parity can only be done in a careful, detailed analysis, which is in preparation in this laboratory.

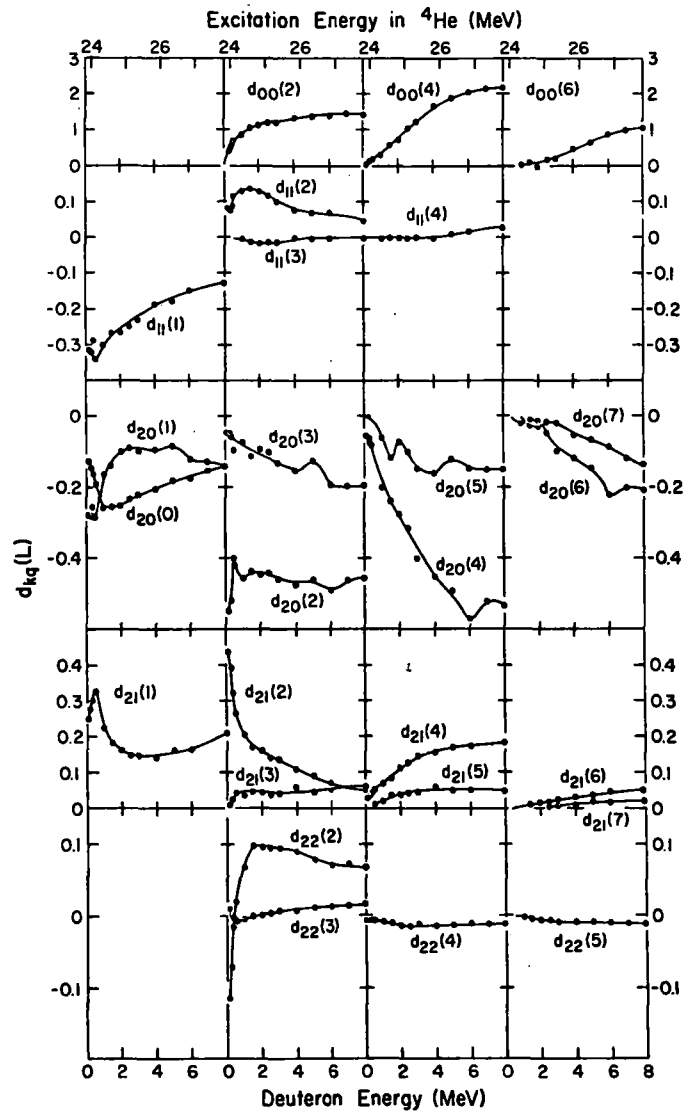


Fig. 5: Normalized Legendre polynomial expansion coefficients  $d_{kq}(L)$  for the differential cross section, and the vector and tensor analyzing powers. The dots are larger than the uncertainties of the fits. At energies below 0.5 MeV the results are from ref. [2].

References

- {1} G. Spalek, R. A. Hardekopf, J. Taylor, Th. Stammach and R. L. Walter, Nucl. Phys. A191 (1972) 449  
R. A. Hardekopf, T. C. Rhea, P. W. Lisowski, R. L. Walter and J. M. Joyce, Nucl. Phys. A191 (1972) 460  
R. A. Hardekopf, P. W. Lisowski, T. C. Rhea and R. L. Walter, Nucl. Phys. A191 (1972) 468
- {2} K. Jeltsch, A. Janett, P. Huber and H. R. Striebel, Helv. Phys. Acta 43 (1970) 279
- {3} H. W. Franz and D. Fick, Nucl. Phys. A122 (1968) 591
- {4} B. P. Ad'yasevich, V. G. Afonenko and D. E. Fomenko, Sov. Journ. Nucl. Phys. 11 (1970) 411
- {5} W. Gruebler, V. König, P. H. Schmelzbach, R. Risler, E. E. White and P. Marmier, Nucl. Phys. A193 (1972) 129
- {6} W. Gruebler, V. König, P. A. Schmelzbach and P. Marmier, Nucl. Phys. A134 (1969) 686  
V. König, W. Gruebler, P. A. Schmelzbach and P. Marmier, Nucl. Phys. A148 (1970) 380  
W. Gruebler, V. König, P. A. Schmelzbach and P. Marmier, Nucl. Phys. A148 (1970) 391
- {7} Proc. 3rd Int. Symp. on Polarization Phenomena, ed. H. H. Barshall and W. Haeberli (University of Wisconsin Press, 1971)
- {8} W. A. Wenzel and W. Whaling, Phys. Rev. 88 (1952) 1149

V. Eidg. Institut für Reaktorforschung, Würenlingen

---

(Dir.: Prof. Dr. H. Granicher)

1. Neutron capture cross sections of  $^{151}\text{Eu}$ ,  $^{153}\text{Eu}$ ,  $^{175}\text{Lu}$  and  $^{176}\text{Lu}$   
in the energy region from 0.01 to 10 eV

---

J. F. Widder

Neutron capture cross sections in the thermal and epithermal energy region are still required for several elements and isotopes. These cross sections are needed for different purposes such as detector applications, fission product poison calculations, burn-up calculations, flux measurements and others.

In order to fulfill requests for neutron data the capture cross sections for the elements Europium and Lutetium have been measured in the energy range from 0.01 through 10 eV using conventional time-of-flight techniques and a Moxon-Rae detector. The cross sections of the isotopes  $^{151}\text{Eu}$ ,  $^{153}\text{Eu}$ ,  $^{175}\text{Lu}$  and  $^{176}\text{Lu}$  were determined by means of additional measurements on samples enriched in  $^{153}\text{Eu}$  and  $^{175}\text{Lu}$ , respectively.

The requests compiled in special NEANDC-Reports (WRENDA) are characterized by high accuracy requirements. Though the experimental techniques for the measurement of such cross sections by means of prompt capture gamma-rays are well known for years, difficulties may occur if high precision is required. For this reason we had to develop new improved methods for the determination of the absolute neutron flux, of background and dead time corrections as well as for the calculation of multiple neutron scattering and gamma-ray attenuation effects in samples in order to reduce the systematic errors.

The accuracy attained in our measurements for the capture cross section values is 2 - 4 % from 0.01 to 1 eV (2 % in the thermal region) and 3 - 5 % above 1 eV. For some resonance cross sections above 4 eV the total error increases up to 10 %.

All data (including systematic and statistical errors) have been transmitted to the NEA Neutron Data Compilation Centre in Saclay, France, and are available on request.

A detailed description is given in EIR-Report No. 217 (1975) (NEANDC(OR)-143) which will appear in the near future.

2. Cross sections important to molten salt reactor studies

E. Ottewitte

Recent studies have indicated the following reactions to be important to the formation of corrosive and radioactive impurities in a molten chloride fast reactor:

(n, $\gamma$ ) for Cl-35, Cl-36, Cl-37, P-32 and S-35,

(n,p) for Cl-35,

(n, $\alpha$ ) for Cl-35.

The absorption cross section of Cl-37 is also critical to the breeding gain in a Cl-37 enriched MSBR.

In this vein EIR personnel are undertaking a complete evaluation of neutron cross sections for pertinent Cl isotopes in ENDF/B format.

To date this work has revealed the need for measurements

(a) to determine the isotopic identity of some of the measured natural Cl resonances,

(b) to determine  $\Gamma_p$  for most of the resonances, and deduce the associated degrees of freedom.

3. Reaction cross section for protons in the energy range of 10 - 70 MeV for Rb, Cs, Cd, Tl and Pb

F. Hegedüs, S. Chakraborty

In connection with the radioisotope production at the SIN injector cyclotron we are measuring reaction cross sections for protons in the energy range of 10 - 70 MeV for Rb, Cs, Cd, Tl and Pb.

Applying the "stacked foil technique" 25 - 30 thin foils of 30 mm in diameter were irradiated simultaneously. The thickness of the foil stack was 4 - 6 g/cm<sup>2</sup> corresponding to a degradation of the incident proton energy of 72 MeV to 40 - 10 MeV. The proton current was measured by means of the <sup>65</sup>Cu (p,pn) <sup>64</sup>Cu reaction induced in thin copper foils placed between target foils. In order to avoid systematic errors the measurements will be repeated with lower incident proton energy and other target arrangement.

After bombardment the gamma spectra of the produced radionuclides in the different target foils were measured. In order to distinguish between (p,xn) and (p,p(x-1)n) type reactions sometimes chemical separation was performed. The evaluation of the spectra allows the determination of the reaction cross sections in function of the proton energy.

PROGRESS REPORT TO NEANEC AND INDC

SOME RECENT NUCLEAR DATA ACTIVITIES AT THE  
ÇEKMECE NUCLEAR RESEARCH AND TRAINING CENTER  
(ÇNAEM), ISTANBUL, TURKEY AND MIDDLE EAST  
TECHNICAL UNIVERSITY, ANKARA, TURKEY

BY

ÇETİN ERTEK

1975

ÇEKMECE NUCLEAR RESEARCH AND TRAINING CENTER  
(ÇNAEM), POST BOX I, HAVA ALANI, ISTANBUL  
TURKEY





TOTAL NEUTRON CROSS SECTION OF TERBIUM  
IN THE THERMAL AND EPITHERMAL ENERGY REGIONS  
AND DETERMINATION OF THE POTENTIAL SCATTERING  
CROSS SECTION

(C. Cansoy, H. Atasoy, and S. Zebitay'an)

The total neutron cross section of Tb 159 has been measured in the energy range from 0.062 to 1 ev with a crystal spectrometer using the Be(10 $\bar{1}$ 1) crystal planes as a monochromator. The data in the left wing of the first neutron resonance in Tb 159 were fitted directly to the one-level Breit-Wigner formula using the method of least squares. The parameters obtained from the analysis are  $\sigma_p = 7.96 \pm 1.33$  b and  $A = 5.50 \pm 0.86$  b x (ev)<sup>1/2</sup>

The experimental values of the total neutron cross section of terbium for the energies between 0.0025 and 0.35 ev are lacking. Therefore, the total neutron cross section of terbium has been measured in the energy range as stated above. In this energy range it is possible to determine the potential scattering cross section  $\sigma_p$ , and this has been done in this work. On the other hand, the parameter "A" due to the far away resonances was also determined.

The total neutron cross section of Tb 159 has been measured for seventy different neutron energies in the energy range from 0.062 to 1 ev with the ÇNAEM crystal spectrometer(1,2). This energy range falls on the left wing of the first neutron of terbium. The spectrometer resolution was 1.405  $\mu$ sec/m using the Be(10 $\bar{1}$ 1) crystal planes as a monochromator.

A sample was made by mounting the oxide Tb<sub>2</sub>O<sub>3</sub> in an aluminum cell. This sample has an inverse thickness 1/N of 87.92 $\pm$ 0.44 b/atom. In calculations of the total neutron cross section of the oxide Tb<sub>2</sub>O<sub>3</sub> the cross section of the oxygen atoms was taken into account and subtracted from the total

cross section. According to the data given in BNL-325 this correction term was found to be almost constant and equal to 5.5 b.

The results are shown in Table I.

Table I

Breit-Wigner Parameters for the Left Wing  
of Terbium Resonance Derived from Analysis  
of Experimental Data

---

$$\begin{aligned}\sigma_p &= 7.96 - 1.33 \text{ b} \\ A &= 5.50 - 0.86 \text{ bx(eV)} \\ J &= 2.11 - 0.24 \text{ bx eV} \\ R &= 7.96 - 0.66 \text{ fm} \\ r_0 &= 1.47 - 0.12 \text{ fm}\end{aligned}$$

---

The total neutron cross section of Tb 159 has been measured by A.Knorr(3) Munich, 1965 in the energy range from 0.00022 to 0.00236 eV. Since the total cross section in this energy range is affected by the left wings of all neutron resonances of Tb 159, the parameter A can be obtained accurately from these experimental data. Therefore, the data given by A.Knorr were fitted directly to the formula,

$$\sigma = \frac{A}{(E)^{1/2}} + B$$

and the result is  $A = 5.49 \text{ bx(eV)}^{1/2}$ . Comparison between this result and the value given in Table I disclose an agreement within experimental error. Analysis also gives the value of  $B = 16.44 \text{ b}$ .

Since the total cross section measured by using QNAEM spectrometer covers the vicinity of the minimum of the left wing of the first neutron resonance in Tb 159, the parameter

$\sigma_p$  can be determined accurately. In fact, the value of 8.64 b for  $\sigma_p$  obtained by using the method of neutron diffraction in Ref.4 is in agreement with the value given in Table I.

#### REFERENCES

Work was performed under the auspices of the Turkish Atomic Energy Commission.

1. R.O.Akyüz, Ç.Cansoy and F.Domaniç, NSE 28, 359(1967)
2. R.O.Akyüz, Ç.Cansoy and F.Domaniç, "A Home-made Neutron Crystal Spectrometer for Research and Training", ÇNAEM 33, Çekmece Nuclear Research and Training Center (1965).
3. M.D. Goldberg et.al. BNL-325, Suppl. 2, Brookhaven National Lab.(1966).
4. R.E.Wood et.al. Phys. Rev. 98, 639 (1955).

#### THE GAMMA-RAY SPECTRUM FROM RADIATIVE CAPTURE OF THE FIRST RESONANCE NEUTRONS IN Sm 149

(C.Cansoy, H.Atasoy and C. Özbaylı )

A 37-cc Ge(Li) detector has been used in conjunction with the ÇNAEM neutron crystal spectrometer to examine the gamma-ray spectrum arising from neutron resonance capture in Sm 149. The effective gamma-ray energy resolution of 0.6-2.4 KeV allowed 17 transitions to be examined in the energy range between 109 and 1806 KeV following the capture of 0.0976 eV resonance neutrons in Sm 149. The spectrum is interpreted in terms of the levels in the compound nucleus, Sm 150. An analysis of the reduced intensities of 38 E1 transitions which consist of 9 secondary and 29 primary transitions indicates that they have a cumulative Porter-Thomas distribution. A similar analysis have been applied to 15 M1 transitions which consist of 4 secondary and 11 primary transitions.

The energy of the first neutron resonance for Sm 149, 0.0976 eV, is very close to the 0.07 eV peak energy of the Maxwellian for the count-rate spectrum of the ÇNAEM spectrometer. Therefore, sufficient gamma-ray intensities were obtained for the spectrum. The reduced gamma-ray intensities are subject to the Porter-Thomas distribution(1). Since the number of the

secondary E1 and M1 transitions is small, a cumulative Porter-Thomas distribution was applied to these transitions together with the primary transitions given by Buss and ~~Smither~~ Smither(2).

Since spin assignments depend on a probability distribution, in some cases they do not give accurate results.

For example, spin assignments for the levels at 1071.8, 1357.7 and 1793.7 KeV are different from that given in previously published studies(2,3). Moreover, there is an ambiguity between two assignments for the levels at 1071.8 and 1357.7 KeV. However, a  $\bar{3}$  or  $\bar{5}$  assignment for the level at 1357.7 KeV is consistent with the result given in Refs.(2 and 4). On the other hand, the  $2^+$  assignment is recommended by Buss and Smither(2) and is consistent with the result for the level at 1416.8 KeV. The  $\bar{3}$  or  $2^-$  assignment(2) is also consistent with our result for the level at 1760.3 KeV. A level is observed in the (d,d') reaction(2,4) at 1819 KeV. The strength of the proton group is proper to a  $2^+$  or  $4^+$  state. Hence, a  $2^+$  or  $6^+$  assignment for the level at 1818.9 KeV gives comparable results with those given in Ref.4 and the  $2^+$  assignment is probably correct. Buss and Smither concluded that any assignment except  $2^+$ ,  $3^+$ ,  $4^+$ , or  $5^+$  would be possible for the level at 2223.7 KeV. This conclusion is correct compared with a 2 or 6 assignment. Finally, a  $2^+$  or  $6^+$  assignment for the level at 2233.5 KeV is consistent with  $2^-$ ,  $3^-$ ,  $4^-$ , or  $5^-$  assignment given in Ref.(2).

#### REFERENCES

- 1.C.E.Porter and R.G.Thomas, Phys. Rev. 104, 483(1956).
- 2.D.J.Buss and R.K.Smither, Phys. Rev. ~~109~~, ~~1219~~ C2,1513 (1970).
- 3.R.K.Smither, Phys. Rev. 150, 964 (1966).
- 4.E. Veje, B.Elbek, B.Herskind, and M.C.Olesen, Nucl. Phys. A109, 489 (1968).

Contribution from Chemistry Department

Middle East Technical University

Ankara-Turkey

Contributing Members:

Dr. N. K. Aras

Dr. O. Birgöl

Dr. H. N. Erten

A. İzmen

İ. Ölmez

H. Göktürk

RANGES OF FRAGMENTS FROM FISSION

OF  $^{235}\text{U}$  WITH THERMAL NEUTRONS\*

<u>Fission Product</u>	<u>Range</u> <u>mg/cm<sup>2</sup> Al</u>
$^{99}\text{Mo}$	3.98±0.02
$^{111}\text{Ag}$	3.55±0.01
$^{115}\text{Cd}$	3.32±0.01
$^{121}\text{Sn}$	3.18±0.02
$^{125}\text{Sn}$	3.21±0.01
$^{127}\text{Sb}$	3.25±0.01
$^{129}\text{Sb}$	3.34
$^{140}\text{Ba}$	2.98±0.01

\* From N. K. Aras, M. P. Menon and G. E. Gordon  
Nucl. Phys. 69, 337 (1965)

YIELDS AND ISOMER RATIOS FROM THERMAL NEUTRON

FISSION OF  $^{235}\text{U}$ \*

<u>Fission Products</u>	<u>Independent Yield</u>	<u>Isomer Ratio</u>
3.8-min $^{134m}\text{I}$	0.50	1.4±0.7
53 -min $^{134m}\text{I}$	0.36	
45 -sec $^{136}\text{I}$	2.95	1.3±0.5
83 -sec $^{136}\text{I}$	2.29	
40 -min $^{130}\text{Sb}$	0.19±0.05	0.66±0.25
5.7-min $^{130}\text{Sb}$	0.29±0.09	
4.1-min $^{132}\text{Sb}$	1.40±0.42	2.1±0.8
2.1-min $^{132}\text{Sb}$	0.68±0.20	

\* H. N. Erten METU J. of Pure and Appl. Sci. 6, 17 (1973)

H. N. Erten Proceedings of IV. National Congress, Turkish  
Scientific and Technical Research Council (1973) Ankara-Turkey.

RANGE OF FRAGMENTS FROM SPONTANEOUS

FISSION OF  $^{252}\text{Cf}^*$

Fission Product	R A N G E			
	mg/cm <sup>2</sup> Al	mg/cm <sup>2</sup> Ni	mg/cm <sup>2</sup> Cu	mg/cm <sup>2</sup> Pd
$^{99}\text{Mo}$	3.85±0.03			
$^{105}\text{Rh}$	3.80±0.13			
$^{111}\text{Ag}$	3.64±0.02			
$^{113}\text{Ag}$	3.63±0.02			
$^{115}\text{Cd}$	3.63±0.02			
$^{127}\text{Sb}$	3.31±0.05			
$^{129}\text{Sb}$	3.32±0.02			
$^{131}\text{I}$	3.46±0.03			
$^{132}\text{Te}$	3.38±0.02			
$^{140}\text{Ba}$	3.03±0.03			
$^{99}\text{Mo}$	3.85±0.05	5.53±0.22	6.07±0.17	
$^{140}\text{Ba}$	3.03±0.03	4.45±0.10	4.97±0.16	5.81±0.08

\* O. Birgül, İ. Ölmez, and N. K. Aras, *Radiochim. Acta*, 18, 198 (1972)  
 A. İzmen, O. Birgül, and N. K. Aras, *J. Inorg. Chem.* 36, 25 (1974)

YIELDS OF PRODUCTS FROM SPONTANEOUS FISSION

OF  $^{252}\text{Cf}^*$

Fission Product	Cumulative Yield	Chain Yield	Ind. Yield	Isomer Ratio
$^{105}\text{Ru}$	5.3±0.3			
$^{105}\text{Rh}$	5.1±0.7			
$^{107}\text{Ru}$	6.3±0.9			
$^{107}\text{Rh}$	6.2±0.9			
$^{108}\text{Ru}$	6.0±0.9			
A=105		5.2±0.4		
A=107		6.3±0.7		
A=108		6.0±0.9		
$^{134}\text{Te}$	3.1±0.4			
$^{134}\text{I}$	3.7±0.7			
$^{134m}\text{I}$			0.69±0.05	1.7±0.3
$^{134g}\text{I}$			0.41±0.05	

\* H. Göktürk, O. Birgül, H. N. Erten, and N. K. Aras, *J. Inorg. Chem.* In press (1975)

H. N. Erten, O. Birgül, and N. K. Aras, to be published

Reproduced by the IAEA in Austria  
December 1975  
75-9756